

AperTO - Archivio Istituzionale Open Access dell'Università di Torino

**RIPEIP1, a gene from the arbuscular mycorrhizal fungus *Rhizophagus irregularis*, is preferentially expressed in planta and may be involved in root colonization**

**This is the author's manuscript**

*Original Citation:*

*Availability:*

This version is available <http://hdl.handle.net/2318/1586695> since 2016-08-05T11:08:44Z

*Published version:*

DOI:10.1007/s00572-016-0697-0

*Terms of use:*

Open Access

Anyone can freely access the full text of works made available as "Open Access". Works made available under a Creative Commons license can be used according to the terms and conditions of said license. Use of all other works requires consent of the right holder (author or publisher) if not exempted from copyright protection by the applicable law.

(Article begins on next page)

This is the author's final version of the contribution published as:

Fiorilli, Valentina; Belmondo, Simone; Khouja, Hassine Radhouane; Abbà, Simona; Faccio, Antonella; Daghino, Stefania; Lanfranco, Luisa. RiPEIP1, a gene from the arbuscular mycorrhizal fungus *Rhizophagus irregularis*, is preferentially expressed in planta and may be involved in root colonization. *MYCORRHIZA*. 26 (6) pp: 609-621.  
DOI: 10.1007/s00572-016-0697-0

The publisher's version is available at:

<http://link.springer.com/content/pdf/10.1007/s00572-016-0697-0>

When citing, please refer to the published version.

Link to this full text:

<http://hdl.handle.net/2318/1586695>

# Mycorrhiza

## RiPEIP1, a gene from the arbuscular mycorrhizal fungus *Rhizophagus irregularis*, is preferentially expressed in planta and may be involved in root colonization

--Manuscript Draft--

<b>Manuscript Number:</b>	MCOR-D-16-00008R1	
<b>Full Title:</b>	RiPEIP1, a gene from the arbuscular mycorrhizal fungus <i>Rhizophagus irregularis</i> , is preferentially expressed in planta and may be involved in root colonization	
<b>Article Type:</b>	Original Article	
<b>Keywords:</b>	Arbuscular Mycorrhizal Symbiosis; <i>Rhizophagus irregularis</i> ; <i>Oidiodendron maius</i> ; Heterologous expression system.	
<b>Corresponding Author:</b>	Valentina Fiorilli, PhD University of Turin Torino, ITALY	
<b>Corresponding Author Secondary Information:</b>		
<b>Corresponding Author's Institution:</b>	University of Turin	
<b>Corresponding Author's Secondary Institution:</b>		
<b>First Author:</b>	Valentina Fiorilli, PhD	
<b>First Author Secondary Information:</b>		
<b>Order of Authors:</b>	Valentina Fiorilli, PhD	
	Simone Belmondo	
	Hassine Radhouane Khouja	
	Simona Abbà, PhD	
	Antonella Faccio	
	Stefania Daghino, PhD	
	Luisa Lanfranco	
<b>Order of Authors Secondary Information:</b>		
<b>Funding Information:</b>	Università degli Studi di Torino (60%)	Prof Luisa Lanfranco
	AGER Foundation (RISINNOVA Project (2010-2369))	PhD Valentina Fiorilli
	Università degli Studi di Torino (SLEPS Project)	Prof Luisa Lanfranco
<b>Abstract:</b>	<p>Transcriptomics and genomics data recently obtained from the arbuscular mycorrhizal (AM) fungus <i>Rhizophagus irregularis</i> have offered new opportunities to decipher the contribution of the fungal partner to the establishment of the symbiotic association. The large number of genes which do not show similarity to known proteins, witnesses the uniqueness of this group of plant-associated fungi. In this work we characterize a gene that was called RiPEIP1 (Preferentially Expressed In Planta). Its expression is strongly induced in the intraradical phase, including arbuscules, and follows the expression profile of the <i>Medicago truncatula</i> phosphate transporter MtPT4, a molecular marker of a functional symbiosis. Indeed, <i>mtpt4</i> mutant plants, which exhibit low mycorrhizal colonization and an accelerated arbuscule turnover, also show a reduced RiPEIP1 mRNA abundance. To further characterize RiPEIP1, in the absence of genetic transformation protocols for AM fungi, we took advantage of two different fungal heterologous systems. When expressed as a GFP fusion in yeast cells, RiPEIP1 localizes in the endomembrane system, in particular to the endoplasmic reticulum, which is consistent with the <i>in silico</i> prediction of four transmembrane domains. We then generated RiPEIP1-expressing strains of the fungus <i>Oidiodendron maius</i>, ericoid</p>	

endomycorrhizal fungus for which transformation protocols are available. Roots of *Vaccinium myrtillus* colonized by RiPEIP1-expressing transgenic strains showed a higher mycorrhization level compared to roots colonized by the *O. maius* wild type strain, suggesting that RiPEIP1 may regulate the root colonization process.

Dear Editor,

Please here enclosed you will find the revised version of the manuscript “*RiPEIP1*, a gene from the arbuscular mycorrhizal fungus *Rhizophagus irregularis*, is preferentially expressed *in planta* and may be involved in root colonization”. This new version has taken in account the editor and referee’s suggestions and requests (text highlighted in yellow). All the changes have been listed and commented in the enclosed rebuttal letter.

We really hope that this new version may satisfy the high standards of Mycorrhiza.

With my best wishes

Valentina Fiorilli

**Editor’s comments:**

Please note that \_Mycorrhiza\_ consistently organizes articles as: Introduction, Materials and Methods, Results, and Discussion. (Methods are not placed at the end as in your manuscript.) Please reorganize your manuscript revision.

**Reply:** the manuscript has been organized according to the Mycorrhiza’s rules.

Lines 98-100: Instead of saying “we identified” which made me confused as to whether you are describing previous work or the current work, could you say something like “four genes were identified?” Although I recognize that you were involved in the 2012 work, the “we” might be misinterpreted as signaling “this study.”

**Reply:** the text has been changed.

Line 106: I share the reviewers’ concerns about calling this an “endomycorrhizal” fungus which imprecisely implies some relationship among ericoid, orchid, and glomeromycotan mycorrhizas. I strongly urge you to replace “endomycorrhizal” with “ericoid mycorrhizal.” (Note that Reviewer #2 incorrectly thought this was an orchid mycorrhiza)

**Reply:** the text has been changed: we have used ericoid mycorrhizal fungus.

Lines 278-279: I suggest rewording this as: “...as it shares with AM fungi the capability to intracellularly colonize root cells.” That is precisely what you intend by calling both “endomycorrhizal.”

**Reply:** the text has been changed according to the suggestion (Line 446).

Line 393: “Table 1” should be “Table S1.”

**Reply:** the text has been corrected.

Lines 667 & 678: “Single” should perhaps be “individual.”

**Reply:** the text has been corrected (line 683)

Line 669: Three asterisks often are used to represent  $P < 0.001$  (not “0.01” as you have done).

**Reply:** we have checked again the statistical data: in this case the p-value was 0.0002228, so three asterisks are correct. The text has been corrected (line 685).

Lines 679-680 & 700-701: If you simultaneously compared all four times, then you likely used a post-hoc test procedure after ANOVA. That procedure should be indicated (e.g., Tukey’s HSD, LSD, etc.).

**Reply:** the text has been corrected in the corresponding Figure legends.

Lines 687-690: Panel d could be omitted because the correlation already is apparent from Panels b and c. It seems inappropriate to use regression for these data in two distinct clusters because “two points determine a line,” a simple correlation coefficient could be stated in the text.

**Reply:** Panel d has been deleted from Fig. 4. The correlation coefficient ( $R^2$ : 0.8433) has been added in the text (line 369).

Lines 690-691: Some panels have only two asterisks and others have three; the different probabilities that they represent should be indicated explicitly.

**Reply:** the text has been modified (line 704).

Lines 692-695: Perhaps the right-hand lane of Panel a should be described.

**Reply:** the sample corresponds to a negative control; this information has been added in the Figure legend (line 707).

Lines 704-706: Panel c is entirely text, and so it should be a TABLE. “Plant” in Line 705 should be “plants.”

**Reply:** Panel c has been transformed in Table 1. The word “plant” has been corrected (line 747).

Line 715: “Pars” should be “parts.”

**Reply:** the word has been corrected (line 726).

Lines 721-725: It would be helpful to explain that the “A” lines are WT and the “B” are transgenic.

**Reply:** In both Panels (a and b) only the last lane on the right corresponds to the wild type (wt) sample. WT has been added on both pictures to make it clear.

**Reviewer #1:** Fiorilli et al. have characterized a presumably an orphan gene that is preferentially expressed in planta in the AM fungus *R. irregularis*. This gene was termed as RiPEIP1, whose role remains unclear but the authors showed that it may be involved in root colonization. The manuscript is well written, clear and concise. The experimental setup is appropriate and I found the use of the ericoid mycorrhizal fungus *O. maius* as an alternative system for heterologous expression to characterize AM fungal gene very interesting and novel. However, my major criticism concerns the expression of RiPEIP1 in *M. truncatula* mycorrhizal roots. The authors collected arbuscule-colonized cortical cells and non-colonized cortical cells from paraffin root sections. It would be interesting to collect some vesicles and/or intraradical spores as well as intraradical hyphae to see whether RiPEIP1 is also expressed in these fungal parts or restricted to arbuscules. I know that this is a challenging task but it will strengthen the manuscript.

**Reply:** Although we do have a long experience in the analysis of laser microdissected cells from mycorrhizal samples, we never tried to collect vesicles or intraradical spores due to the difficulty of sampling (and, to the best of our knowledge, nobody has published data on such material). The non colonized cells from mycorrhizal roots (MNM) is the sample that we consider to contain intercellular hyphae; even if at a morphological inspection hyphae are not evident in the LMD sections, this sample shows fungal transcripts (i.e. RiTef) but never transcripts of MtPT4 which is a marker of arbusculated cells.

Minor comments

Page 2: L29: Please add ericoid endomycorrhizal fungus... to avoid misleading for readers.

**Reply:** the text has been corrected.

Page 3, L42-45: Please site the appropriate references.

**Reply:** the reference Schüßler et al., 2001 has been added.

Page 3, L64-65: No sexual cycle has ever been described although meiosis-related genes were found in the genome. The appropriate reference is: Halary et al. (2011). Conserved meiotic machinery in *Glomus* spp., a putatively ancient asexual fungal lineage. *Genome Biology and Evolution* 3: 950-958.

However, Halary et al. (2013) [PLoS One 8(11) e80729] have reported a complete Putative Sex Pheromone-Sensing Pathway in AM Fungi, meaning that AM fungi are able to undergo sex. An analogy can be done with *Aspergillus* and *Candida albicans*.

**Reply:** the text has been modified and the references have been added.

Page 6: L124-127: Why Lin et al. 2014 sequence was annotated with four additional amino acids at the N-terminus? Please discuss.

**Reply:** We initially characterized the gene sequence through RACE experiments and in several independent 5'-RACE-PCR assays we could never report the presence of these four amino acids at the N terminus. The discrepancy may be based on the fact that probably Lin et al. performed an automatic annotation of the genome sequence. Since this is our interpretation, we did not add further comments in the text.

**Reviewer #2:** Report on the Mycorrhiza Manuscript: MCoR-D-16-00008

"RiPEIP1, an orphan gene from the arbuscular mycorrhizal fungus *Rhizophagus irregularis*, is preferentially expressed in planta and may be involved in root colonization" by Fiorilli and collaborators.

This is a potentially very interesting manuscript describing the functional analysis of a novel AM fungal gene from *Rhizophagus irregularis*. The authors identified the gene on the basis of its induction in planta during symbiosis and carried out a series of experiments to determine its role in symbiosis. I have a series of comments and suggested controls that might help to shape the manuscript at places where, in my opinion, the statements or conclusions from the authors are not fully justified.

#### ABSTRACT AND INTRODUCTION

1. I am not fully happy with the use of the word orphan gene. I think the authors should precise it better. To my knowledge, an orphan gene is such without homologues in other lineages, and therefore, the sentence in line 18 of the abstract "...genes identified as orphan, and often lineage-specific,..." is confusing. I would rather say PEIP1 is probably an arbuscular mycorrhiza specific gene, which is what the authors intend to say, not present in any other organism, besides *R. irregularis* and *Gigaspora* sp.

**Reply:** since the definition of "orphan gene" may be ambiguous we decided not to use it. The text has been changed accordingly; in most cases we used the concept of "genes that do not show similarity to known proteins".

2. I find misleading the statement that *Oidodendron maius* is the only endomycorrhizal fungus for which an established transformation protocol exist. First of all, there are other endomycorrhizal fungi, ie. *Piriformospora indica*, for which a transformation protocols exist. But in addition, it is only in page 9 at the end of the result section where the authors for the first time indicate which type of an endomycorrhizal symbiont *Oidodendron* is: an orchid mycorrhiza! I fully agree with the authors that morphologically seen, this infection is more similar to the AM fungi, but the fungi itself do not have to do with each other much, nor the plant is a host for AM fungi, as the authors in the discussion state. I think it would be fair to state from the beginning which fungus *Oidodendron* is and why it might be a good heterologous host for AM fungi.

**Reply:** We have introduced the detail of the ericoid mycorrhizal fungus already in the abstract and in the Introduction section (line 116-117).

We would like only to highlight that *Piriformospora indica*, although it exerts several beneficial effects on the host plant, is not considered a mycorrhizal fungus but a plant-growth promoting endophyte (Zuccaro et al. 2011. Endophytic life strategies decoded by genome and transcriptome analyses of the mutualistic root symbiont *Piriformospora indica*. PLoS Pathog. 2011 Oct;7(10):e1002290. doi: 10.1371/journal.ppat.1002290).

3. Page 3, line 67, I think this sentence reads not very precise. The AM fungus or the fungal cell is homo- or heterokaryotic, but the nuclei are not. The whole paragraph needs rephrasing.

**Reply:** we agree with the comment. We have changed the sentence into “... has been questioned whether AM fungi are in a heterokaryotic (Hijri and Sanders 2005; Ehinger et al. 2012) or in a homokaryotic condition..”

## RESULTS

4. It is not clear, not in the text (page 5, line 118) nor in M&M, not in the figure legend how this experiment was carried out: How old were the plants? How old was the ERM? How was it collected, from liquid? From solid medium? How was the level of root colonization?

**Reply:** We have added more details in the Results section “... the expression profile of *Glomus\_c13083* was monitored by quantitative RT-PCR (qRT-PCR) in intraradical (IRM) and extraradical (ERM) mycelium obtained from *M. truncatula* mycorrhizal roots 60 days post-inoculation (dpi) in a sandwich system (lines 279-282).

We also added the percentage of AM colonization: “The mycorrhizal status of *M. truncatula* roots was confirmed by the calculation of the total root length colonization ( $62.8\% \pm 2.7$ ).”(Lines 284-285)

5. The expression profiles from figure 1 and 3, are somehow redundant. This information could be collated in one figure and the manuscript will gain in clarity.

In this sense, it is not clear why the expression level in spores is not shown. The authors say they were not detectable but actually in Figure 4, much lower expression levels for PEIP are detected (10 times lower, see later). It would be good to know if there is a basal level of expression in spores or in germinated spores.

**Reply:** on our opinion the two experiments are rather different: Fig. 1 points to the comparison of ERM and IRM while Fig. 3 presents data of a time course of AM colonization; we would therefore prefer to keep the two figures separated.

Dealing with the *RiPEIP1* expression in spores, based on a semi-quantitative RT-PCR assays, Tisserant et al. 2012 (Table S5) (we added the reference in line 286) already showed that the gene is not expressed in spores. Also when we analysed the transcript levels by the more sensitive quantitative RT-PCR assay we could only register very high Ct values (40-41).

6. line 174, the authors write the expression levels in ERM are negligible... I think this is not correct. They show ca. 0.01, which is the level of expression from plants at 7 and 14 days after colonization in Figure 3.

**Reply:** We agree with this comment: it is true that at 7 and 14 dpi the intraradical colonization is very low; the *RiPEIP1* mRNAs we detect thus clearly derive from the ERM. These expression values (referred to the *RiTef*) are in line with those obtained in the experiment shown in Fig. 1: in the ERM *RiPEIP1* transcript levels are always lower than those of the IRM.

We have modified the text into “Since *RiPEIP1* was shown by qRT-PCR to be expressed at low levels in the ERM, gene expression was evaluated in whole mycorrhizal roots...”. (Lines 340-341)

My main criticism is that I am not convinced about the correlation between arbuscules and expression of PEIP. Here below some of the reasons (7,8,9)

7. The statement in line 178 is not totally correct, because while the expression of PT4 is still increasing, the PEIP expression is decreasing, even if it is not statistically significant. Furthermore, PEIP is expressed before PT4, indicating that it might be expressed if not in intercellular hyphae, at earlier stages of arbuscule formation where PT4 is not yet expressed, but I think it would be difficult to have such a precise time-point to detect this.

**Reply:** We agree with the comment about the 60 dpi time point: there is a trend but this is actually not supported by the statistical analysis. It is clear that there is a limitation coming from the experimental system, where a rather high variability in the colonization process among the different plants occurs; this does not allow such a precise level of detail.

8. Then also results in Figure 3c: While there are two samples for arbuscules, the sample of MNM is single, and no other gene besides RiTEF has been analysed. At least another sample would help to clarify this, but in addition, expression of a mycorrhiza-induced plant gene expressed not only in arbuscules (there are plenty of them, maybe some induced in adjacent cells), as well as of a fungal gene induced in colonized roots but not only in arbuscules (maybe MST2) should be measured.

**Reply:** This MNM cell population is actually the most difficult to collect. It is important to stress that one biological replicate corresponds to a minimum of 1500-2000 collected cells that were derived from independent LMD sections and mycorrhizal roots; this sample can therefore be intrinsically considered a pool of biological replicates. The RiTef gene was selected on purpose as a defined marker for the presence of the fungus in the MNM sample (possibly as intercellular hyphae as the fungus is not morphologically evident in the LMD sections). We do not think that the analysis of the MST2 gene will provide more information.

On the plant side, we looked in the literature for works where gene expression in mycorrhizal roots was analysed by the laser microdissection technique. In most cases only arbusculated cells (Gomez et al., 2009 BMC Plant biology; Tisserant et al., 2012 New Phytologist) were considered. When also MNM cells were collected the analysed genes were specific of arbusculated cells or they were expressed in both cell types (Hogekamp et al., 2011 Plant Physiologist; Gaude et al., 2015 BMC Plant biology). As far as we know, there are not very well described plant markers for MNM that may be used to further dissect the AM colonization steps.

9. The level of expression of PEIP1 in Figure 4 for wild type plants is extremely low as compared with the other experiments and not really explainable looking at the pictures depicting colonization.

**Reply:** The explanation is simple: in this case, to provide a more correct comparison of the colonization level in wt and mutant plants, we decided to normalize the RiPEIP1 expression level to the MtTef plant housekeeping gene, while in the other Figures the RiPEIP1 expression values were given referring to the fungal RiTef housekeeping gene.

Considering overall gene expression data, including those from the *mtpt4* mutants, we think that a kind of correlation between RiPEIP1 expression and arbuscule formation does occur. However, we are aware of limits of the experimental techniques and the biological system; for this reason we modified the text by softening the idea of a correlation; in particular, in the Discussion section at line 438 we have modified the sentence "Overall the data suggest (instead of support) a relationship between *RiPEIP1* and arbuscule differentiation."

Finally, it would be interesting if the authors would speculate on the possible cellular function that PEIP could have and on the experiments that, as they say at the end, will be required to elucidate the function of this gene in the AM symbiosis.

**Reply:** at this point of the investigations it is rather difficult to speculate about possible cellular functions. As we hypothesized that RiPEIP1 could be delivered to the plant cell, RiPEIP1-expressing transgenic lines of rice have been recently obtained as a tool to look for altered plants phenotypes including susceptibility to AM colonization and to dissect the metabolic pathway affected by RiPEIP1 and possibly its mechanisms of action. A sentence has been included at the end of the Discussion section (lines 454-457).

[Click here to view linked References](#)

1 ***RiPEIP1*, a gene from the arbuscular mycorrhizal fungus *Rhizophagus irregularis*, is**  
2 **preferentially expressed *in planta* and may be involved in root colonization**

3

4 Valentina Fiorilli<sup>1</sup>, Simone Belmonto<sup>1</sup>, Hassine Radhouane Khouja<sup>1</sup>, Simona Abbà<sup>2</sup>, Antonella  
5 Faccio<sup>2</sup>, Stefania Daghino<sup>1</sup> and Luisa Lanfranco<sup>1</sup>

6

7 <sup>1</sup>Department of Life Science and Systems Biology, University of Torino, via Accademia Albertina  
8 13, 10123 Torino, Italy

9 <sup>2</sup>Institute for Sustainable Plant Protection (IPSP), CNR, Strada delle Cacce 73, 10135 Torino, Italy

10

11 Corresponding author: Valentina Fiorilli

12 e-mail: valentina.fiorilli@unito.it

13

## 14 **ABSTRACT**

15 Transcriptomics and genomics data recently obtained from the arbuscular mycorrhizal (AM) fungus  
16 *Rhizophagus irregularis* have offered new opportunities to decipher the contribution of the fungal  
17 partner to the establishment of the symbiotic association. The large number of genes **which do not**  
18 **show similarity to known proteins**, witnesses the uniqueness of this group of plant-associated fungi.

19 In this work we characterize **a gene** that was called *RiPEIP1* (Preferentially Expressed In Planta).  
20 Its expression is strongly induced in the intraradical phase, including arbuscules, and follows the  
21 expression profile of the *Medicago truncatula* phosphate transporter *MtPT4*, a molecular marker of  
22 a functional symbiosis. Indeed, *mpt4* mutant plants, which exhibit low mycorrhizal colonization  
23 and an accelerated arbuscule turnover, also show a reduced *RiPEIP1* mRNA abundance. To further  
24 characterize *RiPEIP1*, in the absence of genetic transformation protocols for AM fungi, we took  
25 advantage of two different fungal heterologous systems. When expressed as a GFP fusion in yeast  
26 cells, *RiPEIP1* localizes in the endomembrane system, in particular to the endoplasmic reticulum,

27 which is consistent with the *in silico* prediction of four transmembrane domains. We then generated  
28 *RiPEIP1*-expressing strains of the fungus *Oidiodendron maius*, **ericoid** endomycorrhizal fungus for  
29 which transformation protocols are available. Roots of *Vaccinium myrtillus* colonized by *RiPEIP1*-  
30 expressing transgenic strains showed a higher mycorrhization level compared to roots colonized by  
31 the *O. maius* wild type strain, suggesting that *RiPEIP1* may regulate the root colonization process.

32

33 Keywords: Arbuscular Mycorrhizal Symbiosis, *Rhizophagus irregularis*, *Oidiodendron maius*,  
34 Heterologous expression system.

35

36

37

38

39

40

## 41 INTRODUCTION

42 The arbuscular mycorrhiza (AM), one of the most widespread symbiosis on earth, occurs between  
43 about 80% of land plants and soil fungi belonging to the ancient *Glomeromycota* Phylum (Schüßler  
44 et al. 2001; Redecker et al. 2013). This intimate mutualistic association allows the host plant to gain  
45 mineral nutrients and water from the soil *via* the activity of the large network of extraradical  
46 mycelium (Javot et al. 2007; Govindarajulu et al. 2005; Allen and Shachar-Hill 2009) while, in turn,  
47 the fungus acquires plant photoassimilates (up to 20%) that are essential to progress into the  
48 different developmental stages (Pfeffer et al. 1999). AM fungi are important members of the plant  
49 microbiome and provide important ecosystem services; they are therefore of great interest for the  
50 development of a sustainable and low-input agriculture (Gianinazzi et al. 2010).

51 The root colonization process comprises three main stages: i) a presymbiotic phase where the  
52 partners recognize each other through the exchanges of chemical compounds (Bonfante and  
53 Requena 2011; Bonfante and Genre 2015); ii) the root penetration where, after the formation of a  
54 hyphopodium on the root surface, the epidermal cell develops the pre-penetration apparatus to guide  
55 the entrance/accommodation of the fungal hypha (Genre et al. 2005, 2008); iii) the intraradical  
56 fungal growth, which culminates with the development of highly branched intracellular structures,  
57 the arbuscules, where nutrient exchanges between the two partners are thought to occur (Gutjahr  
58 and Parniske 2013). Arbuscule developmental dynamics was elegantly described by live cell  
59 imaging in rice roots: arbuscules were confirmed to be ephemeral structures with a lifetime at  
60 maturity of approximately two to three days (Kobae and Hata 2010).

61 AM fungi display many unusual biological features beside the obligate biotrophism, spores and  
62 hyphae contain multiple nuclei, making classic genetic approaches challenging (Lanfranco and  
63 Young 2012; Young 2015). No sexual cycle has ever been described although meiosis-related genes  
64 and conserved putative sex pheromone-sensing pathway were found in the genome (Halary et al.  
65 2011; 2013; Tisserant et al. 2013; Riley et al. 2014). Moreover, genomic structure was for long time  
66 obscure, and it has been questioned whether AM fungi are in a heterokaryotic (Hijri and Sanders

67 2005; Ehinger et al. 2012) or in a homokaryotic condition (Pawlowska and Taylor 2004). Recent  
68 data from the genome sequence of the model AM fungus *Rhizophagus irregularis* (isolate DAOM  
69 197198; Tisserant et al. 2013), also at the level of a single fungal nucleus (Lin et al. 2014), strongly  
70 support the homokaryotic status.

71 Several transcriptomic studies, mainly based on large-scale gene expression analysis, have been  
72 applied in the last decade to decipher the molecular mechanisms that accompany the formation of  
73 arbuscular mycorrhizas. They focused almost exclusively on the host plant (Salvioli and Bonfante  
74 2013 and references within), whereas only a few studies addressed the fungal partner (Requena et  
75 al. 2002; Breuninger and Requena 2004; Cappellazzo et al. 2007; Kikuchi et al. 2014; Salvioli et al.  
76 2016). A major advance has been obtained with transcriptomics and genomics data of *R. irregularis*  
77 (Tisserant et al. 2012; 2013; Ruzicka et al. 2013; Lin et al. 2014). The genome of *R. irregularis* is  
78 one of the largest (153 Mb) fungal genome sequenced to date, along with those of obligate  
79 biotrophic powdery mildews (Spanu et al. 2010) and the ectomycorrhizal symbiont *Tuber*  
80 *melanosporum* (Martin et al. 2010). The obligate biotrophy of AM fungi is not explained by  
81 genome erosion or any related loss of metabolic complexity in central metabolism. One striking  
82 genomic feature is the lack of genes encoding plant cell wall degrading enzymes in analogy to other  
83 obligate biotrophic pathogens (Spanu et al. 2010) and ectomycorrhizal symbionts (Martin et al.  
84 2010).

85 Tisserant et al. (2012) provided the first genome-wide overview of the transcriptional changes that  
86 occur in the different fungal life stages. In particular, the abundance of c. 18,500 fungal non-  
87 redundant expressed transcripts was analyzed in spores, extra- and intraradical mycelium, and  
88 arbuscules. Interestingly, several transcripts coding for Small Secreted Proteins (SSPs) were  
89 identified as being induced in the intraradical mycelium (IRM) and in arbuscule-containing cells  
90 (ARB), as compared to the extraradical mycelium (ERM). This SSPs list included the recently  
91 described secreted effector protein SP7, which is the first gene described so far to play a crucial role  
92 in the accommodation of the fungus within the plant root. In particular, SP7 counteracts the plant

93 immune response by interacting with the pathogenesis-related transcription factor Ethylene  
94 Response Factor (*ERF19*) in the host nucleus (Kloppholz et al. 2011).  
95 This transcriptomic dataset has been instrumental for the characterization of several fungal genes  
96 (Li et al. 2013; Belmondo et al. 2014; Tamayo et al. 2014), providing new insights into the genetic  
97 program activated during the AM symbiosis and into the genetic characteristics, similarities and  
98 uniqueness of AM organisms. Taking advantage of laser microdissection, four genes which were  
99 preferentially expressed in the intraradical phase, including arbuscules, were identified: three did  
100 not show similarity to known proteins and one showed similarities with ABC transporters (Tisserant  
101 et al. 2012).

102 In this study, we characterize one of these genes, that we called *RiPEIPI* (*Preferentially Expressed*  
103 *In Planta*) because its expression was strongly induced in the intraradical phase. Since stable  
104 transformation protocols are not available for AM fungi (Helber and Requena 2008; Helber et al.,  
105 2011), to characterize *RiPEIPI* we used two heterologous expression systems: *Saccharomyces*  
106 *cerevisiae*, a classical fungal model system and, for the first time, *Oidodendron maius*, an ericoid  
107 mycorrhizal fungus that, in analogy to AM fungi, intracellularly colonizes root cells, and for which  
108 a stable transformation protocol is available (Martino et al. 2007).

109

## 110 MATERIALS AND METHODS

### 111 Plant and fungal material

112 Seeds of *Medicago truncatula* Gaertn cv Jemalong and the *mtp4-2* TILLING mutant (Javot et al.,  
113 2011) were treated as described in Fiorilli et al. (2013). *Rhizophagus irregularis* (Syn. *Glomus*  
114 *intraradices*, DAOM 197198) inoculum was obtained from *in vitro* monoxenic cultures of  
115 *Agrobacterium rhizogenes*-transformed chicory roots (Bécard and Fortin 1988) in two-compartment  
116 Petri plates, as described in Belmondo et al. (2014). Plates were incubated in the dark at 24°C until  
117 the fungal compartment, containing a solid M medium without sucrose (M-C medium), was  
118 profusely colonized by the fungus (approximately 6 weeks).

119 *M. truncatula* wilde type (WT) and *mtpt4-2* mycorrhizal plants were obtained in the sandwich  
120 system (Giovannetti et al. 1993), inoculating seedlings with *R. irregularis* extraradical mycelium  
121 (ERM) between two sterile nitrocellulose membranes. Plants were fertilized with Long-Ashton  
122 nutrient solution containing 32  $\mu\text{M}$   $\text{KH}_2\text{PO}_4$  and grown in climate-controlled rooms at 22°C with a  
123 photoperiod of 14-h light and 10-h dark. **Plants were harvested 60 days post-inoculation (dpi).**

124 *Oidiodendron maius* (CLM1381.98 strain; Martino et al. 2000) was grown in Czapek-Dox medium  
125 (supplemented with 1% agar for the solid medium). Petri dishes were kept in the dark at 25°C in a  
126 dark room at 25°C for 2 months. Flasks were kept under the same conditions on an orbital shaker.

127 *In vitro* endomycorrhizas were synthesized as described by Abbà et al. (2009) with some  
128 modifications. Axenic *V. myrtillus* seedlings (Les Semences du Puy, Le Puy-En-Velay, France)  
129 were inoculated on modified Ingestad's medium (Ingestad, 1971), where four mycelium plug of wt  
130 or transformants strains were previously grown for two months. Plates were placed in a growth  
131 chamber (16 h photoperiod, light at 170  $\mu\text{mol m}^{-2} \text{s}^{-1}$ , temperatures at 23°C day and 21°C night),  
132 and roots were observed after 2 months of incubation. Four Petri dishes, each containing three  
133 seedlings (for a total of twelve replicates), were used for each fungal genotype.

134

### 135 **Quantification of mycorrhizal colonization**

136 *M. truncatula* WT and *mtpt4-2* mycorrhizal roots were stained after two months of inoculation with  
137 0.1% cotton blue in lactic acid and the estimation of mycorrhizal parameters was performed as  
138 described by Trouvelot et al. (1986) using MYCOCALC ([http://](http://www2.dijon.inra.fr/mychintec/Mycocalc-prg/download.html)  
139 [www2.dijon.inra.fr/mychintec/Mycocalc-prg/download.html](http://www2.dijon.inra.fr/mychintec/Mycocalc-prg/download.html)).

140 The degree of *V. myrtillus* mycorrhization was recorded after two months of inoculation by *O.*  
141 *maius* Zn WT or *RiPEIP1*-expressing strains. The magnified intersections method (Villarreal-Ruiz  
142 et al. 2004) was adapted to quantify the percentage of infection of *V. myrtillus* roots after staining  
143 with acid fuchsin. The root system was examined under the microscope using the rectangle around  
144 the cross-hair as intersection area at 200X magnification. A total of 100 intersections per seedling

145 root system were scored. Counts were recorded as percentage of root colonized (RC) by the fungus  
146 using the formula:  $RC\% = 100 \times \frac{\Sigma \text{ of coils counted}}{\Sigma \text{ of epidermal cells}}$  for all the intersections, where  $\Sigma$  is the number  
147 of epidermal cells for all the intersections.

148

#### 149 **Biomass analysis**

150 Conidia were harvested from two month-agar cultures of both WT and transformants by gently  
151 scraping cultures in 9 cm Petri dishes flooded with 1 ml of sterilized water. Conidia were counted in  
152 a Bürker counting chamber (Marienfeld, Germany) and, for each fungus, an aliquot containing a  
153 comparable number of conidia was transferred into liquid medium. After one month, fungal mycelia  
154 were harvested and the biomass weight evaluated. Analyses were carried out on three technical  
155 replicates for each biological condition.

156

#### 157 ***Agrobacterium tumefaciens*-mediated transformation of *Oidiodendron maius***

158 The pCAMBIA0380 (CAMBIA) was used as a backbone to construct the p*RiPEIP1* expression  
159 vector. The hygromycin resistance cassette (containing the *A. nidulans gpdA* promoter, the *hph* gene  
160 encoding resistance to hygromycin, and the *trpC* terminator from *A. nidulans*) was excised from  
161 pAN7-1 (Punt et al. 1987) with *HindIII* and *BglII* and inserted into the pCAMBIA030 at the  
162 *HindIII/BglII* sites to create the pCAMBIA0380\_HYG. The insertion of the Hygromycin resistance  
163 cassette introduced at the end of the *trpC* terminator a *XbaI* restriction site that was not originally  
164 present in the pCAMBIA0380 vector. The vector was then *XbaI-XmaI* digested to insert another  
165 copy of the *A. nidulans gpdA* constitutive promoter, which was modified at the 3' end to carry also a  
166 *KpnI* restriction site before the *XmaI* site. *RiPEIP1* full length cDNA was then amplified using a  
167 forward primer (*RiPEIP1-K*) containing a *KpnI* site and a reverse primer (*RiPEIP1-X*) containing a  
168 *XmaI* site (Table S1). The PCR product was *KpnI* and *XmaI* digested and inserted into the *KpnI*-  
169 *XmaI*-digested pCAMBIA0380\_HYG plasmid under the *A. nidulans gpdA* constitutive promoter.  
170 The resulting recombinant plasmid was introduced into *A. tumefaciens* LBA1100 strain, which was

171 used to transform *O. maius* ungerminated conidia according to the protocol described by Abbà et al.  
172 (2009). Transformants were isolated and transferred into 24-well plates with Czapek-Dox agar  
173 medium supplemented with 100 µg/ml hygromycin B. Transgenic strains were confirmed by PCR  
174 assays and Southern blot hybridization.

175 Genomic DNA of transformants strains was extracted using the CTAB protocol from mycelium  
176 grown for 30 days in liquid Czapek-2% DOX medium. For Southern blot, 10 micrograms of  
177 genomic DNA was digested with *Bgl*II restriction enzyme, size-fractionated on 1% (w/v) agarose  
178 gel and blotted onto nylon membranes following standard procedures (Sambrook and Russel 2001).  
179 Hybridization with a chemiluminescent detection system (ELC Direct DNA labelling and Detection  
180 System, Amersham) was performed according to the manufacturer's recommendation using a probe  
181 corresponding to the full length *RiPEIP1* cDNA sequence using *RiPEIP1* full length (*RiPEIP1*fl)  
182 forward/reverse primer (Table S1). Probe labelling and high stringency hybridization were carried  
183 out using ECL protocol (GE Healthcare, Chalfont St. Giles, U.K.).

184

#### 185 **5'- and 3' RACE**

186 Both 5'- and 3' RACE were performed on total RNA extracted from the mycorrhizal roots with the  
187 SMART RACE cDNA amplification kit (Clontech). The PCR product was obtained using the  
188 primers *RiPEIP1*-race-forward/reverse (Table S1). PCR was performed according to the Clontech  
189 protocol using the Advantage 2 PCR enzyme system and 35 cycles of 95°C for 30 sec, 60°C for 30  
190 sec and 72°C for 2 min, with a final extension at 72°C for 10 min. The RACE products were cloned  
191 into pCRII vector (TOPO cloning kit; Invitrogen) and sequenced.

192

#### 193 **Nucleic acid extraction, cDNA synthesis, RT-PCR assay**

194 Total genomic DNA was extracted from *R. irregularis* ERM and *M. truncatula* shoot using the  
195 DNeasy Plant Mini Kit (Qiagen), according to the manufacturer's instructions. Each primer pair

196 was first tested on plant or fungal genomic DNA as a positive control and to exclude cross  
197 hybridization.

198 Total RNA was extracted from *R. irregularis* ERM and mycorrhizal *M. truncatula* roots using the  
199 Plant RNeasy Kit (Qiagen), according to the manufacturer's instructions.

200 Total RNA was extracted from *O. maius* transformants and WT mycelia using a Tris-HCl extraction  
201 buffer (Tris-HCl 100 mM pH 8, NaCl 100 mM, Na-EDTA 20 mM, PVP 0.1 %, Na-laurylsarcosine  
202 1 % in DEPC-treated H<sub>2</sub>O), followed by phenol (Roti-Phenol, Roth) extraction,  
203 phenol:chloroform:isoamyl alcohol (25:24:1) extraction, chloroform extraction and isopropanol  
204 precipitation (30 min at -80°C). The pellet was then resuspended in DEPC-treated water and  
205 precipitated in 6M LiCl (12 hours at 4°C). Finally, RNA was pelleted by centrifugation, rinsed with  
206 70 % ethanol and resuspended in DEPC-treated H<sub>2</sub>O.

207 Samples were treated with TURBO™ DNase (Ambion) according to the manufacturer's instructions.  
208 RNA samples were routinely checked for DNA contamination by means of RT-PCR (One-RT-  
209 PCR, Qiagen) analysis, using for *R. irregularis* *RiEF1α*, *M. truncatula* *MtTef*, and *O. maius*  
210 *OmTubulin* primers (Table S1).

211 For conventional RT-PCR analyses, RNAs were amplified with *RiPEIP1-qpcr* forward/reverse  
212 primers and for the *O. maius* tubulin housekeeping gene (Table S1) using the One Step RT-PCR kit  
213 (Qiagen). RNA samples were incubated for 30 min at 50°C, followed by 15 min of incubation at  
214 95°C. Amplification reactions were run for 40 cycles at 94°C for 30 s, 60°C for 30 s, and 72°C for  
215 40 s.

216 cDNA synthesis was carried out on about 700 ng of total RNA which was denatured at 65°C for 5  
217 min and then reverse-transcribed at 25°C for 10 min, 42°C for 50 min and 70° for 15 min in a final  
218 volume of 20 µl containing 10 µM random primers, 0.5 mM dNTPs, 4 µl 5X buffer, 2 µl 0.1 M  
219 DTT, and 1 µl Super-ScriptII (Invitrogen).

## 220 **Quantitative RT-PCR**

221 Quantitative RT-PCR (qRT-PCR) assays were performed using an iCycler apparatus (Bio-Rad) as  
222 described in Belmondo et al. (2014) with primers pairs listed in Table S1. All reactions were  
223 performed on three technical replicates and on at least three biological replicates. Baseline range  
224 and Ct values were automatically calculated using iCycler software. Transcript levels were  
225 normalized to Ct values registered for the *RiEF1 $\alpha$*  (González-Guerrero et al. 2010) fungal gene and  
226 the *MtTef* (Hohnjec et al. 2005) plant gene. Only Ct values leading to a Ct mean with a standard  
227 deviation below 0.5 were considered.

228

### 229 **Laser microdissection (LMD)**

230 *M. truncatula* mycorrhizal roots, obtained using the sandwich method, were dissected, fixed and  
231 embedded in paraffin according to the method described in Perez-Tienda et al. (2011). A Leica AS  
232 LMD system (Leica Microsystem, Inc.) was used to collect arbuscule-colonized cortical cells  
233 (ARB) and non-colonized cortical cells (MNM) from paraffin root sections, as described by  
234 Balestrini et al. (2007). Two thousand ARB and MNM cells (for each biological replicate) from *M.*  
235 *truncatula* roots were collected. RNA was extracted following the Pico Pure kit (Arcturus  
236 Engineering) protocol. A DNase treatment was performed using an RNA-free DNase Set (Qiagen)  
237 in a Pico Pure column, according to the manufacturer's instructions. RNA was then quantified using  
238 a NanoDrop 1000 spectrophotometer. DNA contamination in RNA samples was evaluated using  
239 *RiEF1 $\alpha$*  (Table S1) by means of RT-PCR assays carried out using One Step RT-PCR kit (Qiagen).

240

### 241 **Construction of GFP fusion proteins for expression in yeast**

242 The full length cDNA of *RiPEIP1* was amplified from *R. irregularis* cDNA by PCR using the  
243 Phusion DNA-Polymerase (Finnzymes, Espoo, Finland). cDNAs were amplified using a forward  
244 primer containing the *KpnI* site (*RiPEIP1-K*) and a reverse primer containing the *NotI* site  
245 (*RiPEIP1-N*) (Table S1). The PCR products were *KpnI* and *NotI* -digested and inserted into the  
246 *KpnI-NotI*-digested pYES2-GFP plasmid (Blaudez et al. 2003) under the control of the GAL1

247 promoter and allowing a 3' fusion with the enhanced GFP reporter gene. *Saccharomyces cerevisiae*  
248 (BY4742 strain) transformation was performed using the lithium acetate based method described by  
249 Gietz et al. (1992). As a control of subcellular localization, two yeast strains constitutively  
250 expressing the red fluorescent protein fused to Sec13 (marker of both the endoplasmic reticulum  
251 and Golgi stacks) or Cop1 (marker of early Golgi) were analysed in parallel  
252 (<http://yeastgfp.yeastgenome.org/info.php>).

253

## 254 **Microscopy**

255 Fluorescence emission from yeast cells expressing RiPEIP1::GFP, Sec13::RFP or Cop1::RFP was  
256 examined with a Leica TCS-SP2 confocal laser-scanning microscope equipped with a 63x water  
257 immersion objective. GFP was excited at 488 nm (Ar laser) and fluorescence was detected at 515-  
258 530 nm. RFP was excited at 546 nm and fluorescence was detected at 570-650 nm.

259 For acid fuchsin staining mycorrhizal roots were stained with 0.01% (w/v) acid fuchsin in  
260 lactoglycerol (lactic acid-glycerol-water, 14:1:1; Kormanik and McGraw 1982). Confocal  
261 microscopy observations were done using a Leica TCS-SP2 microscope equipped with a 40x long-  
262 distance objective. Acid fuchsin fluorescence was excited at 488nm and detected using a 560-680  
263 nm emission window.

264 For calcofluor white (CFW; Fluorescent Brightener 28, F3543; Sigma-Aldrich) staining *O. maius*  
265 mycelia were let grown on a coverslip. The CFW solution was dropped onto the coverslips  
266 immediately before observation. CFW fluorescence was visualized with a Leica TCS-SP2 confocal  
267 laser-scanning microscope using a 405nm diode and an emission window at 410-460nm.

268

## 269 **Statistical analyses**

270 Statistical analyses were performed through one-way ANOVA and Tukey's post hoc test, using a  
271 probability level of  $p < 0.05$ . All statistical elaborations were performed using PAST statistical  
272 package (version 2.16; Hammer et al. 2001).

273 **RESULTS**

274 ***RiPEIP1* gene isolation**

275 With the aim to identify fungal genes involved in the functioning of arbuscules, the key structures  
276 of the AM symbiosis, we exploited transcriptomics data (Tisserant et al. 2012) generated for the  
277 AM fungus *Rhizophagus irregularis*. We focused our attention on an EST (contig Glomus\_c13083  
278 - v1 assembly) that turned out to be up-regulated in the intraradical phase in microarray experiments  
279 (Tisserant et al. 2012). In order to confirm the microarray data, the expression profile of  
280 Glomus\_c13083 was monitored by quantitative RT-PCR (qRT-PCR) in intraradical (IRM) and  
281 extraradical (ERM) mycelium obtained from *M. truncatula* mycorrhizal roots 60 days post-  
282 inoculation (dpi) in a sandwich system. In particular, RNAs were extracted from the ERM and from  
283 *M. truncatula* roots fragments from which ERM was carefully removed to generate the IRM  
284 sample. The mycorrhizal status of *M. truncatula* roots was confirmed by the calculation of the total  
285 root length colonization (62.8%±2.7). Glomus\_c13083 transcripts were highly abundant in the IRM  
286 compared to ERM (Fig. 1), and they were barely detected in spores (Tisserant et al., 2012; data not  
287 shown). From this expression profile, we called this gene *RiPEIP1* for *Preferentially Expressed In*  
288 *Planta*.

289 The 786 bp full length cDNA sequence of *RiPEIP1* was obtained by RACE assays. The  
290 corresponding genomic sequence (1267 bp), which comprises five introns (Supplementary Fig.  
291 S1A), was also obtained by conventional PCR. The recent release of the complete genome sequence  
292 of *R. irregularis* (Lin et al. 2014) confirmed the presence of this gene in the genome assembly  
293 (RirG\_002110 - GenBank EXX79805.1), although the sequence was annotated with four additional  
294 amino acids at the N-terminus. Considering that the coding sequence isolated through several  
295 independent 5'-RACE-PCR assays never reported the presence of these four amino acids we  
296 considered the shorter cDNA sequence for the further analysis.

297 The predicted protein sequence (261 amino acids) showed no significant similarity (all E-values >  
298 0.2) with proteins deposited in the NCBI “nr” database. The only hit found by a BlastP analysis,

299 spanning more than 50% of the sequence length, was another *R. irregularis* protein with unknown  
300 function (GenBank ESA21063.1, percentage of identity 22%; E-value 0.38). The second round of a  
301 Psi-Blast analysis, including this protein, identified three additional *R. irregularis* proteins  
302 (GenBank EXX76561.1, ESA00383.1, EXX59269.1) of unknown function slightly shorter (less  
303 than 200 amino acids) than RiPEIP1. Interestingly, a TblastN search within an extensive EST  
304 dataset recently published for another AM fungus, *Gigaspora margarita* (Salvioli et al. 2016), led  
305 to the identification of a cDNA sequence (GenBank: GBYF01016486.1; percentage of identity  
306 26%; E-value 0.036) coding for a 182 amino acids polypeptide, which is probably a partial  
307 sequence lacking the C-terminus.

308 TMHMM analysis of the RiPEIP1 amino acid sequence revealed the presence of four  
309 transmembrane-helix domains with cytoplasmic N- and C-terminus regions (Supplementary Fig.  
310 S1B). Additionally, the WoLFPSORT subcellular location predictor identified RiPEIP1 as a  
311 putative integral membrane protein. Remarkably, the sequence from *G. margarita*, notwithstanding  
312 the rather low similarity percentage, presents the same four transmembrane domains topology.

313 The C-terminus region, just after the fourth transmembrane domain, is highly hydrophilic, with a  
314 high percentage of charged (lysine, arginine, aspartate and glutamate) and polar (especially serines)  
315 amino acids. Some serines were also predicted (score > 0.99) by the NetPhos 2.0 Server to be  
316 potentially phosphorylated (Supplementary Fig. S1B). Notably, this region contains three typical  
317 ER-retention/retrieval C-terminus motifs: two KKXX motifs (starting from amino acid 188 and  
318 amino acid 200) and one KKKXX motif (starting from amino acid 246) (Jackson et al. 1990;  
319 Supplementary Fig. S1B).

320

### 321 **RiPEIP1 is localized in the endomembrane system**

322 In order to investigate the sub-cellular localization of RiPEIP1, we expressed a RiPEIP1::GFP  
323 fusion construct in *Saccharomyces cerevisiae* yeast cells. The fluorescent signal was observed

324 outlining the nucleus and extending into a network-like pattern in the cytoplasm (Fig. 2A). To better  
325 characterize this protein localization, we compared the RiPEIP1::GFP fluorescence pattern with that  
326 of two strains constitutively expressing the red fluorescent protein (RFP) fused to Sec13, which is a  
327 marker of the endoplasmic reticulum and Golgi stacks, or Cop1 which is localized in the early  
328 Golgi. Indeed, Sec13::RFP showed a very similar pattern to RiPEIP1::GFP, with the addition of  
329 several bright spots in the cytoplasm (Fig. 2C). Since analogous spots were observed in the  
330 Cop1::RFP line (Fig. 2D), we concluded that the RiPEIP1::GFP fluorescence pattern was  
331 compatible with protein localization in the endoplasmic reticulum and nuclear envelope. These  
332 results are in line with *in silico* predictions.

333

### 334 ***RiPEIP1* expression profiles**

335 To monitor the dynamics of *RiPEIP1* expression pattern along the colonization process, we set up a  
336 time course experiment of *M. truncatula* plants inoculated with *R. irregularis* in the sandwich  
337 system and sampled 7, 14, 28 and 60 days post-inoculation (dpi). Morphological analyses of roots  
338 revealed almost no intraradical fungal structures at 7 or 14 dpi. Mycorrhization frequency increased  
339 from 28 to 60 dpi, although arbuscules, detected starting from 28 dpi, decreased at 60 dpi  
340 (Supplementary Fig. S2). Since *RiPEIP1* was shown by qRT-PCR to be expressed at **low** levels in  
341 the ERM, gene expression was evaluated in whole mycorrhizal roots, without a distinction between  
342 IRM and ERM. *RiPEIP1* mRNA abundance increased in parallel to the development of the  
343 intraradical phase, and in particular to arbuscules formation, as demonstrated by morphological data  
344 and by the parallel mRNA accumulation of *MtPT4*, the *M. truncatula* phosphate transporter-  
345 encoding gene which is considered a molecular marker of arbuscule-containing cells (Harrison et al.  
346 2002; Fig. 3 A,B).

347 Using the laser microdissection, we investigated in more detail the *RiPEIP1* expression profile  
348 during the intraradical phase by comparing gene expression in arbusculated cells (ARB) and in non-  
349 colonized cortical cells from mycorrhizal roots (MNM). We used primers to the fungal

350 housekeeping gene *RiTEFα* to monitor the presence of fungal structures in the two cell types, and  
351 primers to *MtPT4* to confirm the presence of arbuscules (Fig. 3C). Since the transcript for the fungal  
352 housekeeping gene *RiTEFα*, but not *MtPT4*, was also detected in the MNM cell population, we  
353 considered this sample representative of intercellular hyphae. As witnessed by the detection of  
354 *MtPT4* mRNA, *RiPEIP1* was only expressed in the ARB cell population, indicating that, in the  
355 intraradical phase, *RiPEIP1* expression occurred mainly in arbuscules and presumably not in  
356 intercellular hyphae (Fig. 3C).

357 To gather information on the relationship between *RiPEIP1* expression and arbuscule functionality,  
358 we analysed *RiPEIP1* expression profile in the *M. truncatula mtpt4-2* mutant line, which is  
359 defective of MtPT4. Inactivation of MtPT4 causes low mycorrhizal colonization and an increased  
360 number of stunted arbuscules as a result of accelerated arbuscules turnover (Javot et al. 2011; Fig  
361 S3). As expected, a lower colonization level, based on relative abundance of fungal to plant *Tef*  
362 transcripts, was observed for *mtpt4-2* compared to wt plants (Fig. 4A). To have an overview of  
363 arbuscule abundance in the wt and *mtpt4-2* plants, we checked the expression level of the blue  
364 copper-binding protein1 (*MtBCP1*), a protein localized in the plasma membrane of cortical cells  
365 before and during the growth arbuscules and in the periarbuscular membrane surrounding arbuscule  
366 trunks (Pumplin and Harrison 2009). *mtpt4-2* mycorrhizal plants showed a lower level of *MtBCP1*  
367 transcripts compared to wt plants (Fig. 4B). Similarly, *RiPEIP1* mRNA abundance was lower in the  
368 *mtpt4-2* genotype (Fig. 4C). *MtBCP1* and *RiPEIP1* expression levels showed a positive correlation  
369 in wt and *mtpt4-2* genotypes ( $R^2:0.8433$ ). These data clearly indicate that *RiPEIP1* expression is  
370 therefore associated to arbuscule development.

371

### 372 **Heterologous expression of *RiPEIP1* in *Oidiodendron maius***

373 To gain further information on *RiPEIP1* function a novel fungal heterologous expression system has  
374 been exploited. In particular, we expressed *RiPEIP1* in the ericoid mycorrhizal fungus  
375 *Oidiodendron maius*, for which a protocol of genetic transformation is available (Martino et al.

376 2007). By means of *A. tumefaciens*-mediated genetic transformation, transgenic *O. maius* strains  
377 expressing *RiPEIP1* under a constitutive promoter were obtained. We confirmed the presence of  
378 *RiPEIP1* in *O. maius* genome by PCR and Southern blot analyses (Supplementary Fig. S4). Three  
379 transformants (BA2, BA4 and BC6) with a single genomic insertion were selected for further  
380 analyses (Supplementary Fig. S4).

381 *RiPEIP1* expression in free-living mycelia of *O. maius* transformants was confirmed by RT-PCR  
382 assays (Fig. 5A). As shown in Fig 5B the growth rate of *RiPEIP1*-expressing mycelia was similar to  
383 that of the wt strain. A phenotypic analysis carried out on free-living mycelia stained with  
384 calcoflour white showed no difference in hyphal morphology (Supplementary Fig. S5).

385 To investigate the impact of *RiPEIP1* expression on the establishment of the mycorrhizal symbiosis,  
386 seedlings of *Vaccinium myrtillus*, a common host plant for ericoid fungi, were colonized *in vitro*  
387 with wt or *RiPEIP1*-expressing strains. Plates with *V. myrtillus* seedlings without fungal inoculation  
388 were also set up. As expected, after 2 months uninoculated seedlings were dead (Fig. 6A). Root  
389 colonization level of inoculated plants was analysed through the morphological evaluation of the  
390 numbers of coils/root intersections. Interestingly, roots colonized by *O. maius RiPEIP1*-expressing  
391 strains showed a statistically significant higher mycorrhization degree compared to roots colonized  
392 by the wt strain (Fig. 6B: Fig S6). Moreover, morphological changes were also observed in the root  
393 apparatus colonized by *RiPEIP1*-expressing strains (Fig 7): in particular, a stimulation of root  
394 branching was observed. Roots colonized by the transgenic strains formed lateral roots up to the 6<sup>th</sup>  
395 order while the roots colonized by the wt strain only developed up to 4<sup>th</sup> order lateral roots (Table  
396 1).

397

## 398 **DISCUSSION**

399 Among plant-associated microbes, AM fungi form the most ecologically and agriculturally  
400 important mutualistic association with plant roots in terrestrial ecosystems. Yet, the genetic  
401 determinants that control the fungal development *in planta*, which are necessary to support a long-

402 lasting interaction between the partners, are still largely unknown. Transcriptomic (Tisserant et al.  
403 2012) and genomic (Tisserant et al. 2013; Lin et al. 2014) data recently obtained for *R. irregularis*  
404 have offered new opportunities to decipher the contribution of the fungal partner to the  
405 establishment of the symbiotic association. A large number of genes expressed in the intraradical  
406 and the extraradical phases do not show similarity with proteins listed in databanks and may  
407 therefore be AM-specific. This may be an indicator of the uniqueness of Glomeromycota. In this  
408 work, we have focused on the characterization of one of these genes that was called *RiPEIP1* based  
409 on its expression profiles.

410 Based on bioinformatics analyses, *RiPEIP1* is a protein with no similarity to known sequences;  
411 consistently with *in silico* predictions, *RiPEIP1* seems to be a transmembrane protein localized in  
412 particular in the endoplasmic reticulum and nuclear envelope when expressed as a GFP fusion in  
413 yeast cells. It is worth to note that a similar sequence was found in the recently published  
414 transcriptome (Salvioli et al. 2016) of another AM fungus, *G. margarita*. Even if the sequence is  
415 only partial, lacking the C-terminus portion, and the percentage of identity is relatively low (22%),  
416 the two proteins share the same 4 transmembrane domains topology. Moreover, RNA-seq data  
417 showed an up-regulation of about 4 folds in mycorrhizal roots, as compared to germinating spores  
418 (Salvioli et al. 2016). Only the search within genomic and transcriptomic data from other AM fungi,  
419 once available, will clarify whether *RiPEIP1*-related sequences are a specific feature of  
420 Glomeromycota and whether they may have a general role in the *in planta* phase.

421 *RiPEIP1* expression is strongly induced in the intraradical phase, and the time course experiment  
422 showed that the highest expression levels were reached in mature mycorrhizal roots; *RiPEIP1*  
423 mRNA abundance perfectly matches the expression profile of *MtPT4* (at 28 and 60 dpi), a  
424 phosphate transporter essential for the acquisition of Pi delivered by the AM fungus (Javot et al.  
425 2007) and thus considered a marker of a functional symbiosis. We therefore suggest that *RiPEIP1*  
426 expression is, to some extent, related to arbuscules formation. This hypothesis is supported by the  
427 fact that *RiPEIP1* transcripts were detected in laser microdissected arbuscule-containing cells, while

428 they were absent in adjacent cortical cells that likely contained only intercellular hyphae. To better  
429 understand the relationship with arbuscule development, we analysed *RiPEIP1* expression in the *M.*  
430 *truncatula mpt4-2* mutant line that is defective of MtPT4. MtPT4 function was shown to be critical  
431 for the AM symbiosis since its inactivation led to an altered arbuscules morphology, with premature  
432 senescence (Javot et al. 2007). As expected, we observed a reduced level of fungal colonization in  
433 *mpt4-2* mutants, as monitored by *RiTEF $\alpha$*  transcripts abundance, in comparison with colonized  
434 roots of wt plants. Interestingly, *mpt4-2* mycorrhizal roots showed lower levels of *RiPEIP1*  
435 mRNAs. Transcripts for *MtBCP1*, coding for a protein localized in the periarbuscular membrane  
436 and considered a molecular marker of arbuscule development and of colonization of the root system  
437 (Pumplin and Harrison 2009), were also found expressed at lower levels in the *mpt4-2* genotype.  
438 Overall the data suggest a relationship between *RiPEIP1* and arbuscule differentiation.  
439 The involvement of *RiPEIP1* in the intraradical phase of the colonization process was also  
440 supported by the heterologous expression of *RiPEIP1* in the ericoid mycorrhizal fungus *O. maius*.  
441 In the absence of genetic transformation protocols for AM fungi, AM fungal genes have been  
442 characterized by heterologous expression in filamentous fungi in few studies. To our knowledge,  
443 this approach was limited to pathogenic systems such as *Magnaporthe oryzae* (Kloppholz et al.  
444 2011) or *Colletotrichum lindemuthianum* (Tollot et al. 2009). We suggest that *O. maius* could  
445 represent an additional, possibly more suitable biological system for the characterization of AM  
446 fungal genes, as it shares with AM fungi the capability to intracellularly colonize root cells.  
447 Roots colonized by *O. maius RiPEIP1*-expressing strains showed a higher mycorrhization degree  
448 compared to roots colonized by the wt strain. Although no *RiPEIP1* homolog has been found in the  
449 complete *O. maius* genome sequence (Kohler et al. 2015) and *V. myrtillus* is not a host for AM  
450 fungi, the stimulation of mycorrhization observed in this heterologous mycorrhizal system suggests  
451 a general role for *RiPEIP1* in endosymbiosis establishment or functioning. Remarkably, *O. maius*  
452 transgenic strains induced changes on *V. myrtillus* root morphology with the stimulation of lateral  
453 roots formation up to the 6<sup>th</sup> order. The molecular basis of this phenomenon are unknown and

454 deserve further investigations. To this purpose, RiPEIP1-expressing transgenic lines of rice have  
455 been recently obtained as a tool to look for altered plants phenotypes including susceptibility to AM  
456 colonization and to dissect the metabolic pathway affected by RiPEIP1 and possibly its mechanisms  
457 of action.

458 In summary, although the mechanism of action still remain obscure, we showed that *RiPEIP1*, a  
459 gene from the AM fungus *R. irregularis*, is preferentially expressed *in planta* and may play a role in  
460 the root accommodation of fungal structures. Our data also underlies the potential of the  
461 endomycorrhizal fungus *O. maius* to characterize genes from AM fungi.

462

#### 463 **ACKNOWLEDGMENTS**

464 Research was funded by the BIOBIT-Converging Technology project (WP2) and the University  
465 grant (60%) to LL. VF fellowship was funded by the RISINNOVA Project (grant number 2010-  
466 2369, AGER Foundation). We thank Maria J. Harrison for the *mtpt4-2* mutant, Nuria Ferrol for the  
467 RFP yeast strains, Andrea Genre for confocal microscopy observations, Raffaella Balestrini for the  
468 help on laser microdissection and Paola Bonfante and Silvia Perotto for fruitful discussions and  
469 critical reading of the manuscript.

470 **REFERENCES**

- 471 Abbà S, Khouja HR, Martino E, Archer DB, Perotto S (2009) SOD1-targeted gene disruption in the  
472 ericoid mycorrhizal fungus *Oidiodendron maius* reduces conidiation and the capacity for  
473 mycorrhization. *Mol. Plant Microbe Interact* 22:1412-1421. doi: 10.1094/MPMI-22-11-1412
- 474 Allen JW, Shachar-Hill Y (2009) Sulfur transfer through an arbuscular mycorrhiza. *Plant Physiol.*  
475 149: 549-560. doi: 10.1104/pp.108.129866
- 476 Balestrini R, Gómez-Ariza J, Lanfranco L, Bonfante, P (2007) Laser microdissection reveals that  
477 transcripts for five plant and one fungal phosphate transporter genes are contemporaneously present  
478 in arbusculated cells. *Mol Plant Microbe Interact.* 20:1055-1062. doi.org/10.1094/MPMI-20-9-1055
- 479 Bécard G, Fortin JA (1988) Early events of vesicular–arbuscular mycorrhiza formation on Ri T-  
480 DNA transformed roots. *New Phytol* 108:211-218. doi: 10.1111/j.1469-8137.1988.tb03698.x
- 481 Belmondo, S, Fiorilli, V, Pérez-Tienda, J, Ferrol, N, Marmeisse, R, Lanfranco, L (2014) A  
482 dipeptide transporter from the arbuscular mycorrhizal fungus *Rhizophagus irregularis* is  
483 upregulated in the intraradical phase. *Front Plant Sci* 3;5: 436. doi.org/10.3389/fpls.2014.00436
- 484 Blaudez D, Kohler A, Martin F, Sanders D, Chalot, M (2003) Poplar metal tolerance protein 1  
485 confers zinc tolerance and is an oligomeric vacuolar zinc transporter with an essential leucine zipper  
486 motif. *Plant Cell* 1512: 2911-28. doi: 10.1105/tpc.017541
- 487 Bonfante P, Genre A (2015) Arbuscular mycorrhizal dialogues: do you speak 'plantish' or 'fungish'?  
488 *Trends Plant Sci* 20:150-154. doi: 10.1016/j.tplants.2014.12.002
- 489 Bonfante P, Requena N (2011) Dating in the dark: how roots respond to fungal signals to establish  
490 arbuscular mycorrhizal symbiosis. *Curr Opin Plant Biol* 14:451-457. doi: 10.1016/j.pbi.2011.03.014

491 Breuninger M, Requena N (2004) Recognition events in AM symbiosis: analysis of fungal gene  
492 expression at the early appressorium stage. *Fungal Genet Biol* 41:794-804.  
493 doi:10.1016/j.fgb.2004.04.002

494 Cappellazzo G, Lanfranco L, Bonfante P (2007) A limiting source of organic nitrogen induces  
495 specific transcriptional responses in the extraradical structures of the endomycorrhizal fungus  
496 *Glomus intraradices*. *Curr Genet* 51:59-70. doi: 10.1007/s00294-006-0101-2

497 Ehinger MO, Croll D, Koch AM, Sanders IR (2012) Significant genetic and phenotypic changes  
498 arising from clonal growth of a single spore of an arbuscular mycorrhizal fungus over multiple  
499 generations. *New Phytol* 196:853-561. doi: 10.1111/j.1469-8137.2012.04278.x

500 Jackson MR, Nilsson T, Peterson PA (1990) Identification of a consensus motif for retention of  
501 transmembrane proteins in the endoplasmic reticulum. *EMBO J* 9, 3153–3162

502 Kikuchi Y, Hijikata N, Yokoyama K, Ohtomo RY, Handa Y, Kawaguchi M, Katsuharu Saito K,  
503 Ezawa T (2014) Polyphosphate accumulation is driven by transcriptome alterations that lead near-  
504 synchronous and near-equivalent uptake of inorganic cations in an arbuscular mycorrhizal fungus.  
505 *New Phytol* 204:638-649. doi: 10.1111/nph.12937

506 Kormanik PP, McGraw AC (1982) Quantification of vesicular-arbuscular mycorrhizae in plant  
507 roots. In NC Schenk (ed) *Methods and principles of mycorrhizal research* American  
508 Phytopathological Society, St Paul, MN, p37-47

509 Fiorilli V, Lanfranco L, Bonfante, P (2013) The expression of *GintPT*, the phosphate transporter of  
510 *Rhizophagus irregularis*, depends on the symbiotic status and phosphate availability. *Planta*  
511 237:1267-1277. doi: 10.1007/s00425-013-1842-z

512 Genre A, Chabaud M, Timmers T, Bonfante P, Barker DG (2005). Arbuscular mycorrhizal fungi  
513 elicit a novel intracellular apparatus in *Medicago truncatula* root epidermal cells before infection.  
514 Plant Cell 17:3489-3499. doi: 10.1105/tpc.105.035410

515 Genre A, Chabaud M, Faccio A, Barker DG, Bonfante P (2008) Pre-penetration apparatus assembly  
516 precedes and predicts the colonization patterns of arbuscular mycorrhizal fungi within the root  
517 cortex of both *Medicago truncatula* and *Daucus carota*. Plant Cell 20:1407-1420. doi:  
518 10.1105/tpc.108.059014

519 Gianinazzi S, Gollotte A, Binet MN, van Tuinen D, Redecker D, Wipf D (2010) Agroecology: the  
520 key role of arbuscular mycorrhizas in ecosystem services. Mycorrhiza 20:519-530. doi:  
521 10.1007/s00572-010-0333-3

522 Gietz D, St Jean A, Woods RA, Schies RH (1992) Improved method for high efficiency  
523 transformation of intact yeast cells. Nucleic Acids Res 20:1425

524 Giovannetti M, Sbrana C, Avio L, Citernesi AS, Logi C (1993) Differential hyphal morphogenesis  
525 in arbuscular mycorrhizal fungi during pre-infection stages. New Phytol 125:587-593. doi:  
526 10.1111/j.1469-8137.1993.tb03907.x

527 González-Guerrero M, Oger E, Benabdellah K, Azcón-Aguilar C, Lanfranco L, Ferrol N (2010)  
528 Characterization of a CuZn superoxide dismutase gene in the arbuscular mycorrhizal fungus  
529 *Glomus intraradices*. Curr Genet 56:265-74. doi: 10.1007/s00294-010-0298-y

530 Govindarajulu M, Pfeffer PE, Jin HR, Abubaker J, Douds DD, Allen JW, Bücking H, Lammers PJ  
531 Shachar-Hil Y (2005) Nitrogen transfer in the arbuscular mycorrhizal symbiosis. Nature 435:819-  
532 823. doi:10.1038/nature03610

533 Gutjahr C, Parniske M (2013) Cell and developmental biology of arbuscular mycorrhiza symbiosis.  
534 Annu Rev Cell Dev Biol 29:593-617. doi: 10.1146/annurev-cellbio-101512-122413.

535 Halary S, Malik SB, Lildhar L, Slamovits CH, Hijri M, Corradi N (2011) Conserved Meiotic  
536 Machinery in *Glomus* spp., a Putatively Ancient Asexual Fungal Lineage. *Genome Biol Evol* 3:  
537 950-958. doi: 10.1093/gbe/evr089.

538 Halary S, Daubois L, Terrat Y, Ellenberger S, Wöstemeyer J, Hijri M (2013) Mating type gene  
539 homologues and putative sex pheromone-sensing pathway in arbuscular mycorrhizal fungi, a  
540 presumably asexual plant root symbiont. *Plos One* 8(11) e80729. doi:  
541 10.1371/journal.pone.0080729.

542 Hammer Ø, Harper DAT, Ryan PD (2001) PAST: paleontological statistics software package for  
543 education and data analysis. *Palaeontol Electron* 4, 9.

544 Harrison MJ, Dewbre GR, Liu J (2002) A phosphate transporter from *Medicago truncatula*  
545 involved in the acquisition of phosphate released by arbuscular mycorrhizal fungi. *Plant Cell*  
546 14:2413-2429. doi: 10.1105/tpc.004861

547 Helber N, Requena N (2008) Expression of the fluorescence markers DsRed and GFP fused to a  
548 nuclear localization signal in the arbuscular mycorrhizal fungus *Glomus intraradices*, *New Phytol*  
549 177: 537-548. doi: 10.1111/j.1469-8137.2007.02257.x

550 Helber N, Wippel N, Schaarschmidt S, Hause B, Requena N (2011) A versatile monosaccharide  
551 transporter that operates in the arbuscular mycorrhizal fungus *Glomus sp.* is crucial for the  
552 symbiotic relationship with plants. *Plant Cell* 23:3812-3823. doi: 10.1105/tpc.111.089813

553 Hijri M, Sanders IR (2005) Low gene copy number shows that arbuscular mycorrhizal fungi inherit  
554 genetically different nuclei. *Nature* 433:160-163. doi:10.1038/nature03069

555 Hohnjec N, Vieweg MF, Pühler A, Becker A, Küster H (2005) Overlaps in the transcriptional  
556 profiles of *Medicago truncatula* roots inoculated with two different *Glomus* fungi provide insights

557 into the genetic program activated during arbuscular mycorrhiza. *Plant Physiol* 137:1283-1301. doi:  
558 10.1104/pp.104.056572

559 Javot H, Penmetsa RV, Breuillin F, Bhattarai KK, Noar RD, Gomez SK, Zhang Q, Cook DR,  
560 Harrison MJ (2011) *Medicago truncatula mtpt4* mutants reveal a role for nitrogen in the regulation  
561 of arbuscule degeneration in arbuscular mycorrhizal symbiosis. *Plant J* 68:954-965. doi:  
562 10.1111/j.1365-313X.2011.04746.x

563 Javot H, Penmetsa RV, Terzaghi N, Cook DR, Harrison MJ (2007) A *Medicago truncatula*  
564 phosphate transporter indispensable for the arbuscular mycorrhizal symbiosis. *Proc Natl Acad Sci U*  
565 *S A* 104:1720-1725. doi: 10.1073/pnas.0608136104

566 Klopffholz S, Kuhn H, Requena N (2011) A secreted fungal effector of *Glomus intraradices*  
567 promotes symbiotic biotrophy. *Curr Biol* 21:1204-1209. doi: 10.1016/j.cub.2011.06.044

568 Kobae Y, Hata, S (2010) Dynamics of periarbuscular membranes visualized with a fluorescent  
569 phosphate transporter in arbuscular mycorrhizal roots of rice. *Plant Cell Physiol* 51:341-53.  
570 doi:10.1093/pcp/pcq013

571 Kohler A, Kuo A, Nagy LG, Morin E, Barry KW, Buscot F, Canbäck B, Choi C, Cichocki N, Clum  
572 A, Colpaert J, Copeland A, Costa MD, Doré J, Floudas D, Gay G, Girlanda M, Henrissat B,  
573 Herrmann S, Hess J, Högberg N, Johansson T, Khouja HR, LaButti K, Lahrmann U, Levasseur A,  
574 Lindquist EA, Lipzen A, Marmeisse R, Martino E, Murat C, Ngan C Y, Nehls U, Plett J M, Pringle  
575 A, Ohm R A, Perotto S, Peter M, Riley R, Rineau F, Ruytinx J, Salamov A, Shah F, Sun H, Tarkka,  
576 M Tritt, A Veneault-Fourrey, C Zuccaro, A Tunlid, A Grigoriev IV, Hibbett DS, Martin F (2015)  
577 Convergent losses of decay mechanisms and rapid turnover of symbiosis genes in mycorrhizal  
578 mutualists *Nat Genet* 47:410-415. doi:10.1038/ng.3223

579 Lanfranco L, Young JP (2012) Genetic and genomic glimpses of the elusive arbuscular mycorrhizal  
580 fungi. *Curr Opin Plant Biol* 15:454-461. doi: 10.1016/j.pbi.2012.04.003

581 Li T, Hu YJ, Hao ZP, Li H, Wang YS, Chen BD (2013) First cloning and characterization of two  
582 functional aquaporin genes from an arbuscular mycorrhizal fungus *Glomus intraradices*. *New*  
583 *Phytol* 197:617-30. doi: 10.1111/nph.12011

584 Lin K, Limpens E, Zhang Z, Ivanov S, Saunders DG, Mu D, Pang E, Cao H, Cha H, Lin T, Zhou Q,  
585 Shang Y, Li Y, Sharma T, van Velzen R, de Ruijter N, Aanen DK, Win J, Kamoun S, Bisseling T,  
586 Martin F, Kohler A, Murat C, Balestrini R, Coutinho PM, Jaillon O, Montanini B, Morin E, Noel B,  
587 Percudani R, Porcel B, Rubini A, Amicucci A, Amselem J, Anthouard V, Arcioni S, Artiguenave F,  
588 Aury JM, Ballario P, Bolchi A, Brenna A, Brun A, Buée M, Cantarel B, Chevalier G, Couloux A,  
589 Da Silva C, Denoeud F, Duplessis S, Ghignone S, Hilselberger B, Iotti M, Marçais B, Mello A,  
590 Miranda M, Pacioni G, Quesneville H, Riccioni C, Ruotolo R, Splivallo R, Stocchi V, Tisserant E,  
591 Viscomi AR, Zambonelli A, Zampieri E, Henrissat B, Lebrun MH, Paolocci F, Bonfante P,  
592 Ottonello S, Wincker P (2010) Périgord black truffle genome uncovers evolutionary origins and  
593 mechanisms of symbiosis. *Nature* 464:1033-1038. doi: 10.1038/nature08867

594 Martino E, Turnau K, Girlanda M, Bonfante P, Perotto S (2000) Ericoid mycorrhizal fungi from  
595 heavy metal polluted soils: their identification and growth in the presence of zinc ions. *Mycol Res*  
596 104:338-344. doi:10.1017/S0953756299001252

597 Martino E, Murat C, Vallino M, Bena A, Perotto S, and Spanu P (2007) Imaging mycorrhizal  
598 fungal transformants that express EGFP during ericoid endosymbiosis *Curr Genet* 52:65-75. doi:  
599 10.1007/s00294-007-0139-9

600 Pawlowska TE, Taylor JW (2004) Organization of genetic variation in individuals of arbuscular  
601 mycorrhizal fungi. *Nature* 427:733-737. doi:10.1038/nature02290

602 Pérez-Tienda J., Balestrini R, Fiorilli V, Azcón-Aguilar C, Ferrol N (2011) GintAMT2, a new  
603 member of the ammonium transporter family in the arbuscular mycorrhizal fungus *Glomus*  
604 *intraradices*. Fungal Genet Biol 48:1044-1055.doi: 10.1016/j.fgb.2011.08.003

605 Pfeffer PE, Douds DD, Bécard G, Shachar-Hill Y (1999) Carbon uptake and the metabolism and  
606 transport of lipids in an arbuscular mycorrhiza. Plant Physiol 120:587-598. doi: [http://dx.doi.org/10.](http://dx.doi.org/10.1104/pp.120.2.587)  
607 1104/pp.120.2.587

608 Pumplin N, Harrison MJ (2009) Live-cell imaging reveals periarbuscular membrane domains and  
609 organelle location in *Medicago truncatula* roots during arbuscular mycorrhizal symbiosis. Plant  
610 Physiol 151:809-819. doi: 10.1104/pp.109.141879

611 Punt PJ, Oliver RP, Dingemanse MA, Pouwels PH, van den Hondel CA (1987) Transformation of  
612 *Aspergillus* based on the hygromycin B resistance marker from *Escherichia coli*. Gene 56:117-24

613 Redecker D, Schüssler A, Stockinger H, Stürmer SL, Morton JB, Walker C (2013) An evidence-  
614 based consensus for the classification of arbuscular mycorrhizal fungi (Glomeromycota)  
615 Mycorrhiza 23:515-531. doi: 10.1007/s00572-013-0486-y

616 Requena N, Mann P, Hampp R, Franken P (2002) Early developmentally regulated genes in the  
617 arbuscular mycorrhizal fungus *Glomus mosseae*: GmGIN1, a novel gene encoding a protein with  
618 homology to the C-terminus of metazoan hedgehog proteins. Plant Soil 244:129-139

619 Riley R, Salamov AA, Brown DW, Nagy LG, Floudas D, Held BW, Levasseur A, Lombard V,  
620 Morin E, Otiillar R, Lindquist EA, Sun H, LaButti KM, Schmutz J, Jabbour D, Luo H, Baker SE,  
621 Pisabarro AG, Walton JD, Blanchette RA, Henrissat B, Martin F, Cullen D, Hibbett DS, Grigoriev  
622 IV (2014) Extensive sampling of basidiomycete genomes demonstrates inadequacy of the white-  
623 rot/brown-rot paradigm for wood decay fungi. Proc Natl Acad Sci U S A 111:9923-9928. doi:  
624 10.1073/pnas.1400592111

625 Ruzicka D, Chamala S, Barrios-Masias FH, Martin F, Smith S, Jackson LE, Brad Barbazuk W,  
626 Schachtman DP (2013) Inside arbuscular mycorrhizal roots - Molecular probes to understand the  
627 symbiosis. *Plant genome* 6:1-13. doi:10.3835/plantgenome2012.06.0007

628 Salvioli A, Bonfante P (2013) Systems biology and "omics" tools: a cooperation for next-generation  
629 mycorrhizal studies. *Plant Sci* 204:107-114. doi: 10.1016/j.plantsci.2013.01.001

630 Salvioli A, Ghignone S, Novero M, Navazio L, Venice F, Bagnaresi P, Bonfante P (2016)  
631 Symbiosis with an endobacterium increases the fitness of a mycorrhizal fungus, raising its  
632 bioenergetic potential. *ISME J* 10:130-144. doi: 10.1038/ismej201591

633 Sambrook J, Russel DW (2001) *Molecular Cloning: A Laboratory Manual, Volume 1, 2, 3* Cold  
634 Spring Harbour Laboratory Press, Cold Spring Harbour, New York.

635 Schüßler A, Schwarzott D, Walker C (2001). A new fungal phylum, the Glomeromycota:  
636 phylogeny and evolution. *Mycol Res* 105: 1413-1421.

637 Spanu PD, Abbott JC, Amselem J, Burgis TA, Soanes DM, Stüber K, Ver Loren van, Themaat E,  
638 Brown JK, Butcher S A, Gurr SJ, Lebrun MH, Ridout CJ, Schulze-Lefert P, Talbot NJ,  
639 Ahmadinejad N, Ametz C, Barton GR, Benjdia M, Bidzinski P, Bindschedler LV, Both M, Brewer  
640 MT, Cadle-Davidson L, Cadle-Davidson MM, Collemare J, Cramer R, Frenkel O, Godfrey D,  
641 Harriman J, Hoede C, King BC, Klages S, Kleemann J, Knoll D, Koti PS, Kreplak J, López-Ruiz  
642 FJ, Lu X, Maekawa T, Mahanil S, Micali C, Milgroom MG, Montana G, Noir S, O'Connell RJ,  
643 Oberhaensli S, Parlange F, Pedersen C, Quesneville H, Reinhardt R, Rott M, Sacristán S, Schmidt  
644 SM, Schön M, Skamnioti P, Sommer H, Stephens A, Takahara H, Thordal-Christensen H,  
645 Vigouroux M, Wessling R, Wicker T, Panstruga R (2010) Genome expansion and gene loss in  
646 powdery mildew fungi reveal tradeoffs in extreme parasitism. *Science* 330:1543-1546. doi:  
647 10.1126/science.1194573.

648 Tamayo E, Gómez-Gallego T, Azcón-Aguilar C, Ferrol N (2014) Genome-wide analysis of copper,  
649 iron and zinc transporters in the arbuscular mycorrhizal fungus *Rhizophagus irregularis*. *Front Plant*  
650 *Sci* 14;5:547. <http://dx.doi.org/10.3389/fpls.2014.00547>

651 Tisserant E, Kohler A, Dozolme-Seddas P, Balestrini R, Benabdellah K, Colard A, Croll D, Da  
652 Silva C, Gomez S K, Koul R, Ferrol N, Fiorilli V, Formey D, Franken P, Helber N, Hijri M,  
653 Lanfranco L, Lindquist E, Liu Y, Malbreil M, Morin E, Poulain J, Shapiro H, van Tuinen D,  
654 Waschke A, Azcón-Aguilar C, Bécard G, Bonfante P, Harrison MJ, Küster H, Lammers P,  
655 Paszkowski U, Requena N, Rensing SA, Roux C, Sanders IR, Shachar-Hill Y, Tuskan G, Young JP,  
656 Gianinazzi-Pearson V, Martin F (2012) The transcriptome of the arbuscular mycorrhizal fungus  
657 *Glomus intraradices* (DAOM 197198) reveals functional tradeoffs in an obligate symbiont. *New*  
658 *Phytol* 193:755-769. doi: 10.1111/j.1469-8137.2011.03948.x

659 Tisserant E, Malbreil M, Kuo A, Kohler A, Symeonidi A, Balestrini R, Charron P, Duensing N,  
660 Frei dit Frey N, Gianinazzi-Pearson V, Gilbert LB, Handa Y, Herr JR, Hijri M, Koul R, Kawaguchi,  
661 M Krajinski, F Lammers PJ, Masclaux FG, Murat C, Morin E, Ndikumana S, Pagni M, Petitpierre  
662 D, Requena N, Rosikiewicz P, Riley R, Saito K, San Clemente H, Shapiro H, van Tuinen D, Bécard  
663 G, Bonfante P, Paszkowski U, Shachar-Hill YY, Tuskan GA, Young JP, Sanders IR, Henrissat B,  
664 Rensing SA, Grigoriev IV, Corradi N, Roux C, Martin F (2013) Genome of an arbuscular  
665 mycorrhizal fungus provides insight into the oldest plant symbiosis. *Proc Natl Acad Sci U S A*  
666 110:20117-20122. doi: 10.1073/pnas.1313452110

667 Tollot M, Wong Sak Hoi J, van Tuinen D, Arnould C, Chatagnier O, Dumas B, Gianinazzi-Pearson  
668 V, Seddas PM (2009) An STE12 gene identified in the mycorrhizal fungus *Glomus intraradices*  
669 restores infectivity of a hemibiotrophic plant pathogen. *New Phytol* 181:693-707. doi:  
670 10.1111/j.1469-8137.2008.02696.x

671 Villarreal-Ruiz L, Anderson IC, Alexander IJ (2004) Interaction between an isolate from the  
672 *Hymenoscyphus ericae* aggregate and roots of *Pinus* and *Vaccinium*. *New Phytol* 164:183-192. doi:  
673 10.1111/j.1469-8137.2004.01167.x

674 Young JPW (2015) Genome diversity in arbuscular mycorrhizal fungi. *Curr Opin Plant Biol*  
675 23:113-119. doi: 10.1016/j.pbi.2015.06.005

676

677

678

679

680 **FIGURE LEGENDS**

681 **Figure 1** *RiPEIP1* is up-regulated in the intraradical mycelium. Expression of *RiPEIP1* (relative to  
682 *RiTef*) assessed by qRT-PCR in intraradical mycelium (IRM) and extraradical mycelium (ERM)  
683 from mycorrhizal roots of *M. truncatula* grown in the sandwich system (n= 5). Individual data for  
684 each condition are shown as dots and the median as black bars. Asterisks indicate a statistically  
685 significant difference ( $p < 0.001$ , ANOVA, Tukey's post-hoc test)

686 **Figure 2** Confocal imaging of *RiPEIP1::GFP* localization in yeast cells. The observed fluorescence  
687 pattern (a) is compatible with GFP localization in the endoplasmic reticulum and nuclear (n)  
688 envelope. A brightfield image of the same cells is shown in panel b. *RiPEIP1::GFP* localization is  
689 confirmed by a comparison with the fluorescence pattern from constitutively expressed *Sec13::RFP*  
690 (c), which labels the endoplasmic reticulum/nuclear envelope (n) and Golgi stacks, and *Cop1::GFP*  
691 (d), which targets the early Golgi stacks (arrowheads). Bars: 5  $\mu\text{m}$

692 **Figure 3** *RiPEIP1* gene expression along the AM colonization process. Relative expression of  
693 *MtPT4* (a) and *RiPEIP1* (b) assessed by qRT-PCR in a time course experiment of root colonization  
694 at 7, 14, 28 and 60 days post-inoculation (dpi). Single data for each condition are shown as dots and  
695 the median as black bars. Different letters indicate statistically significant difference ( $p < 0.05$ ,  
696 ANOVA, Tukey's post-hoc test). (c) Gel electrophoresis of RT-PCR products obtained from two  
697 independent samples of RNA from laser-microdissected arbuscule-containing cells (ARB) and one  
698 sample of not colonized cortical cells from mycorrhizal roots (MNM) using primers specific for  
699 *MtPT4*, *RiTef* or *RiPEIP1*. No RNA sample (-)

700 **Figure 4** *RiPEIP1* gene expression is affected in the *mtp4-2* mutant line. The AM colonization of  
701 wt and *mtp4-2* genotypes was evaluated through the assessment of fungal *RiTef* mRNA abundance  
702 (a); *MtBCP* expression was used as a marker of AM intraradical phase (b). The relative expression  
703 of *RiPEIP1* in wt and *mtp4-2* roots is shown in panel (c). Asterisks indicate a statistically  
704 significant difference (\*\* $p < 0.01$ , \*\*\*  $p < 0.001$ , ANOVA, Tukey's post-hoc test)

705 **Figure 5** Expression of *RiPEIP1* in *Oidiodendron maius* does not affect the growth of free-living  
706 mycelia. Gel electrophoresis of RT-PCR products obtained from wt and three *RiPEIP1*-expressing  
707 (BA2, BA4, BC6) free-living strains using *RiPEIP1* specific primers; - : negative control (a). Dry  
708 weight of free-living mycelia of wt and transgenic strains grown in liquid cultures (b)

709 **Figure 6** *RiPEIP1*-expressing strains led to a higher *Vaccinium myrtillus* root colonization level  
710 compared to the WT strain. (a) *In vitro* mycorrhization system between *V. myrtillus* seedlings and  
711 *O. maius*. Non inoculated *V. myrtillus* seedlings were unable to correctly develop (right panel) (b)  
712 The percentage of root colonization of *V. myrtillus* seedlings colonized with the *O. maius* wt or the  
713 three *RiPEIP1*-expressing strains was quantified after staining with acid fuchsin. Different letters  
714 indicate statistically significant difference ( $p < 0.05$ , ANOVA, Tukey's post-hoc test)

715 **Figure 7** Representative details of the *V. myrtillus* root system colonized by *O. maius* wt (a) or BC6  
716 *RiPEIP1*-expressing (b) strains after two months of inoculation. Note the stimulation of root  
717 branching in roots colonized by the *RiPEIP1*-expressing strain. Bar = 1 cm.

718

## 719 **Supplementary material**

720 **Figure S1** Nucleotide and deduced amino acid sequences of *RiPEIP1*. a) *RiPEIP1* genomic DNA  
721 sequence showing the presence of five introns. b) *RiPEIP1* protein sequence showing the 4  
722 transmembrane domains (underlined), the typical ER-retention/retrieval motifs (bold) and the  
723 predicted phosphorylation sites (red). See text for details

724 **Figure S2** Colonization level of *M. truncatula* roots at 28 and 60 days post inoculation (dpi)  
725 assessed accordingly to Trouvelot et al (1986). F%: frequency of mycorrhization in the root system  
726 (a), a%: arbuscules abundance in mycorrhizal parts of root fragments (b). Different letters indicate  
727 statistically significant difference ( $p < 0.05$  ANOVA, Tukey's post-hoc test)

728 **Figure S3** Mycorrhizal phenotype of *M. truncatula* wt (**a, b**) and *mtpt4-2* (**c, d**) roots colonized by  
729 *R. irregularis*. Roots were harvested 60 dpi, stained with acid fuchsin and observed with a confocal  
730 microscope. Arbuscules in *mtpt4-2* are degenerated as described in Javot et al. (2011). Bars = 25  
731  $\mu\text{m}$

732 **Figure S4** Molecular analyses of *O. maius* transgenic strains expressing *RiPEIP1*. (**a**) Gel  
733 electrophoresis of PCR products obtained from genomic DNA of wt and transgenic strains using  
734 *RiPEIP1* specific primers (**b**) Southern blot of genomic DNA from wt and transgenic strains  
735 restricted with *Bgl*III enzyme and hybridized with the *RiPEIP1* probe. Lanes corresponding to BC6,  
736 BA2, BA4 samples exhibited a single genomic insertion.

737 **Figure S5** Phenotype of *O. maius* free living mycelia from wt and *RiPEIP1*-expressing strain BA2  
738 as revealed by calcoflour white staining. Laser-scanning microscope observation of one-month-old  
739 *O. maius* wt and transgenic strains stained with calcofluor white. Transmitted light images are  
740 shown on the right (**b, d**) and the corresponding fluorescence images on the left (**a, c**). Bars: 10  $\mu\text{m}$

741 **Figure S6** Mycorrhizal phenotype of *O. maius* wt and *RiPEIP1*-expressing strain BC6.  
742 Mycorrhized *V. myrtillus* roots were stained with acid fuchsin and observed 2 months after fungal  
743 inoculation. *O. maius* transgenic strains showed an increased number of coils (asterisk) in epidermal  
744 cells compared to the wt.

745

746 **Table 1.** Average values and standard deviation of the number of lateral roots of the different  
 747 orders in plants colonized by the wt or the transgenic strains (BA2, BA4, BC6)

748

	Root orders	samples			
		BA2	BA4	BC6	WT
Lateral roots average values	1°	14 ± 7	14.6 ± 7.2	16 ± 10.3	9.6 ± 2
	2°	33.3 ± 25	39 ± 14.9	51.6 ± 38.4	17.3 ± 4
	3°	23 ± 24	31 ± 18.1	52 ± 28.7	10.3 ± 1.1
	4°	8.6 ± 9.8	15 ± 14	27 ± 18.5	2.3 ± 4
	5°	0.7 ± 1.1	6.3 ± 7	13.3 ± 8.7	0
	6°	0.3 ± 0.5	1.7 ± 1.5	2.3 ± 1.5	0

749

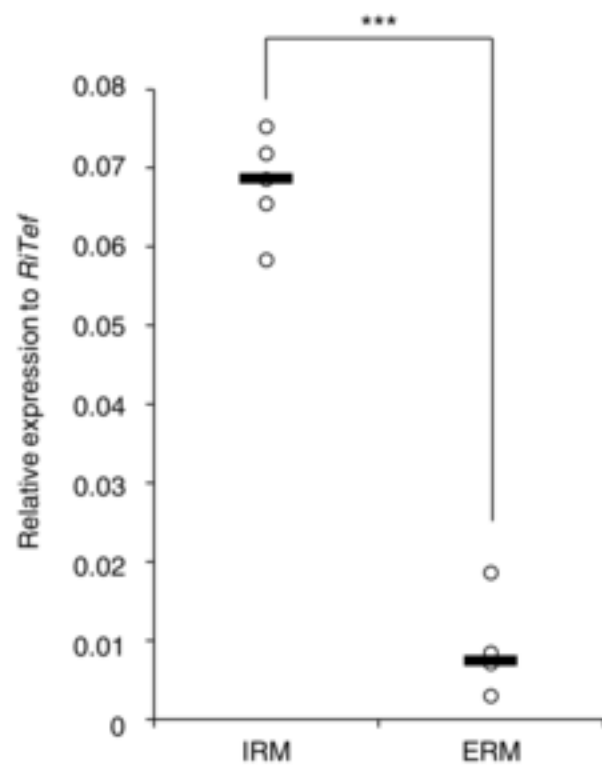
750

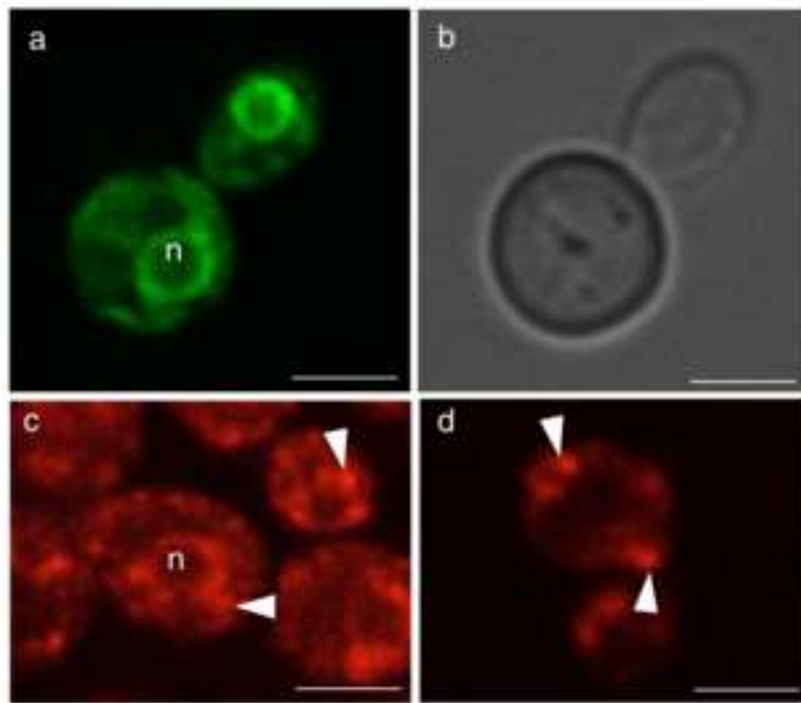
751 **Table S1.** List of primers used in this study. Sites for GATEWAY recombination or restriction  
 752 enzymes are underlined.

Primer ID	Primer sequences [5'-3']
RiEF $\alpha$ f	GCTATTTTGATCATTGCCGCC
RiEF $\alpha$ r	TCATTA <del>AAAACGTTCTTCCGACC</del>
MtTEFf	AAGCTAGGAGGTATTGACAAG
MtTEFr	ACTGTGCAGTAGTACTTGGTG
MtPT4 f	TCGCGCGCCATGTTTGTGT
MtPT4r	CGCAAGAAGAATGTTAGCCC
RiPEIP1-attB-forward	<u>GGGGACAAGTTTGTACAAAAAAGCAGGCT</u> ATGTCAGCTAAATTTATCAAGC
RiPEIP1-attB-reverse	<u>GGGGACCACTTTGTACAAGAAAGCTGGGT</u> CTTTAAACATTTTCATTAACA <del>CTC</del>
RiPEIP1fF:	ATGTCAGCTAAATTTATCAAGC
RiPEIP1fR:	CTTTAAACATTTTCATTAACA <del>CTC</del> TCG
RiPEIP1-N	<u>GTCAGCGGCCGC</u> CTTTAAACATTTTCATTAAC
RiPEIP1-K	<u>GATCGGTACC</u> ATGTCAGCTAAATTTATC
RiPEIP1-X	<u>GCATCCCGGG</u> CTTTAAACATTTTCATTAAC
RiPEIP1-race-forward	AGTAGAAGCACTAAAGGTGCCAAGAAAAGT
RiPEIP1-race-reverse	TAACACTCATCTCGGGACTGACTTCATTCT
RiPEIP1-qpcrF	AAGAAAGTAAACGTGTGGCT
RiPEIP1-qpcrR	TAACACTCATCTCGGGACTG
OmTubulin-forward	GTTTCCATGAAGGAGGTTGAGG
OmTubulin-reverse	CAGAGAGCAGTCTGGACGTTGT

753

754

**Figure 1**

**Figure 2**

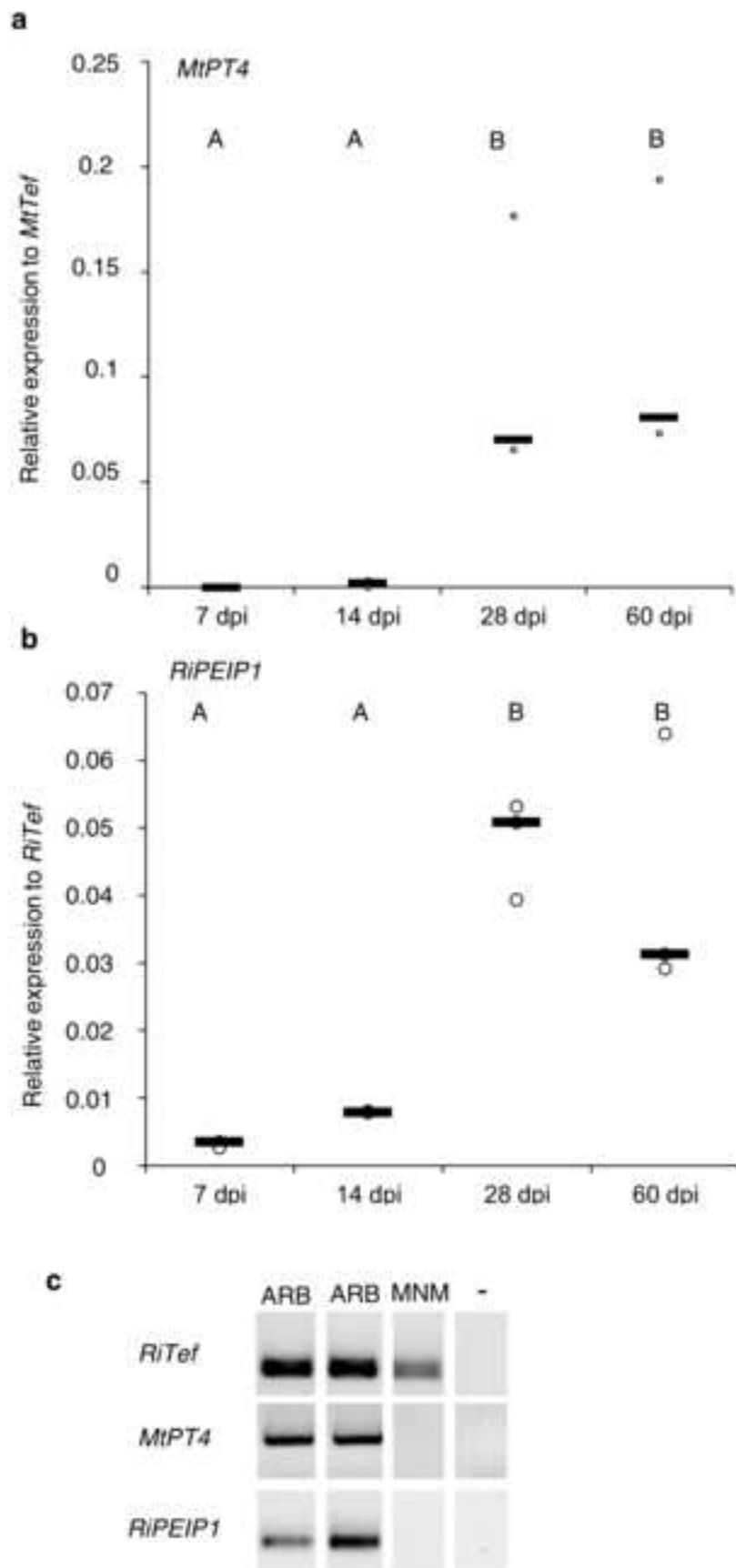


Figure 3

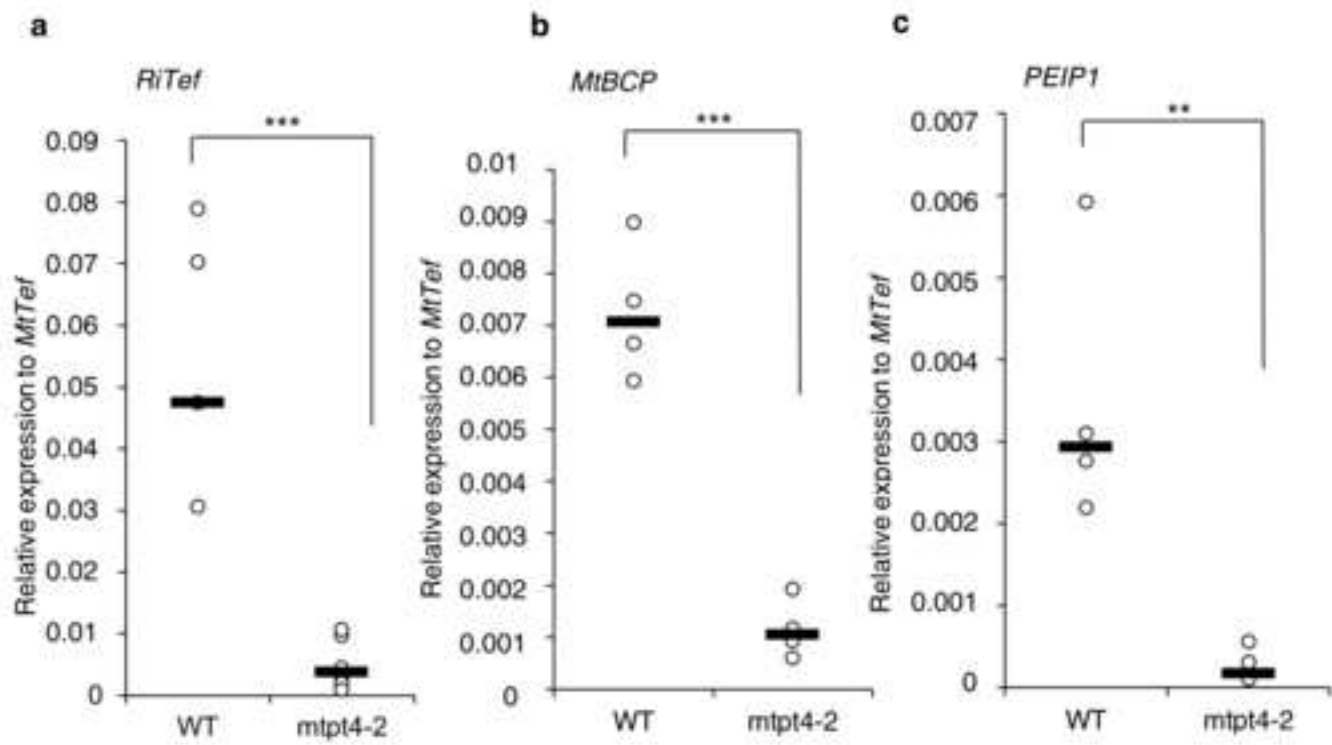
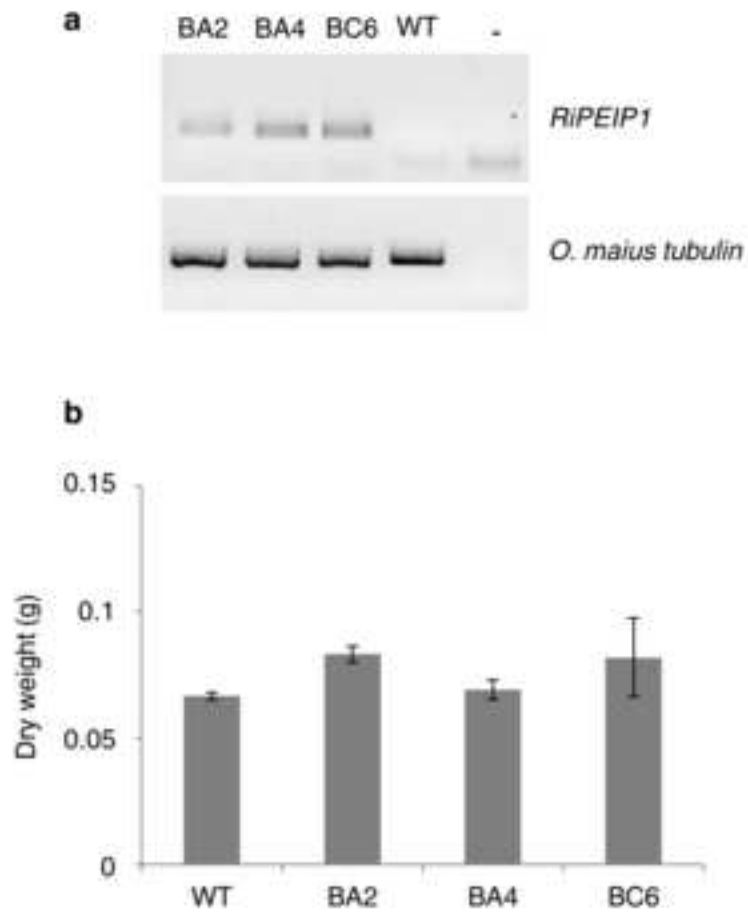
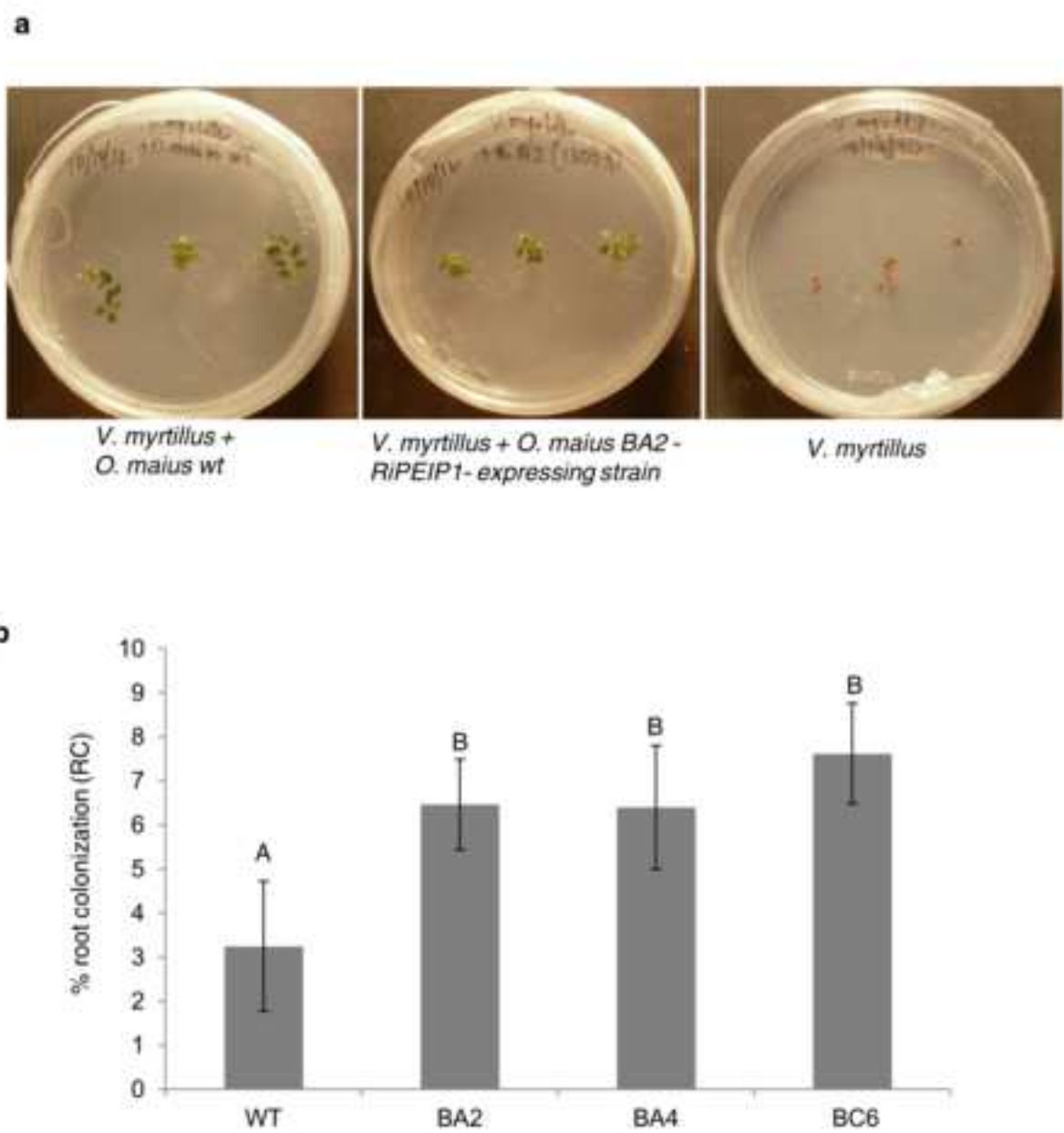
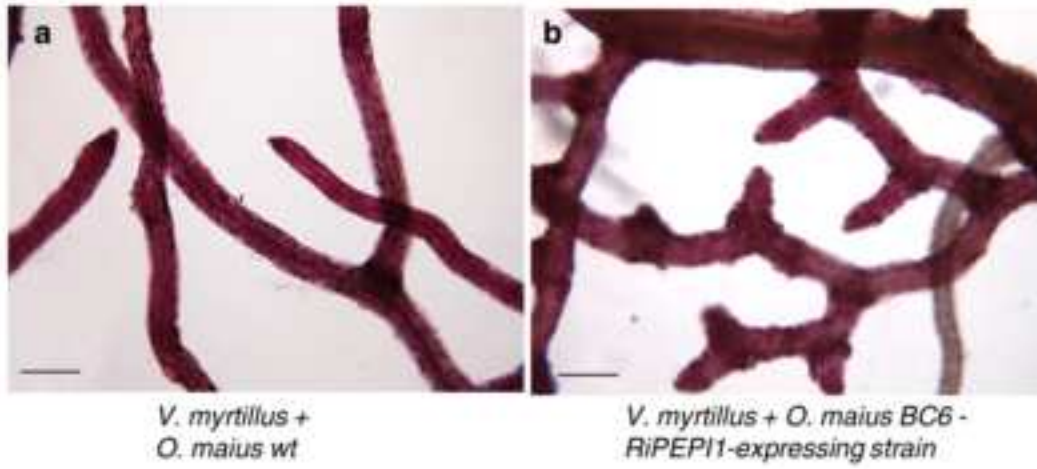


Figure 4

**Figure 5**

**Figure 6**

**Figure 7**

## A

```

A T N T C A G C T S A R A T T T S T C A R A G C A T T E N T T T T T S T N C A A A T T C T C A T C A T C A R T N G G A A T N T G T G S T A G T C G T E N T G A A T T A T S A R T T T C A R T 100
M S A K F I K H L F F I O I L I M I G I G I C E I
T C A R A T T T S A T A A A A T S T T A T T T T A T T E N T T T T T T T T S T S T S A T T E N T T C A T T T C C C G T T C T T T C T T T T C G T T C S T T C G T T C G T T C T T S A A G 200
R A T T T N G A G G T N G T N C A A T T G G C G G A A G T S A T S A G T C T C A C A A G A A G T S T T C A C A T C C G G A A G A T T G G G A C T A C T T S T T T S G T T A C A C A A A A G C A 300
V V Q L A E V N K S Q Q E V I Q H P E D W D Y L F G Y T K S I
T A G C G T S A T T T T T T T T T C G T T A R T C T T C C T T T T A T A A A G A A T T A A T A S T S A T T A T T T T T T T S T T T T S G T S C A A T T T T S T A A G A A T A T T 400
A T I F I R I Y Y
A T T G A T E N T E N T A C T T S T T T C G T T C G G A T T T T A G G T G G G C A A T T C T T T T T G A A T T T T T T T T T A A A A A A A A A A T T S A A A A T T S A A A A T T A S A A T 500
W I I I L V S F G I L G
G A T T A A A T S T S T S T S T S T S T S T S T T T T A T N G G A T G G G C C T T G G A T T C A T T T S A T S A A A G A T G A A A A A A T S T S A A A A T T A T S G T S A T A T C A A 600
W A L D S F N R R W K N I E N Y S D N S K
A A T T G T S T N C G T S T A T T T T T T T T T A A A A A A A A A A T T T A A C G T A A G A T C G A C T T E N T A T S G A T T A A A A A T S T T T T T T T T T T T T C G T S A A 700
H V T
C G T T C C T E N T A C T A T S G T S T T T T C A A G T A A G C C A G A T A T T T A T T T A T S T C A A T C G A A A T C T C A A T C T C G A A T C T C A T S T T T T T C A T T A 800
L L I L W C F A I
T T S A G T E N T A C C A A G T A T A C C A T T T T A C A A G A T C A A T A A T T G A A A C A T S T T C C A A T C A T C C T S T T C A T S C A C A G T G T A C C A A G A T T A T T A A 900
I P S V T I L A R S D K L R T C S E S S Y S Y T V S A R L L S
T C A T T A T A C G C A T T T T G C A T C T S T T C T T G C A T A T S T T A T T A S A C A G T S A T A T T C A A T S T S T T A T T T C G T T G T S A T T A A A C A T C A A 1000
K C H A Y L A S L I L A Y I I I I T V I I Q L L I H I V V I K K Q
A A A A A T S G T S T A A A C C A C C A A A T T T N C A A G A C C A A A A A A A T S A A G T S A A A A A G A T S A A C G T S T G C T S A A A A G A A A T S G T T A A G A T 1100
K E I S M K P P P N L Q E P K K I K V R R S K R V A K K R N S L R S
C G A T T T C T C T S T T C A A G T A C A A G A T A A G T A T T C A C C A A G A T A A A A A A A A A T A A A A A G T N G T N G A A G T N T T N G A A G T N G T N G A A G 1200
I S A Y S A S T R L S I V T E D D E I E K S H K S S R S I R S S R S
T A C T A A A G G T C C C A A G A A G T T A A G A A T G A A G T C A G T C C C G A G A T S A G T G T T A A T G A A A A T G T T T A
T K G A K K V K N I V S P I M S V N I N V *

```

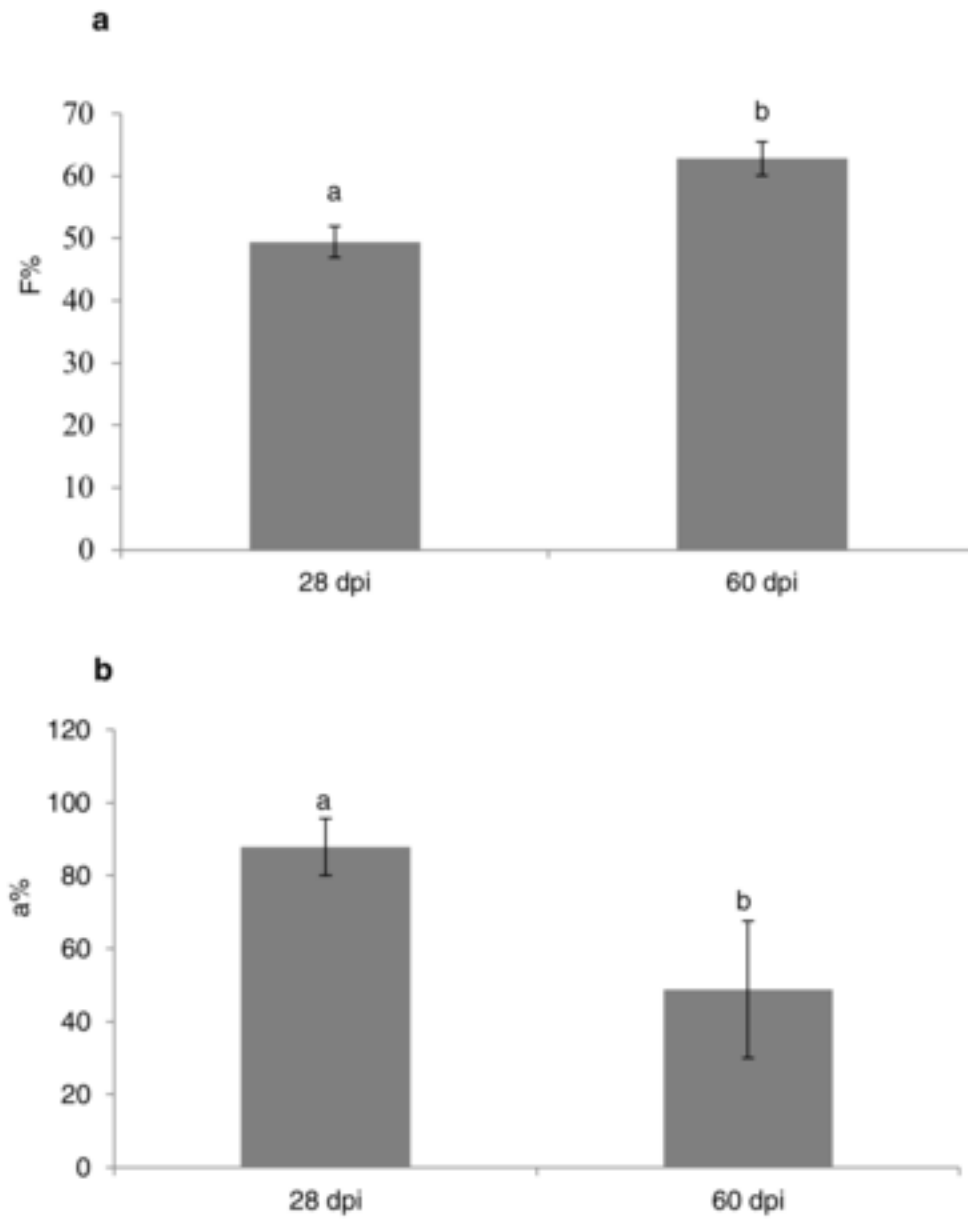
## B

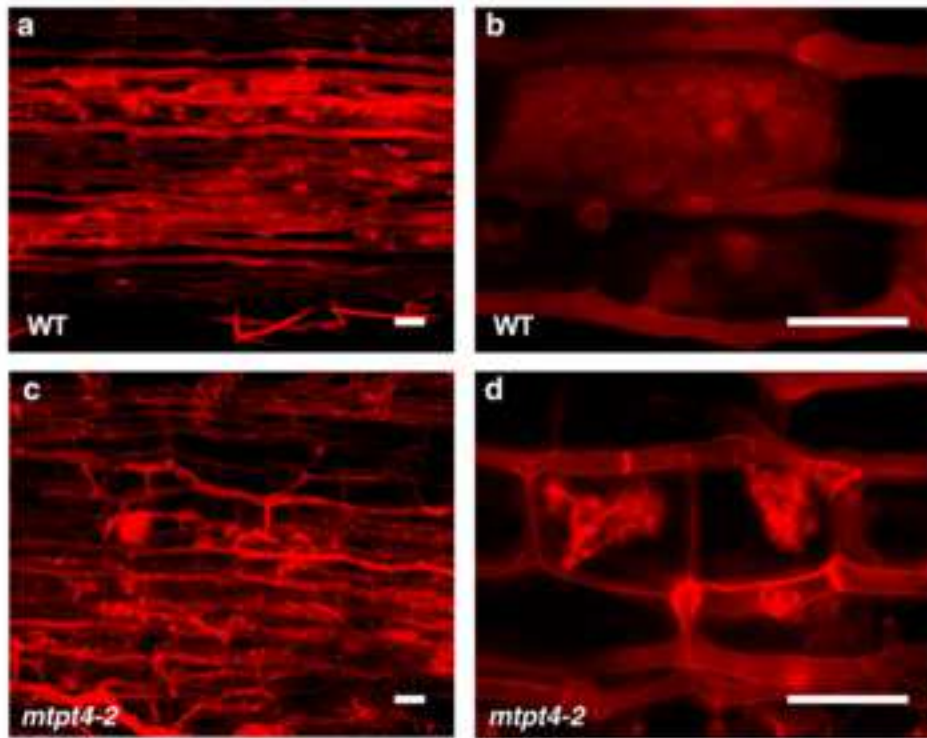
```

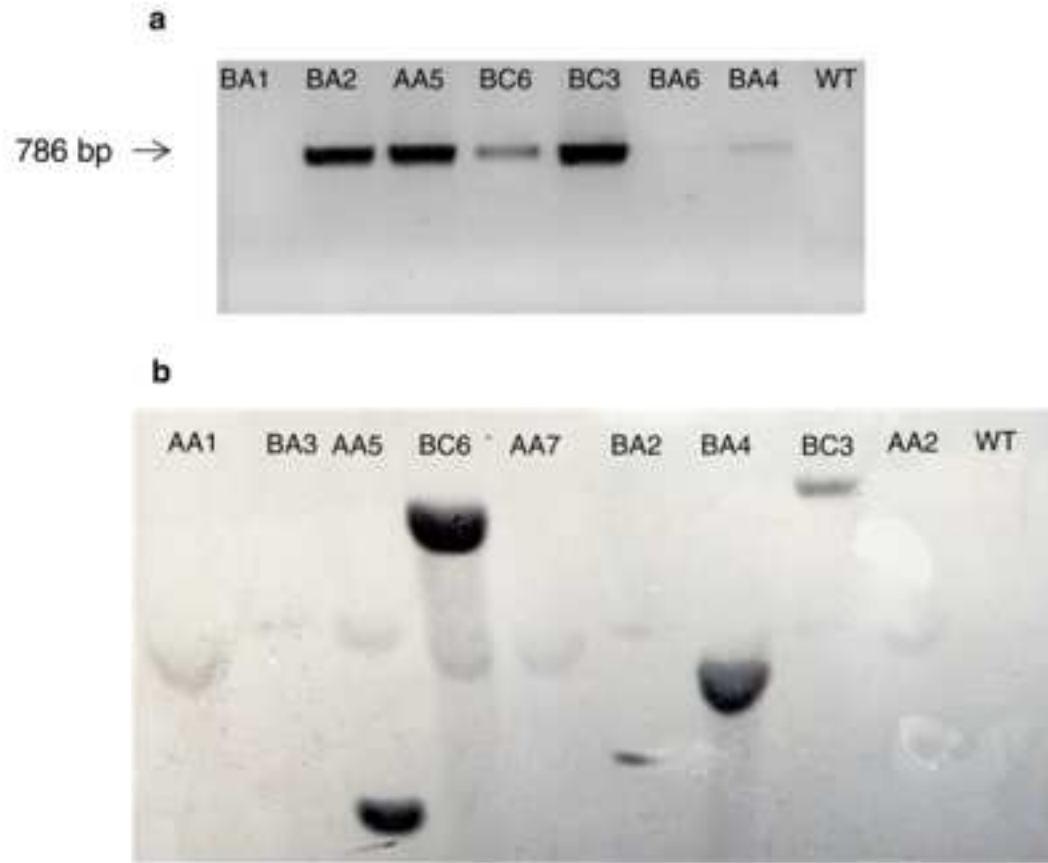
M S A K F I K H L F F I O I L I M I G I G I C E V
V Q L A E V N K S Q Q E V I Q H P E D W D Y L F G
Y T K S I A T I F I R I Y Y W I I I L V S F G I L
G W A L D S F N R R W K N I E N Y S D N S K N V T
L L I L W C F A I I P S V T I L A R S D K L R T C
S E S S Y S Y T V S A R L L S H C N A Y L A S L F
L A Y I F I I T V I I O L L F N F V V I K H Q K E
I S M K P P P N L Q E P K K I K V R R S K R V A K
K R N S L R S I S A Y S A S T R L S I V T E D D E
E K S N K S S R S I R S S R S T K G A K K V K N E
V S P E M S V N E N V

```

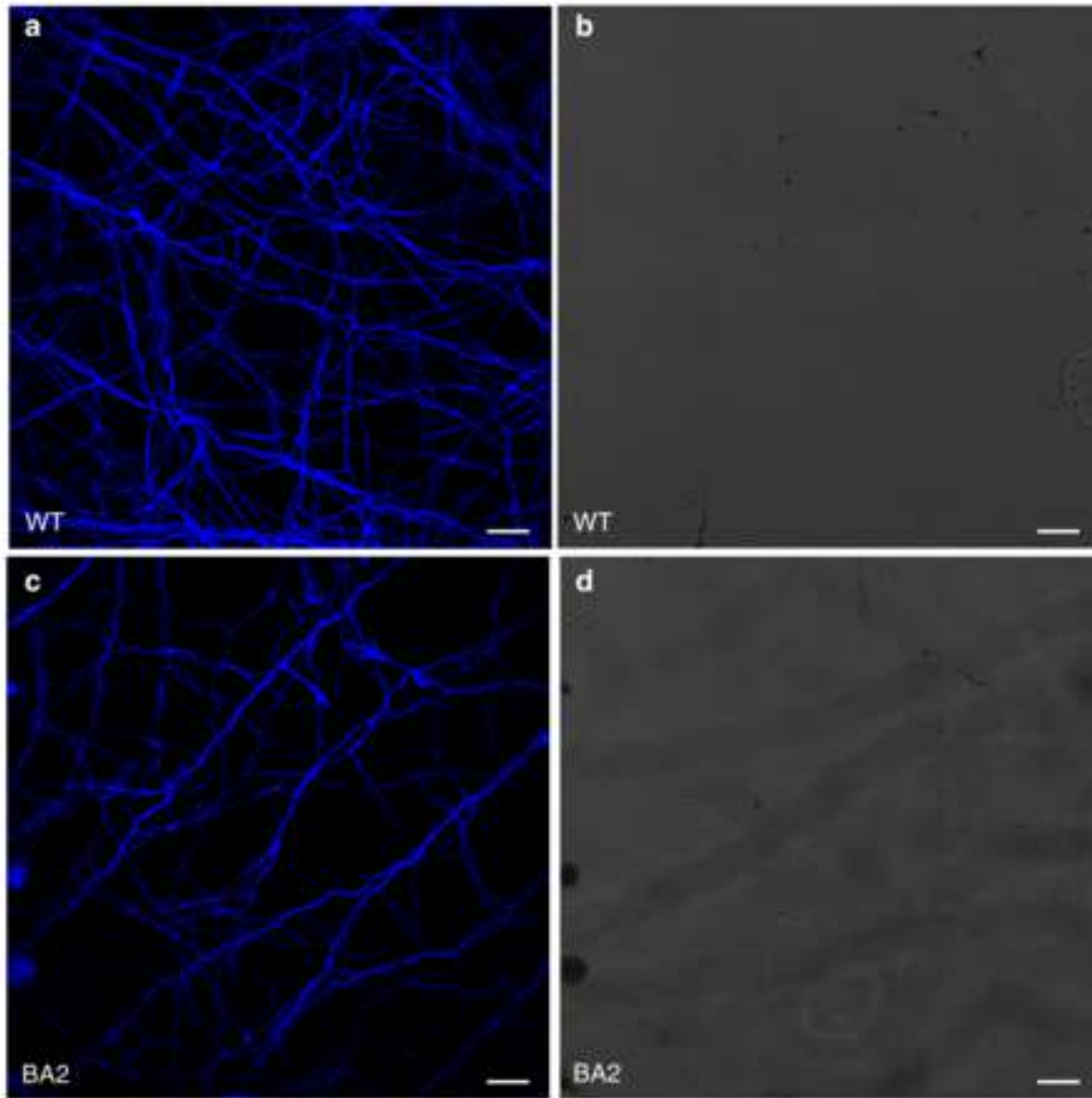
Figure S1

**Figure S2**

**Figure S3**



**Figure S4**

**Figure S5**

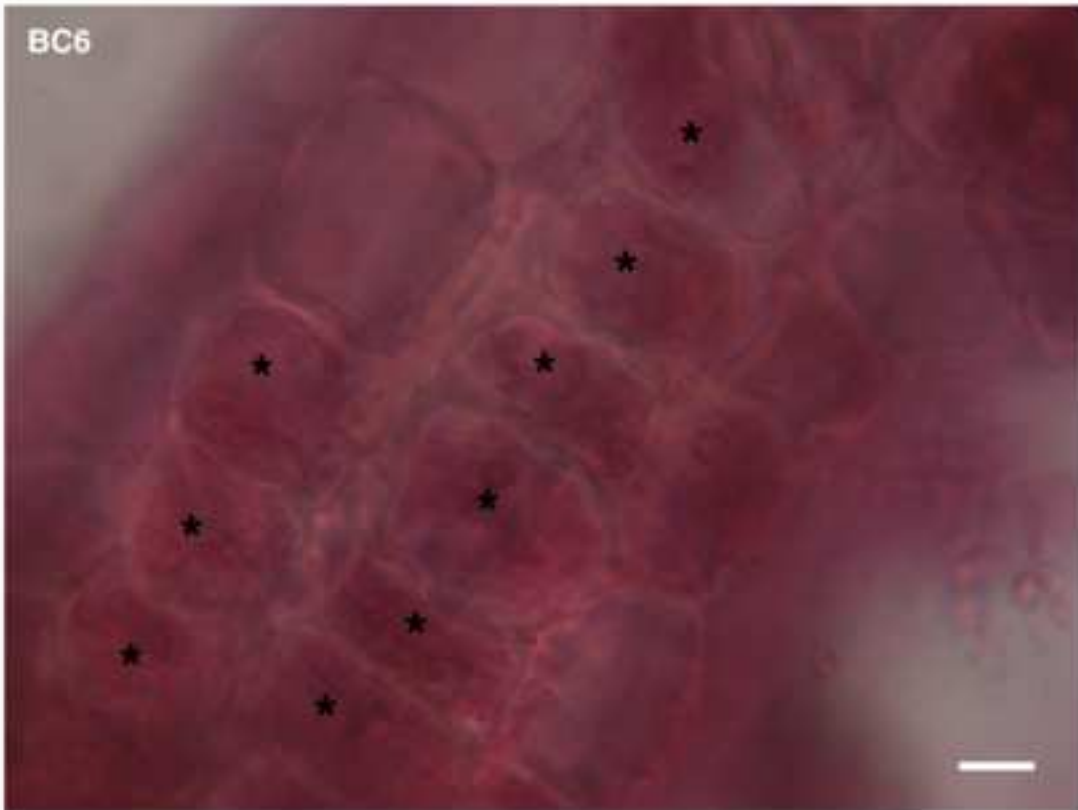
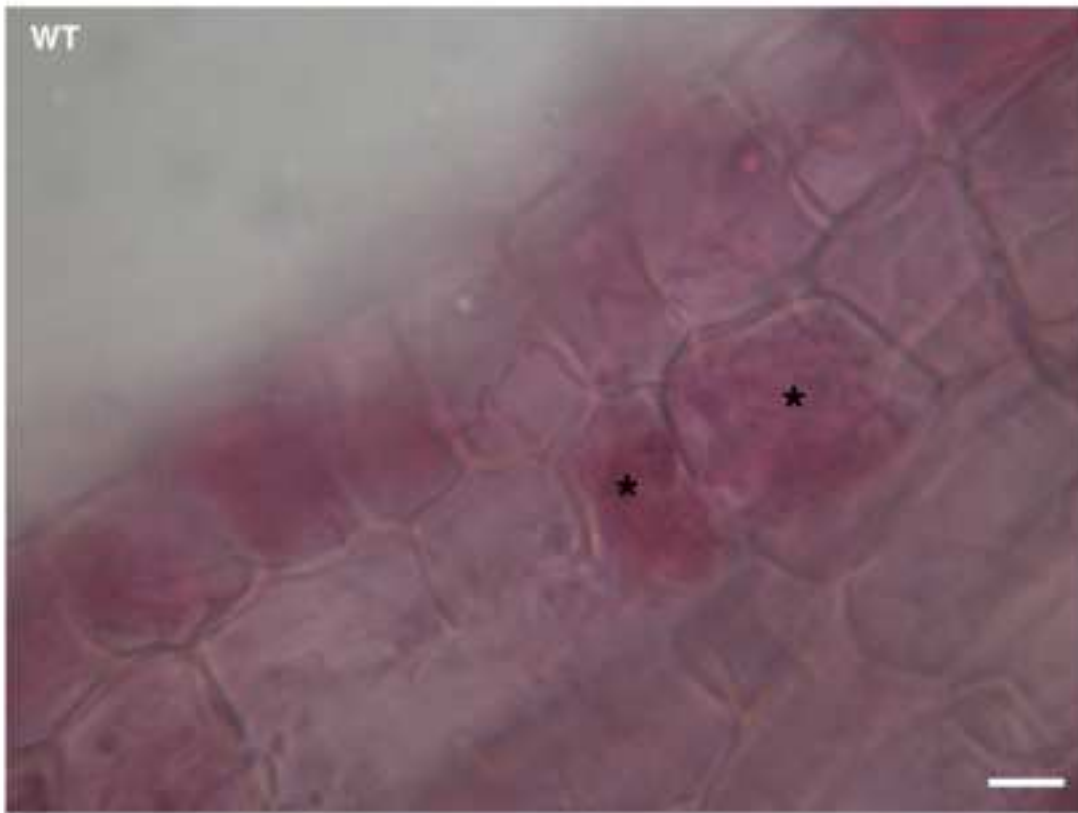


**Figure S6**

[Click here to view linked References](#)

1 ***RiPEIP1*, an orphan gene from the arbuscular mycorrhizal fungus *Rhizophagus irregularis*, is**  
2 **preferentially expressed *in planta* and may be involved in root colonization**

3

4 Valentina Fiorilli<sup>1</sup>, Simone Belmonto<sup>1</sup>, Hassine Radhouane Khouja<sup>1</sup>, Simona Abbà<sup>2</sup>, Antonella  
5 Faccio<sup>2</sup>, Stefania Daghino<sup>1</sup> and Luisa Lanfranco<sup>1</sup>

6

7 <sup>1</sup>Department of Life Science and Systems Biology, University of Torino, via Accademia Albertina  
8 13, 10123 Torino, Italy

9 <sup>2</sup>Institute for Sustainable Plant Protection (IPSP), CNR, Strada delle Cacce 73, 10135 Torino, Italy

10

11 Corresponding author: Valentina Fiorilli

12 e-mail: valentina.fiorilli@unito.it

13

14 **ABSTRACT**

15 Transcriptomics and genomics data recently obtained from the arbuscular mycorrhizal (AM) fungus  
16 *Rhizophagus irregularis* have offered new opportunities to decipher the contribution of the fungal  
17 partner to the establishment of the symbiotic association. The large number of genes identified as  
18 orphan, and often lineage-specific, witnesses the uniqueness of this group of plant-associated fungi.  
19 In this work we characterize an orphan gene that was called *RiPEIP1* (*Preferentially Expressed In*  
20 *Planta*). Its expression is strongly induced in the intraradical phase, including arbuscules, and  
21 follows the expression profile of the *Medicago truncatula* phosphate transporter *MtPT4*, a  
22 molecular marker of a functional symbiosis. Indeed, *mtpt4* mutant plants, which exhibit low  
23 mycorrhizal colonization and an accelerated arbuscule turnover, also show a reduced *RiPEIP1*  
24 mRNA abundance. To further characterize *RiPEIP1*, in the absence of genetic transformation  
25 protocols for AM fungi, we took advantage of two different fungal heterologous systems. When  
26 expressed as a GFP fusion in yeast cells, RiPEIP1 localizes in the endomembrane system, in

27 particular to the endoplasmic reticulum, which is consistent with the *in silico* prediction of four  
28 transmembrane domains. We then generated *RiPEIP1*-expressing strains of the fungus  
29 *Oidiodendron maius*, the only endomycorrhizal fungus for which transformation protocols are  
30 available. Roots of *Vaccinium myrtillus* colonized by *RiPEIP1*-expressing transgenic strains  
31 showed a higher mycorrhization level compared to roots colonized by the *O. maius* wild type strain,  
32 suggesting that *RiPEIP1* may regulate the root colonization process.

33

34 Keywords: Arbuscular Mycorrhizal Symbiosis, *Rhizophagus irregularis*, *Oidiodendron maius*,  
35 Heterologous expression system.

36

37

38

39

40

41

## 42 INTRODUCTION

43 The arbuscular mycorrhiza (AM), one of the most widespread symbiosis on earth, occurs between  
44 about 80% of land plants and soil fungi belonging to the ancient *Glomeromycota* Phylum  
45 (Redecker et al. 2013). This intimate mutualistic association allows the host plant to gain mineral  
46 nutrients and water from the soil *via* the activity of the large network of extraradical mycelium  
47 (Javot et al. 2007; Govindarajulu et al. 2005; Allen and Shachar-Hill 2009) while, in turn, the  
48 fungus acquires plant photoassimilates (up to 20%) that are essential to progress into the different  
49 developmental stages (Pfeffer et al. 1999). AM fungi are important members of the plant  
50 microbiome and provide important ecosystem services; they are therefore of great interest for the  
51 development of a sustainable and low-input agriculture (Gianinazzi et al. 2010).

52 The root colonization process comprises three main stages: i) a presymbiotic phase where the  
53 partners recognize each other through the exchanges of chemical compounds (Bonfante and  
54 Requena 2011; Bonfante and Genre 2015); ii) the root penetration where, after the formation of a  
55 hyphopodium on the root surface, the epidermal cell develops the pre-penetration apparatus to guide  
56 the entrance/accommodation of the fungal hypha (Genre et al. 2005, 2008); iii) the intraradical  
57 fungal growth, which culminates with the development of highly branched intracellular structures,  
58 the arbuscules, where nutrient exchanges between the two partners are thought to occur (Gutjahr  
59 and Parniske 2013). Arbuscule developmental dynamics was elegantly described by live cell  
60 imaging in rice roots: arbuscules were confirmed to be ephemeral structures with a lifetime at  
61 maturity of approximately two to three days (Kobae and Hata 2010).

62 AM fungi display many unusual biological features beside the obligate biotrophism, spores and  
63 hyphae contain multiple nuclei, making classic genetic approaches challenging (Lanfranco and  
64 Young 2012; Young 2015). No sexual cycle has ever been described although meiosis-related genes  
65 were found in the genome (Tisserant et al. 2013; Riley et al. 2014). Moreover, their genomic  
66 structure was for long time obscure, and it has been questioned whether nuclei were in a  
67 heterokaryotic (Hijri and Sanders 2005; Ehinger et al. 2012) or in a homokaryotic condition

68 (Pawlowska and Taylor 2004). Recent data from the genome sequence of the model AM fungus  
69 *Rhizophagus irregularis* (isolate DAOM 197198; Tisserant et al. 2013), also at the level of a single  
70 fungal nucleus (Lin et al. 2014), strongly support the homokaryotic status.

71 Several transcriptomic studies, mainly based on large-scale gene expression analysis, have been  
72 applied in the last decade to decipher the molecular mechanisms that accompany the formation of  
73 arbuscular mycorrhizas. They focused almost exclusively on the host plant (Salvioli and Bonfante  
74 2013 and references within), whereas only a few studies addressed the fungal partner (Requena et  
75 al. 2002; Breuninger and Requena 2004; Cappellazzo et al. 2007; Kikuchi et al. 2014; Salvioli et al.  
76 2016). A major advance has been obtained with transcriptomics and genomics data of *R. irregularis*  
77 (Tisserant et al. 2012; 2013; Ruzicka et al. 2013; Lin et al. 2014). The genome of *R. irregularis* is  
78 one of the largest (153 Mb) fungal genome sequenced to date, along with those of obligate  
79 biotrophic powdery mildews (Spanu et al. 2010) and the ectomycorrhizal symbiont *Tuber*  
80 *melanosporum* (Martin et al. 2010). The obligate biotrophy of AM fungi is not explained by  
81 genome erosion or any related loss of metabolic complexity in central metabolism. One striking  
82 genomic feature is the lack of genes encoding plant cell wall degrading enzymes in analogy to other  
83 obligate biotrophic pathogens (Spanu et al. 2010) and ectomycorrhizal symbionts (Martin et al.  
84 2010).

85 Tisserant et al. (2012) provided the first genome-wide overview of the transcriptional changes that  
86 occur in the different fungal life stages. In particular, the abundance of c. 18,500 fungal non-  
87 redundant expressed transcripts was analyzed in spores, extra- and intraradical mycelium, and  
88 arbuscules. Interestingly, several transcripts coding for Small Secreted Proteins (SSPs) were  
89 identified as being induced in the intraradical mycelium (IRM) and in arbuscule-containing cells  
90 (ARB), as compared to the extraradical mycelium (ERM). This SSPs list included the recently  
91 described secreted effector protein SP7, which is the first gene described so far to play a crucial role  
92 in the accommodation of the fungus within the plant root. In particular, SP7 counteracts the plant

93 immune response by interacting with the pathogenesis-related transcription factor Ethylene  
94 Response Factor (*ERF19*) in the host nucleus (Kloppholz et al. 2011).

95 This transcriptomic dataset has been instrumental for the characterization of several fungal genes  
96 (Li et al. 2013; Belmondo et al. 2014; Tamayo et al. 2014), providing new insights into the genetic  
97 program activated during the AM symbiosis and into the genetic characteristics, similarities and  
98 uniqueness of AM organisms. Taking advantage of laser microdissection, we identified four genes  
99 which were preferentially expressed in the intraradical phase, including arbuscules: three were  
100 orphan genes and one showed similarities with ABC transporters (Tisserant et al. 2012).

101 In this study, we characterize one of these orphan genes, that we called *RiPEIP1* (*Preferentially*  
102 *Expressed In Planta*) because its expression was strongly induced in the intraradical phase. Since  
103 stable transformation protocols are not available for AM fungi (Helber and Requena 2008; Helber et  
104 al., 2011), to characterize *RiPEIP1* we used two heterologous expression systems: *Saccharomyces*  
105 *cerevisiae*, a classical fungal model system and, for the first time, *Oidodendron maius*, the only  
106 endomycorrhizal fungus for which a stable transformation protocol is available (Martino et al.  
107 2007).

108

## 109 **RESULTS**

### 110 ***RiPEIP1* gene isolation**

111 With the aim to identify fungal genes involved in the functioning of arbuscules, the key structures  
112 of the AM symbiosis, we exploited transcriptomics data (Tisserant et al. 2012) generated for the  
113 AM fungus *Rhizophagus irregularis*. We focused our attention on an EST (contig Glomus\_c13083  
114 - v1 assembly) that turned out to be up-regulated in the intraradical phase in microarray experiments  
115 (Tisserant et al. 2012). In order to confirm the microarray data, the expression profile of  
116 Glomus\_c13083 was monitored in intraradical (IRM) and extraradical (ERM) mycelium by  
117 quantitative RT-PCR (qRT-PCR). In particular, RNAs were extracted from ERM and from *M.*  
118 *truncatula* roots fragments from which ERM was carefully removed to generate the IRM sample.

119 *Glomus\_c13083* transcripts were highly abundant in the IRM compared to ERM (Fig. 1), and they  
120 were barely detected in spores (data not shown). From this expression profile, we called this gene  
121 *RiPEIP1* for *Preferentially Expressed In Planta*.

122 The 786 bp full length cDNA sequence of *RiPEIP1* was obtained by RACE assays. The  
123 corresponding genomic sequence (1267 bp), which comprises five introns (Supplementary Fig.  
124 S1A), was also obtained by conventional PCR. The recent release of the complete genome sequence  
125 of *R. irregularis* (Lin et al. 2014) confirmed the presence of this gene in the genome assembly  
126 (RirG\_002110 - GenBank EXX79805.1), although the sequence was annotated with four additional  
127 amino acids at the N-terminus. Considering that the coding sequence isolated through several  
128 independent 5'-RACE-PCR assays never reported the presence of these four amino acids we  
129 considered the shorter cDNA sequence for the further analysis.

130 The predicted protein sequence (261 amino acids) showed no significant similarity (all E-values >  
131 0.2) with proteins deposited in the NCBI "nr" database. The only hit found by a BlastP analysis,  
132 spanning more than 50% of the sequence length, was another *R. irregularis* protein with unknown  
133 function (GenBank ESA21063.1, percentage of identity 22%; E-value 0.38). The second round of a  
134 Psi-Blast analysis, including this protein, identified three additional *R. irregularis* proteins  
135 (GenBank EXX76561.1, ESA00383.1, EXX59269.1) of unknown function slightly shorter (less  
136 than 200 amino acids) than *RiPEIP1*. Interestingly, a TblastN search within an extensive EST  
137 dataset recently published for another AM fungus, *Gigaspora margarita* (Salvioli et al. 2016), led  
138 to the identification of a cDNA sequence (GenBank: GBYF01016486.1; percentage of identity  
139 26%; E-value 0.036) coding for a 182 amino acids polypeptide, which is probably a partial  
140 sequence lacking the C-terminus.

141 TMHMM analysis of the *RiPEIP1* amino acid sequence revealed the presence of four  
142 transmembrane-helix domains with cytoplasmic N- and C-terminus regions (Supplementary Fig.  
143 S1B). Additionally, the WoLFPSORT subcellular location predictor identified *RiPEIP1* as a

144 putative integral membrane protein. Remarkably, the sequence from *G. margarita*, notwithstanding  
145 the rather low similarity percentage, presents the same four transmembrane domains topology.  
146 The C-terminus region, just after the fourth transmembrane domain, is highly hydrophilic, with a  
147 high percentage of charged (lysine, arginine, aspartate and glutamate) and polar (especially serines)  
148 amino acids. Some serines were also predicted (score > 0.99) by the NetPhos 2.0 Server to be  
149 potentially phosphorylated (Supplementary Fig. S1B). Notably, this region contains three typical  
150 ER-retention/retrieval C-terminus motifs: two KKXX motifs (starting from amino acid 188 and  
151 amino acid 200) and one KKKXX motif (starting from amino acid 246) (Jackson et al. 1990;  
152 Supplementary Fig. S1B).

153

#### 154 **RiPEIP1 is localized in the endomembrane system**

155 In order to investigate the sub-cellular localization of RiPEIP1, we expressed a RiPEIP1::GFP  
156 fusion construct in *Saccharomyces cerevisiae* yeast cells. The fluorescent signal was observed  
157 outlining the nucleus and extending into a network-like pattern in the cytoplasm (Fig. 2A). To better  
158 characterize this protein localization, we compared the RiPEIP1::GFP fluorescence pattern with that  
159 of two strains constitutively expressing the red fluorescent protein (RFP) fused to Sec13, which is a  
160 marker of the endoplasmic reticulum and Golgi stacks, or Cop1 which is localized in the early  
161 Golgi. Indeed, Sec13::RFP showed a very similar pattern to RiPEIP1::GFP, with the addition of  
162 several bright spots in the cytoplasm (Fig. 2C). Since analogous spots were observed in the  
163 Cop1::RFP line (Fig. 2D), we concluded that the RiPEIP1::GFP fluorescence pattern was  
164 compatible with protein localization in the endoplasmic reticulum and nuclear envelope. These  
165 results are in line with *in silico* predictions.

166

#### 167 ***RiPEIP1* expression profiles**

168 To monitor the dynamics of *RiPEIP1* expression pattern along the colonization process, we set up a  
169 time course experiment of *M. truncatula* plants inoculated with *R. irregularis* in the sandwich

170 system and sampled 7, 14, 28 and 60 days post-inoculation (dpi). Morphological analyses of roots  
171 revealed almost no intraradical fungal structures at 7 or 14 dpi. Mycorrhization frequency increased  
172 from 28 to 60 dpi, although arbuscules, detected starting from 28 dpi, decreased at 60 dpi  
173 (Supplementary Fig. S2). Since *RiPEIP1* was shown by qRT-PCR to be expressed at negligible  
174 levels in the ERM, gene expression was evaluated in whole mycorrhizal roots, without a distinction  
175 between IRM and ERM. *RiPEIP1* mRNA abundance increased in parallel to the development of the  
176 intraradical phase, and in particular to arbuscules formation, as demonstrated by morphological data  
177 and by the parallel mRNA accumulation of *MtPT4*, the *M. truncatula* phosphate transporter-  
178 encoding gene which is considered a molecular marker of arbuscule-containing cells (Harrison et al.  
179 2002; Fig. 3 A,B).

180 Using the laser microdissection, we investigated in more detail the *RiPEIP1* expression profile  
181 during the intraradical phase by comparing gene expression in arbusculated cells (ARB) and in non-  
182 colonized cortical cells from mycorrhizal roots (MNM). We used primers to the fungal  
183 housekeeping gene *RiTEFa* to monitor the presence of fungal structures in the two cell types, and  
184 primers to *MtPT4* to confirm the presence of arbuscules (Fig. 3C). Since the transcript for the fungal  
185 housekeeping gene *RiTEFa*, but not *MtPT4*, was also detected in the MNM cell population, we  
186 considered this sample representative of intercellular hyphae. As witnessed by the detection of  
187 *MtPT4* mRNA, *RiPEIP1* was only expressed in the ARB cell population, indicating that, in the  
188 intraradical phase, *RiPEIP1* expression occurred mainly in arbuscules and presumably not in  
189 intercellular hyphae (Fig. 3C).

190 To gather information on the relationship between *RiPEIP1* expression and arbuscule functionality,  
191 we analysed *RiPEIP1* expression profile in the *M. truncatula* *mpt4-2* mutant line, which is  
192 defective of MtPT4. Inactivation of MtPT4 causes low mycorrhizal colonization and an increased  
193 number of stunted arbuscules as a result of accelerated arbuscules turnover (Javot et al. 2011; Fig  
194 S3). As expected, a lower colonization level, based on relative abundance of fungal to plant *Tef*  
195 transcripts, was observed for *mpt4-2* compared to wt plants (Fig. 4A). To have an overview of

196 arbuscule abundance in the wt and *mtpt4-2* plants, we checked the expression level of the blue  
197 copper-binding protein1 (*MtBCP1*), a protein localized in the plasma membrane of cortical cells  
198 before and during the growth arbuscules and in the periarbuscular membrane surrounding arbuscule  
199 trunks (Pumplin and Harrison 2009). *mtpt4-2* mycorrhizal plants showed a lower level of *MtBCP1*  
200 transcripts compared to wt plants (Fig. 4B). Similarly, *RiPEIP1* mRNA abundance was lower in the  
201 *mtpt4-2* genotype (Fig. 4C). *MtBCP1* and *RiPEIP1* expression levels showed a positive correlation  
202 in wt and *mtpt4-2* genotypes (Fig. 4D). These data clearly indicate that *RiPEIP1* expression is  
203 therefore associated to arbuscule development.

204

#### 205 **Heterologous expression of *RiPEIP1* in *Oidiodendron maius***

206 To gain further information on *RiPEIP1* function a novel fungal heterologous expression system has  
207 been exploited. In particular, we expressed *RiPEIP1* in the ericoid mycorrhizal fungus  
208 *Oidiodendron maius*, the only endomycorrhizal fungus for which a protocol of genetic  
209 transformation is available (Martino et al. 2007). By means of *A. tumefaciens*-mediated genetic  
210 transformation, transgenic *O. maius* strains expressing *RiPEIP1* under a constitutive promoter were  
211 obtained. We confirmed the presence of *RiPEIP1* in *O. maius* genome by PCR and Southern blot  
212 analyses (Supplementary Fig. S4). Three transformants (BA2, BA4 and BC6) with a single genomic  
213 insertion were selected for further analyses (Supplementary Fig. S4).

214 *RiPEIP1* expression in free-living mycelia of *O. maius* transformants was confirmed by RT-PCR  
215 assays (Fig. 5A). As shown in Fig 5B the growth rate of *RiPEIP1*-expressing mycelia was similar to  
216 that of the wt strain. A phenotypic analysis carried out on free-living mycelia stained with  
217 calcoflour white showed no difference in hyphal morphology (Supplementary Fig. S5).

218 To investigate the impact of *RiPEIP1* expression on the establishment of the mycorrhizal symbiosis,  
219 seedlings of *Vaccinium myrtillus*, a common host plant for ericoid fungi, were colonized *in vitro*  
220 with wt or *RiPEIP1*-expressing strains. Plates with *V. myrtillus* seedlings without fungal inoculation  
221 were also set up. As expected, after 2 months uninoculated seedlings were dead (Fig. 6A). Root

222 colonization level of inoculated plants was analysed through the morphological evaluation of the  
223 numbers of coils/root intersections. Interestingly, roots colonized by *O. maius RiPEIP1*-expressing  
224 strains showed a statistically significant higher mycorrhization degree compared to roots colonized  
225 by the wt strain (Fig. 6B: Fig S6). Moreover, morphological changes were also observed in the root  
226 apparatus colonized by *RiPEIP1*-expressing strains (Fig 7): in particular, a stimulation of root  
227 branching was observed. Roots colonized by the transgenic strains formed lateral roots up to the 6<sup>th</sup>  
228 order while the roots colonized by the wt strain only developed up to 4<sup>th</sup> order lateral roots (Fig. 7  
229 C).

230

## 231 **DISCUSSION**

232 Among plant-associated microbes, AM fungi form the most ecologically and agriculturally  
233 important mutualistic association with plant roots in terrestrial ecosystems. Yet, the genetic  
234 determinants that control the fungal development *in planta*, which are necessary to support a long-  
235 lasting interaction between the partners, are still largely unknown. Transcriptomic (Tisserant et al.  
236 2012) and genomic (Tisserant et al. 2013; Lin et al. 2014) data recently obtained for *R. irregularis*  
237 have offered new opportunities to decipher the contribution of the fungal partner to the  
238 establishment of the symbiotic association. A large number of genes expressed in the intraradical  
239 and the extraradical phases have been described as orphan and lineage-specific. This may be an  
240 indicator of the uniqueness of Glomeromycota. In this work, we have focused on the  
241 characterization of an orphan gene that was called *RiPEIP1* based on its expression profiles.

242 Based on bioinformatics analyses, RiPEIP1 is a protein with no similarity to known sequences;  
243 consistently with *in silico* predictions, RiPEIP1 seems to be a transmembrane protein localized in  
244 particular in the endoplasmic reticulum and nuclear envelope when expressed as a GFP fusion in  
245 yeast cells. It is worth to note that a similar sequence was found in the recently published  
246 transcriptome (Salvioli et al. 2016) of another AM fungus, *G. margarita*. Even if the sequence is  
247 only partial, lacking the C-terminus portion, and the percentage of identity is relatively low (22%),

248 the two proteins share the same 4 transmembrane domains topology. Moreover, RNA-seq data  
249 showed an up-regulation of about 4 folds in mycorrhizal roots, as compared to germinating spores  
250 (Salvioli et al. 2016). Only the search within genomic and transcriptomic data from other AM fungi,  
251 once available, will clarify whether *RiPEIP1*-related sequences are a specific feature of  
252 Glomeromycota and whether they may have a general role in the *in planta* phase.

253 *RiPEIP1* expression is strongly induced in the intraradical phase, and the time course experiment  
254 showed that the highest expression levels were reached in mature mycorrhizal roots; *RiPEIP1*  
255 mRNA abundance perfectly matches the expression profile of *MtPT4* (at 28 and 60 dpi), a  
256 phosphate transporter essential for the acquisition of Pi delivered by the AM fungus (Javot et al.  
257 2007) and thus considered a marker of a functional symbiosis. We therefore suggest that *RiPEIP1*  
258 expression is, to some extent, related to arbuscules formation. This hypothesis is supported by the  
259 fact that *RiPEIP1* transcripts were detected in laser microdissected arbuscule-containing cells, while  
260 they were absent in adjacent cortical cells that likely contained only intercellular hyphae. To better  
261 understand the relationship with arbuscule development, we analysed *RiPEIP1* expression in the *M.*  
262 *truncatula mpt4-2* mutant line that is defective of MtPT4. MtPT4 function was shown to be critical  
263 for the AM symbiosis since its inactivation led to an altered arbuscules morphology, with premature  
264 senescence (Javot et al. 2007). As expected, we observed a reduced level of fungal colonization in  
265 *mpt4-2* mutants, as monitored by *RiTEFα* transcripts abundance, in comparison with colonized  
266 roots of wt plants. Interestingly, *mpt4-2* mycorrhizal roots showed lower levels of *RiPEIP1*  
267 mRNAs. Transcripts for *MtBCP1*, coding for a protein localized in the periarbuscular membrane  
268 and considered a molecular marker of arbuscule development and of colonization of the root system  
269 (Pumplin and Harrison 2009), were also found expressed at lower levels in the *mpt4-2* genotype.

270 Overall the data support a relationship between *RiPEIP1* and arbuscule differentiation.

271 The involvement of *RiPEIP1* in the intraradical phase of the colonization process was also  
272 supported by the heterologous expression of *RiPEIP1* in the ericoid mycorrhizal fungus *O. maius*.

273 In the absence of genetic transformation protocols for AM fungi, AM fungal genes have been

274 characterized by heterologous expression in filamentous fungi in few studies. To our knowledge,  
275 this approach was limited to pathogenic systems such as *Magnaporthe oryzae* (Kloppholz et al.  
276 2011) or *Colletotrichum lindemuthianum* (Tollot et al. 2009). We suggest that *O. maius* could  
277 represent an additional, possibly more suitable biological system for the characterization of AM  
278 fungal genes, as it shares with AM fungi the capability to form an endomycorrhizal association and  
279 to colonize root cells at an intracellular level.

280 Roots colonized by *O. maius* *RiPEIP1*-expressing strains showed a higher mycorrhization degree  
281 compared to roots colonized by the wt strain. Although no *RiPEIP1* homolog has been found in the  
282 complete *O. maius* genome sequence (Kohler et al. 2015) and *V. myrtillus* is not a host for AM  
283 fungi, the stimulation of mycorrhization observed in this heterologous mycorrhizal system suggests  
284 a general role for *RiPEIP1* in endosymbiosis establishment or functioning. Remarkably, *O. maius*  
285 transgenic strains induced changes on *V. myrtillus* root morphology with the stimulation of lateral  
286 roots formation up to the 6<sup>th</sup> order. The molecular basis of this phenomenon are unknown and  
287 deserve further investigations.

288 In summary, although the mechanism of action still remain obscure, we showed that *RiPEIP1*, an  
289 orphan gene from the AM fungus *R. irregularis*, is preferentially expressed *in planta* and may play  
290 a role in the root accommodation of fungal structures. Our data also underlies the potential of the  
291 endomycorrhizal fungus *O. maius* to characterize genes from AM fungi.

292

## 293 **MATERIALS AND METHODS**

### 294 **Plant and fungal material**

295 Seeds of *Medicago truncatula* Gaertn cv Jemalong and the *mpt4-2* TILLING mutant (Javot et al.,  
296 2011) were treated as described in Fiorilli et al. (2013). *Rhizophagus irregularis* (Syn. *Glomus*  
297 *intraradices*, DAOM 197198) inoculum was obtained from *in vitro* monoxenic cultures of  
298 *Agrobacterium rhizogenes*-transformed chicory roots (Bécard and Fortin 1988) in two-compartment  
299 Petri plates, as described in Belmondo et al. (2014). Plates were incubated in the dark at 24°C until

300 the fungal compartment, containing a solid M medium without sucrose (M-C medium), was  
301 profusely colonized by the fungus (approximately 6 weeks).

302 *M. truncatula* wilde type (WT) and *mtpt4-2* mycorrhizal plants were obtained in the sandwich  
303 system (Giovannetti et al. 1993), inoculating seedlings with *R. irregularis* extraradical mycelium  
304 (ERM) between two sterile nitrocellulose membranes. Plants were fertilized with Long-Ashton  
305 nutrient solution containing 32  $\mu\text{M}$   $\text{KH}_2\text{PO}_4$  and grown in climate-controlled rooms at 22°C with a  
306 photoperiod of 14-h light and 10-h dark.

307 *Oidiodendron maius* (CLM1381.98 strain; Martino et al. 2000) was grown in Czapek-Dox medium  
308 (supplemented with 1% agar for the solid medium). Petri dishes were kept in the dark at 25°C in a  
309 dark room at 25°C for 2 months. Flasks were kept under the same conditions on an orbital shaker.

310 *In vitro* endomycorrhizas were synthesized as described by Abbà et al. (2009) with some  
311 modifications. Axenic *V. myrtilillus* seedlings (Les Semences du Puy, Le Puy-En-Velay, France)  
312 were inoculated on modified Ingestad's medium (Ingestad, 1971), where four mycelium plug of wt  
313 or transformants strains were previously grown for two months. Plates were placed in a growth  
314 chamber (16 h photoperiod, light at 170  $\mu\text{mol m}^{-2} \text{s}^{-1}$ , temperatures at 23°C day and 21°C night),  
315 and roots were observed after 2 months of incubation. Four Petri dishes, each containing three  
316 seedlings (for a total of twelve replicates), were used for each fungal genotype.

317

### 318 **Quantification of mycorrhizal colonization**

319 *M. truncatula* WT and *mtpt4-2* mycorrhizal roots were stained after two months of inoculation with  
320 0.1% cotton blue in lactic acid and the estimation of mycorrhizal parameters was performed as  
321 described by Trouvelot et al. (1986) using MYCOCALC ([http://](http://www2.dijon.inra.fr/mychintec/Mycocalc-prg/download.html)  
322 [www2.dijon.inra.fr/mychintec/Mycocalc-prg/download.html](http://www2.dijon.inra.fr/mychintec/Mycocalc-prg/download.html)).

323 The degree of *V. myrtilillus* mycorrhization was recorded after two months of inoculation by *O.*  
324 *maius* Zn WT or *RiPEIP1*-expressing strains. The magnified intersections method (Villarreal-Ruiz  
325 et al. 2004) was adapted to quantify the percentage of infection of *V. myrtilillus* roots after staining

326 with acid fuchsin. The root system was examined under the microscope using the rectangle around  
327 the cross-hair as intersection area at 200X magnification. A total of 100 intersections per seedling  
328 root system were scored. Counts were recorded as percentage of root colonized (RC) by the fungus  
329 using the formula:  $RC\% = 100 \times \frac{\Sigma \text{ of coils counted}}{\Sigma \text{ of cells counted}}$  for all the intersections, where  $\Sigma$  is the number  
330 of epidermal cells for all the intersections.

331

### 332 **Biomass analysis**

333 Conidia were harvested from two month-agar cultures of both WT and transformants by gently  
334 scraping cultures in 9 cm Petri dishes flooded with 1 ml of sterilized water. Conidia were counted in  
335 a Bürker counting chamber (Marienfeld, Germany) and, for each fungus, an aliquot containing a  
336 comparable number of conidia was transferred into liquid medium. After one month, fungal mycelia  
337 were harvested and the biomass weight evaluated. Analyses were carried out on three technical  
338 replicates for each biological condition.

339

### 340 ***Agrobacterium tumefaciens*-mediated transformation of *Oidiodendron maius***

341 The pCAMBIA0380 (CAMBIA) was used as a backbone to construct the p*RiPEIP1* expression  
342 vector. The hygromycin resistance cassette (containing the *A. nidulans gpdA* promoter, the *hph* gene  
343 encoding resistance to hygromycin, and the *trpC* terminator from *A. nidulans*) was excised from  
344 pAN7-1 (Punt et al. 1987) with *HindIII* and *BglII* and inserted into the pCAMBIA030 at the  
345 *HindIII/BglII* sites to create the pCAMBIA0380\_HYG. The insertion of the Hygromycin resistance  
346 cassette introduced at the end of the *trpC* terminator a *XbaI* restriction site that was not originally  
347 present in the pCAMBIA0380 vector. The vector was then *XbaI-XmaI* digested to insert another  
348 copy of the *A. nidulans gpdA* constitutive promoter, which was modified at the 3' end to carry also a  
349 *KpnI* restriction site before the *XmaI* site. *RiPEIP1* full length cDNA was then amplified using a  
350 forward primer (*RiPEIP1-K*) containing a *KpnI* site and a reverse primer (*RiPEIP1-X*) containing a  
351 *XmaI* site (Table S1). The PCR product was *KpnI* and *XmaI* digested and inserted into the *KpnI*-

352 *Xma*I-digested pCAMBIA0380\_HYG plasmid under the *A. nidulans* *gpdA* constitutive promoter.  
353 The resulting recombinant plasmid was introduced into *A. tumefaciens* LBA1100 strain, which was  
354 used to transform *O. maius* ungerminated conidia according to the protocol described by Abbà et al.  
355 (2009). Transformants were isolated and transferred into 24-well plates with Czapek-Dox agar  
356 medium supplemented with 100 µg/ml hygromycin B. Transgenic strains were confirmed by PCR  
357 assays and Southern blot hybridization.

358 Genomic DNA of transformants strains was extracted using the CTAB protocol from mycelium  
359 grown for 30 days in liquid Czapek-2% DOX medium. For Southern blot, 10 micrograms of  
360 genomic DNA was digested with *Bgl*II restriction enzyme, size-fractionated on 1% (w/v) agarose  
361 gel and blotted onto nylon membranes following standard procedures (Sambrook and Russel 2001).  
362 Hybridization with a chemiluminescent detection system (ELC Direct DNA labelling and Detection  
363 System, Amersham) was performed according to the manufacturer's recommendation using a probe  
364 corresponding to the full length *RiPEIP1* cDNA sequence using *RiPEIP1* full length (RiPEIP1fl)  
365 forward/reverse primer (Table 1). Probe labelling and high stringency hybridization were carried  
366 out using ECL protocol (GE Healthcare, Chalfont St. Giles, U.K.).

367

### 368 **5'- and 3' RACE**

369 Both 5'- and 3' RACE were performed on total RNA extracted from the mycorrhizal roots with the  
370 SMART RACE cDNA amplification kit (Clontech). The PCR product was obtained using the  
371 primers *RiPEIP1*-race-forward/reverse (Table 1). PCR was performed according to the Clontech  
372 protocol using the Advantage 2 PCR enzyme system and 35 cycles of 95°C for 30 sec, 60°C for 30  
373 sec and 72°C for 2 min, with a final extension at 72°C for 10 min. The RACE products were cloned  
374 into pCRII vector (TOPO cloning kit; Invitrogen) and sequenced.

375

### 376 **Nucleic acid extraction, cDNA synthesis, RT-PCR assay**

377 Total genomic DNA was extracted from *R. irregularis* ERM and *M. truncatula* shoot using the  
378 DNeasy Plant Mini Kit (Qiagen), according to the manufacturer's instructions. Each primer pair  
379 was first tested on plant or fungal genomic DNA as a positive control and to exclude cross  
380 hybridization.

381 Total RNA was extracted from *R. irregularis* ERM and mycorrhizal *M. truncatula* roots using the  
382 Plant RNeasy Kit (Qiagen), according to the manufacturer's instructions.

383 Total RNA was extracted from *O. maius* transformants and WT mycelia using a Tris-HCl extraction  
384 buffer (Tris-HCl 100 mM pH 8, NaCl 100 mM, Na-EDTA 20 mM, PVP 0.1 %, Na-laurylsarcosine  
385 1 % in DEPC-treated H<sub>2</sub>O), followed by phenol (Roti-Phenol, Roth) extraction,  
386 phenol:chloroform:isoamyl alcohol (25:24:1) extraction, chloroform extraction and isopropanol  
387 precipitation (30 min at -80°C). The pellet was then resuspended in DEPC-treated water and  
388 precipitated in 6M LiCl (12 hours at 4°C). Finally, RNA was pelleted by centrifugation, rinsed with  
389 70 % ethanol and resuspended in DEPC-treated H<sub>2</sub>O.

390 Samples were treated with TURBO™ DNase (Ambion) according to the manufacturer's instructions.

391 RNA samples were routinely checked for DNA contamination by means of RT-PCR (One-RT-  
392 PCR, Qiagen) analysis, using for *R. irregularis* *RiEF1α*, *M. truncatula* *MtTef*, and *O. maius*  
393 *OmTubulin* primers (Table 1).

394 For conventional RT-PCR analyses, RNAs were amplified with *RiPEIP1-qpcr* forward/reverse  
395 primers and for the *O. maius* tubulin housekeeping gene (Table 1) using the One Step RT-PCR kit  
396 (Qiagen). RNA samples were incubated for 30 min at 50°C, followed by 15 min of incubation at  
397 95°C. Amplification reactions were run for 40 cycles at 94°C for 30 s, 60°C for 30 s, and 72°C for  
398 40 s.

399 cDNA synthesis was carried out on about 700 ng of total RNA which was denatured at 65°C for 5  
400 min and then reverse-transcribed at 25°C for 10 min, 42°C for 50 min and 70° for 15 min in a final  
401 volume of 20 µl containing 10 µM random primers, 0.5 mM dNTPs, 4 µl 5X buffer, 2 µl 0.1 M  
402 DTT, and 1 µl Super-ScriptII (Invitrogen).

### 403 **Quantitative RT-PCR**

404 Quantitative RT-PCR (qRT-PCR) assays were performed using an iCycler apparatus (Bio-Rad) as  
405 described in Belmondo et al. (2014) with primers pairs listed in Table S1. All reactions were  
406 performed on three technical replicates and on at least three biological replicates. Baseline range  
407 and Ct values were automatically calculated using iCycler software. Transcript levels were  
408 normalized to Ct values registered for the *RiEF1 $\alpha$*  (González-Guerrero et al. 2010) fungal gene and  
409 the *MtTef* (Hohnjec et al. 2005) plant gene. Only Ct values leading to a Ct mean with a standard  
410 deviation below 0.5 were considered.

411

### 412 **Laser microdissection (LMD)**

413 *M. truncatula* mycorrhizal roots, obtained using the sandwich method, were dissected, fixed and  
414 embedded in paraffin according to the method described in Perez-Tienda et al. (2011). A Leica AS  
415 LMD system (Leica Microsystem, Inc.) was used to collect arbuscule-colonized cortical cells  
416 (ARB) and non-colonized cortical cells (MNM) from paraffin root sections, as described by  
417 Balestrini et al. (2007). Two thousand ARB and MNM cells (for each biological replicate) from *M.*  
418 *truncatula* roots were collected. RNA was extracted following the Pico Pure kit (Arcturus  
419 Engineering) protocol. A DNase treatment was performed using an RNA-free DNase Set (Qiagen)  
420 in a Pico Pure column, according to the manufacturer's instructions. RNA was then quantified using  
421 a NanoDrop 1000 spectrophotometer. DNA contamination in RNA samples was evaluated using  
422 *RiEF1 $\alpha$*  (Table 1) by means of RT-PCR assays carried out using One Step RT-PCR kit (Qiagen).

423

### 424 **Construction of GFP fusion proteins for expression in yeast**

425 The full length cDNA of *RiPEIP1* was amplified from *R. irregularis* cDNA by PCR using the  
426 Phusion DNA-Polymerase (Finnzymes, Espoo, Finland). cDNAs were amplified using a forward  
427 primer containing the *KpnI* site (*RiPEIP1-K*) and a reverse primer containing the *NotI* site  
428 (*RiPEIP1-N*) (Table S1). The PCR products were *KpnI* and *NotI* -digested and inserted into the

429 *KpnI-NotI*-digested pYES2-GFP plasmid (Blaudez et al. 2003) under the control of the GAL1  
430 promoter and allowing a 3' fusion with the enhanced GFP reporter gene. *Saccharomyces cerevisiae*  
431 (BY4742 strain) transformation was performed using the lithium acetate based method described by  
432 Gietz et al. (1992). As a control of subcellular localization, two yeast strains constitutively  
433 expressing the red fluorescent protein fused to Sec13 (marker of both the endoplasmic reticulum  
434 and Golgi stacks) or Cop1 (marker of early Golgi) were analysed in parallel  
435 (<http://yeastgfp.yeastgenome.org/info.php>).

436

### 437 **Microscopy**

438 Fluorescence emission from yeast cells expressing RiPEIP1::GFP, Sec13::RFP or Cop1::RFP was  
439 examined with a Leica TCS-SP2 confocal laser-scanning microscope equipped with a 63x water  
440 immersion objective. GFP was excited at 488 nm (Ar laser) and fluorescence was detected at 515-  
441 530 nm. RFP was excited at 546 nm and fluorescence was detected at 570-650 nm.

442 For acid fuchsin staining mycorrhizal roots were stained with 0.01% (w/v) acid fuchsin in  
443 lactoglycerol (lactic acid-glycerol-water, 14:1:1; Kormanik and McGraw 1982). Confocal  
444 microscopy observations were done using a Leica TCS-SP2 microscope equipped with a 40x long-  
445 distance objective. Acid fuchsin fluorescence was excited at 488nm and detected using a 560-680  
446 nm emission window.

447 For calcofluor white (CFW; Fluorescent Brightener 28, F3543; Sigma-Aldrich) staining *O. maius*  
448 mycelia were let grown on a coverslip. The CFW solution was dropped onto the coverslips  
449 immediately before observation. CFW fluorescence was visualized with a Leica TCS-SP2 confocal  
450 laser-scanning microscope using a 405nm diode and an emission window at 410-460nm.

451

### 452 **Statistical analyses**

453 Statistical analyses were performed through one-way ANOVA and Tukey's post hoc test, using a  
454 probability level of  $p < 0.05$ . All statistical elaborations were performed using PAST statistical  
455 package (version 2.16; Hammer et al. 2001).

456

#### 457 **ACKNOWLEDGMENTS**

458 Research was funded by the BIOBIT-Converging Technology project (WP2) and the University  
459 grant (60%) to LL. VF fellowship was funded by the RISINNOVA Project (grant number 2010-  
460 2369, AGER Foundation). We thank Maria J. Harrison for the *mtpt4-2* mutant, Nuria Ferrol for the  
461 RFP yeast strains, Andrea Genre for confocal microscopy observations, Raffaella Balestrini for the  
462 help on laser microdissection and Paola Bonfante and Silvia Perotto for fruitful discussions and  
463 critical reading of the manuscript.

464 **REFERENCES**

- 465 Abbà S, Khouja HR, Martino E, Archer DB, Perotto S (2009) SOD1-targeted gene disruption in the  
466 ericoid mycorrhizal fungus *Oidiodendron maius* reduces conidiation and the capacity for  
467 mycorrhization. *Mol. Plant Microbe Interact* 22:1412-1421. doi: 10.1094/MPMI-22-11-1412
- 468 Allen JW, Shachar-Hill Y (2009) Sulfur transfer through an arbuscular mycorrhiza. *Plant Physiol.*  
469 149: 549-560. doi: 10.1104/pp.108.129866
- 470 Balestrini R, Gómez-Ariza J, Lanfranco L, Bonfante, P (2007) Laser microdissection reveals that  
471 transcripts for five plant and one fungal phosphate transporter genes are contemporaneously present  
472 in arbusculated cells. *Mol Plant Microbe Interact.* 20:1055-1062. doi.org/10.1094/MPMI-20-9-1055
- 473 Bécard G, Fortin JA (1988) Early events of vesicular–arbuscular mycorrhiza formation on Ri T-  
474 DNA transformed roots. *New Phytol* 108:211-218. doi: 10.1111/j.1469-8137.1988.tb03698.x
- 475 Belmondo, S, Fiorilli, V, Pérez-Tienda, J, Ferrol, N, Marmeisse, R, Lanfranco, L (2014) A  
476 dipeptide transporter from the arbuscular mycorrhizal fungus *Rhizophagus irregularis* is  
477 upregulated in the intraradical phase. *Front Plant Sci* 3;5: 436. doi.org/10.3389/fpls.2014.00436
- 478 Blaudez D, Kohler A, Martin F, Sanders D, Chalot, M (2003) Poplar metal tolerance protein 1  
479 confers zinc tolerance and is an oligomeric vacuolar zinc transporter with an essential leucine zipper  
480 motif. *Plant Cell* 1512: 2911-28. doi: 10.1105/tpc.017541
- 481 Bonfante P, Genre A (2015) Arbuscular mycorrhizal dialogues: do you speak 'plantish' or 'fungish'?  
482 *Trends Plant Sci* 20:150-154. doi: 10.1016/j.tplants.2014.12.002
- 483 Bonfante P, Requena N (2011) Dating in the dark: how roots respond to fungal signals to establish  
484 arbuscular mycorrhizal symbiosis. *Curr Opin Plant Biol* 14:451-457. doi: 10.1016/j.pbi.2011.03.014

485 Breuninger M, Requena N (2004) Recognition events in AM symbiosis: analysis of fungal gene  
486 expression at the early appressorium stage. *Fungal Genet Biol* 41:794-804.  
487 doi:10.1016/j.fgb.2004.04.002

488 Cappellazzo G, Lanfranco L, Bonfante P (2007) A limiting source of organic nitrogen induces  
489 specific transcriptional responses in the extraradical structures of the endomycorrhizal fungus  
490 *Glomus intraradices*. *Curr Genet* 51:59-70. doi: 10.1007/s00294-006-0101-2

491 Ehinger MO, Croll D, Koch AM, Sanders IR (2012) Significant genetic and phenotypic changes  
492 arising from clonal growth of a single spore of an arbuscular mycorrhizal fungus over multiple  
493 generations. *New Phytol* 196:853-561. doi: 10.1111/j.1469-8137.2012.04278.x

494 Jackson MR, Nilsson T, Peterson PA (1990) Identification of a consensus motif for retention of  
495 transmembrane proteins in the endoplasmic reticulum. *EMBO J* 9, 3153–3162

496 Kikuchi Y, Hijikata N, Yokoyama K, Ohtomo RY, Handa Y, Kawaguchi M, Katsuharu Saito K,  
497 Ezawa T (2014) Polyphosphate accumulation is driven by transcriptome alterations that lead near-  
498 synchronous and near-equivalent uptake of inorganic cations in an arbuscular mycorrhizal fungus.  
499 *New Phytol* 204:638-649. doi: 10.1111/nph.12937

500 Kormanik PP, McGraw AC (1982) Quantification of vesicular-arbuscular mycorrhizae in plant  
501 roots. In NC Schenk (ed) *Methods and principles of mycorrhizal research* American  
502 Phytopathological Society, St Paul, MN, p37-47

503 Fiorilli V, Lanfranco L, Bonfante, P (2013) The expression of *GintPT*, the phosphate transporter of  
504 *Rhizophagus irregularis*, depends on the symbiotic status and phosphate availability. *Planta*  
505 237:1267-1277. doi: 10.1007/s00425-013-1842-z

506 Genre A, Chabaud M, Timmers T, Bonfante P, Barker DG (2005). Arbuscular mycorrhizal fungi  
507 elicit a novel intracellular apparatus in *Medicago truncatula* root epidermal cells before infection.  
508 Plant Cell 17:3489-3499. doi: 10.1105/tpc.105.035410

509 Genre A, Chabaud M, Faccio A, Barker DG, Bonfante P (2008) Pre-penetration apparatus assembly  
510 precedes and predicts the colonization patterns of arbuscular mycorrhizal fungi within the root  
511 cortex of both *Medicago truncatula* and *Daucus carota*. Plant Cell 20:1407-1420. doi:  
512 10.1105/tpc.108.059014

513 Gianinazzi S, Gollotte A, Binet MN, van Tuinen D, Redecker D, Wipf D (2010) Agroecology: the  
514 key role of arbuscular mycorrhizas in ecosystem services. Mycorrhiza 20:519-530. doi:  
515 10.1007/s00572-010-0333-3

516 Gietz D, St Jean A, Woods RA, Schies RH (1992) Improved method for high efficiency  
517 transformation of intact yeast cells. Nucleic Acids Res 20:1425

518 Giovannetti M, Sbrana C, Avio L, Citernesi AS, Logi C (1993) Differential hyphal morphogenesis  
519 in arbuscular mycorrhizal fungi during pre-infection stages. New Phytol 125:587-593. doi:  
520 10.1111/j.1469-8137.1993.tb03907.x

521 González-Guerrero M, Oger E, Benabdellah K, Azcón-Aguilar C, Lanfranco L, Ferrol N (2010)  
522 Characterization of a CuZn superoxide dismutase gene in the arbuscular mycorrhizal fungus  
523 *Glomus intraradices*. Curr Genet 56:265-74. doi: 10.1007/s00294-010-0298-y

524 Govindarajulu M, Pfeffer PE, Jin HR, Abubaker J, Douds DD, Allen JW, Bücking H, Lammers PJ  
525 Shachar-Hil Y (2005) Nitrogen transfer in the arbuscular mycorrhizal symbiosis. Nature 435:819-  
526 823. doi:10.1038/nature03610

527 Gutjahr C, Parniske M (2013) Cell and developmental biology of arbuscular mycorrhiza symbiosis  
528 *Annu Rev Cell Dev Biol* 29:593-617. doi: 10.1146/annurev-cellbio-101512-122413

529 Hammer Ø, Harper DAT, Ryan PD (2001) PAST: paleontological statistics software package for  
530 education and data analysis. *Palaeontol Electron* 4, 9.

531 Harrison MJ, Dewbre GR, Liu J (2002) A phosphate transporter from *Medicago truncatula*  
532 involved in the acquisition of phosphate released by arbuscular mycorrhizal fungi. *Plant Cell*  
533 14:2413-2429. doi: 10.1105/tpc.004861

534 Helber N, Requena N (2008) Expression of the fluorescence markers DsRed and GFP fused to a  
535 nuclear localization signal in the arbuscular mycorrhizal fungus *Glomus intraradices*, *New Phytol*  
536 177: 537-548. doi: 10.1111/j.1469-8137.2007.02257.x

537 Helber N, Wippel N, Schaarschmidt S, Hause B, Requena N (2011) A versatile monosaccharide  
538 transporter that operates in the arbuscular mycorrhizal fungus *Glomus sp.* is crucial for the  
539 symbiotic relationship with plants. *Plant Cell* 23:3812-3823. doi: 10.1105/tpc.111.089813

540 Hijri M, Sanders IR (2005) Low gene copy number shows that arbuscular mycorrhizal fungi inherit  
541 genetically different nuclei. *Nature* 433:160-163. doi:10.1038/nature03069

542 Hohnjec N, Vieweg MF, Pühler A, Becker A, Küster H (2005) Overlaps in the transcriptional  
543 profiles of *Medicago truncatula* roots inoculated with two different *Glomus* fungi provide insights  
544 into the genetic program activated during arbuscular mycorrhiza. *Plant Physiol* 137:1283-1301. doi:  
545 10.1104/pp.104.056572

546 Javot H, Penmetsa RV, Breuillin F, Bhattarai KK, Noar RD, Gomez SK, Zhang Q, Cook DR,  
547 Harrison MJ (2011) *Medicago truncatula mtpt4* mutants reveal a role for nitrogen in the regulation  
548 of arbuscule degeneration in arbuscular mycorrhizal symbiosis. *Plant J* 68:954-965. doi:  
549 10.1111/j.1365-313X.2011.04746.x

550 Javot H, Penmetsa RV, Terzaghi N, Cook DR, Harrison MJ (2007) A *Medicago truncatula*  
551 phosphate transporter indispensable for the arbuscular mycorrhizal symbiosis. Proc Natl Acad Sci U  
552 S A 104:1720-1725. doi: 10.1073/pnas.0608136104

553 Klopffholz S, Kuhn H, Requena N (2011) A secreted fungal effector of *Glomus intraradices*  
554 promotes symbiotic biotrophy. Curr Biol 21:1204-1209. doi: 10.1016/j.cub.2011.06.044

555 Kobae Y, Hata, S (2010) Dynamics of periarbuscular membranes visualized with a fluorescent  
556 phosphate transporter in arbuscular mycorrhizal roots of rice. Plant Cell Physiol 51:341-53.  
557 doi:10.1093/pcp/pcq013

558 Kohler A, Kuo A, Nagy LG, Morin E, Barry KW, Buscot F, Canbäck B, Choi C, Cichocki N, Clum  
559 A, Colpaert J, Copeland A, Costa MD, Doré J, Floudas D, Gay G, Girlanda M, Henrissat B,  
560 Herrmann S, Hess J, Högberg N, Johansson T, Khouja HR, LaButti K, Lahrmann U, Levasseur A,  
561 Lindquist EA, Lipzen A, Marmeisse R, Martino E, Murat C, Ngan C Y, Nehls U, Plett J M, Pringle  
562 A, Ohm R A, Perotto S, Peter M, Riley R, Rineau F, Ruytinx J, Salamov A, Shah F, Sun H, Tarkka,  
563 M Tritt, A Veneault-Fourrey, C Zuccaro, A Tunlid, A Grigoriev IV, Hibbett DS, Martin F (2015)  
564 Convergent losses of decay mechanisms and rapid turnover of symbiosis genes in mycorrhizal  
565 mutualists Nat Genet 47:410-415. doi:10.1038/ng.3223

566 Lanfranco L, Young JP (2012) Genetic and genomic glimpses of the elusive arbuscular mycorrhizal  
567 fungi. Curr Opin Plant Biol 15:454-461. doi: 10.1016/j.pbi.2012.04.003

568 Li T, Hu YJ, Hao ZP, Li H, Wang YS, Chen BD (2013) First cloning and characterization of two  
569 functional aquaporin genes from an arbuscular mycorrhizal fungus *Glomus intraradices*. New  
570 Phytol 197:617-30. doi: 10.1111/nph.12011

571 Lin K, Limpens E, Zhang Z, Ivanov S, Saunders DG, Mu D, Pang E, Cao H, Cha H, Lin T, Zhou Q,  
572 Shang Y, Li Y, Sharma T, van Velzen R, de Ruijter N, Aanen DK, Win J, Kamoun S, Bisseling T,

573 Martin F, Kohler A, Murat C, Balestrini R, Coutinho PM, Jaillon O, Montanini B, Morin E, Noel B,  
574 Percudani R, Porcel B, Rubini A, Amicucci A, Amselem J, Anthouard V, Arcioni S, Artiguenave F,  
575 Aury JM, Ballario P, Bolchi A, Brenna A, Brun A, Buée M, Cantarel B, Chevalier G, Couloux A,  
576 Da Silva C, Denoeud F, Duplessis S, Ghignone S, Hilselberger B, Iotti M, Marçais B, Mello A,  
577 Miranda M, Pacioni G, Quesneville H, Riccioni C, Ruotolo R, Splivallo R, Stocchi V, Tisserant E,  
578 Viscomi AR, Zambonelli A, Zampieri E, Henrissat B, Lebrun MH, Paolocci F, Bonfante P,  
579 Ottonello S, Wincker P (2010) Périgord black truffle genome uncovers evolutionary origins and  
580 mechanisms of symbiosis. *Nature* 464:1033-1038. doi: 10.1038/nature08867

581 Martino E, Turnau K, Girlanda M, Bonfante P, Perotto S (2000) Ericoid mycorrhizal fungi from  
582 heavy metal polluted soils: their identification and growth in the presence of zinc ions. *Mycol Res*  
583 104:338-344. doi:10.1017/S0953756299001252

584 Martino E, Murat C, Vallino M, Bena A, Perotto S, and Spanu P (2007) Imaging mycorrhizal  
585 fungal transformants that express EGFP during ericoid endosymbiosis *Curr Genet* 52:65-75. doi:  
586 10.1007/s00294-007-0139-9

587 Pawlowska TE, Taylor JW (2004) Organization of genetic variation in individuals of arbuscular  
588 mycorrhizal fungi. *Nature* 427:733-737. doi:10.1038/nature02290

589 Pérez-Tienda J, Testillano PS, Balestrini R, Fiorilli V, Azcón-Aguilar C, Ferrol N (2011)  
590 GintAMT2, a new member of the ammonium transporter family in the arbuscular mycorrhizal  
591 fungus *Glomus intraradices*. *Fungal Genet Biol* 48:1044-1055. doi: 10.1016/j.fgb.2011.08.003

592 Pfeffer PE, Douds DD, Bécard G, Shachar-Hill Y (1999) Carbon uptake and the metabolism and  
593 transport of lipids in an arbuscular mycorrhiza. *Plant Physiol* 120:587-598. doi: [http://dx.doi.org/10.](http://dx.doi.org/10.1104/pp.120.2.587)  
594 1104/pp.120.2.587

595 Pumplín N, Harrison MJ (2009) Live-cell imaging reveals periarbuscular membrane domains and  
596 organelle location in *Medicago truncatula* roots during arbuscular mycorrhizal symbiosis. *Plant*  
597 *Physiol* 151:809-819. doi: 10.1104/pp.109.141879

598 Punt PJ, Oliver RP, Dingemans MA, Pouwels PH, van den Hondel CA (1987) Transformation of  
599 *Aspergillus* based on the hygromycin B resistance marker from *Escherichia coli*. *Gene* 56:117-24

600 Redecker D, Schüssler A, Stockinger H, Stürmer SL, Morton JB, Walker C (2013) An evidence-  
601 based consensus for the classification of arbuscular mycorrhizal fungi (Glomeromycota)  
602 *Mycorrhiza* 23:515-531. doi: 10.1007/s00572-013-0486-y

603 Requena N, Mann P, Hampp R, Franken P (2002) Early developmentally regulated genes in the  
604 arbuscular mycorrhizal fungus *Glomus mosseae*: GmGIN1, a novel gene encoding a protein with  
605 homology to the C-terminus of metazoan hedgehog proteins. *Plant Soil* 244:129-139

606 Riley R, Salamov AA, Brown DW, Nagy LG, Floudas D, Held BW, Levasseur A, Lombard V,  
607 Morin E, Otiillar R, Lindquist EA, Sun H, LaButti KM, Schmutz J, Jabbour D, Luo H, Baker SE,  
608 Pisabarro AG, Walton JD, Blanchette RA, Henrissat B, Martin F, Cullen D, Hibbett DS, Grigoriev  
609 IV (2014) Extensive sampling of basidiomycete genomes demonstrates inadequacy of the white-  
610 rot/brown-rot paradigm for wood decay fungi. *Proc Natl Acad Sci U S A* 111:9923-9928. doi:  
611 10.1073/pnas.1400592111

612 Ruzicka D, Chamala S, Barrios-Masias FH, Martin F, Smith S, Jackson LE, Brad Barbazuk W,  
613 Schachtman DP (2013) Inside arbuscular mycorrhizal roots - Molecular probes to understand the  
614 symbiosis. *Plant genome* 6:1-13. doi:10.3835/plantgenome2012.06.0007

615 Salvioli A, Bonfante P (2013) Systems biology and "omics" tools: a cooperation for next-generation  
616 mycorrhizal studies. *Plant Sci* 204:107-114. doi: 10.1016/j.plantsci.2013.01.001

617 Salvioli A, Ghignone S, Novero M, Navazio L, Venice F, Bagnaresi P, Bonfante P (2016)  
618 Symbiosis with an endobacterium increases the fitness of a mycorrhizal fungus, raising its  
619 bioenergetic potential. ISME J 10:130-144. doi: 101038/ismej201591

620 Sambrook J, Russel DW (2001) Molecular Cloning: A Laboratory Manual, Volume 1, 2, 3 Cold  
621 Spring Harbour Laboratory Press, Cold Spring Harbour, New York

622 Spanu PD, Abbott JC, Amselem J, Burgis TA, Soanes DM, Stüber K, Ver Loren van, Themaat E,  
623 Brown JK, Butcher S A, Gurr SJ, Lebrun MH, Ridout CJ, Schulze-Lefert P, Talbot NJ,  
624 Ahmadinejad N, Ametz C, Barton GR, Benjdia M, Bidzinski P, Bindschedler LV, Both M, Brewer  
625 MT, Cadle-Davidson L, Cadle-Davidson MM, Collemare J, Cramer R, Frenkel O, Godfrey D,  
626 Harriman J, Hoede C, King BC, Klages S, Kleemann J, Knoll D, Koti PS, Kreplak J, López-Ruiz  
627 FJ, Lu X, Maekawa T, Mahanil S, Micali C, Milgroom MG, Montana G, Noir S, O'Connell RJ,  
628 Oberhaensli S, Parlange F, Pedersen C, Quesneville H, Reinhardt R, Rott M, Sacristán S, Schmidt  
629 SM, Schön M, Skamnioti P, Sommer H, Stephens A, Takahara H, Thordal-Christensen H,  
630 Vigouroux M, Wessling R, Wicker T, Panstruga R (2010) Genome expansion and gene loss in  
631 powdery mildew fungi reveal tradeoffs in extreme parasitism. Science 330:1543-1546. doi:  
632 10.1126/science.1194573.

633 Tamayo E, Gómez-Gallego T, Azcón-Aguilar C, Ferrol N (2014) Genome-wide analysis of copper,  
634 iron and zinc transporters in the arbuscular mycorrhizal fungus *Rhizophagus irregularis*. Front Plant  
635 Sci 14;5:547. <http://dx.doi.org/10.3389/fpls.2014.00547>

636 Tisserant E, Kohler A, Dozolme-Seddas P, Balestrini R, Benabdellah K, Colard A, Croll D, Da  
637 Silva C, Gomez S K, Koul R, Ferrol N, Fiorilli V, Formey D, Franken P, Helber N, Hijri M,  
638 Lanfranco L, Lindquist E, Liu Y, Malbreil M, Morin E, Poulain J, Shapiro H, van Tuinen D,  
639 Waschke A, Azcón-Aguilar C, Bécard G, Bonfante P, Harrison MJ, Küster H, Lammers P,  
640 Paszkowski U, Requena N, Rensing SA, Roux C, Sanders IR, Shachar-Hill Y, Tuskan G, Young JP,

641 Gianinazzi-Pearson V, Martin F (2012) The transcriptome of the arbuscular mycorrhizal fungus  
642 *Glomus intraradices* (DAOM 197198) reveals functional tradeoffs in an obligate symbiont. New  
643 Phytol 193:755-769. doi: 10.1111/j.1469-8137.2011.03948.x

644 Tisserant E, Malbreil M, Kuo A, Kohler A, Symeonidi A, Balestrini R, Charron P, Duensing N,  
645 Frei dit Frey N, Gianinazzi-Pearson V, Gilbert LB, Handa Y, Herr JR, Hijri M, Koul R, Kawaguchi,  
646 M Krajinski, F Lammers PJ, Masclaux FG, Murat C, Morin E, Ndikumana S, Pagni M, Petitpierre  
647 D, Requena N, Rosikiewicz P, Riley R, Saito K, San Clemente H, Shapiro H, van Tuinen D, Bécard  
648 G, Bonfante P, Paszkowski U, Shachar-Hill YY, Tuskan GA, Young JP, Sanders IR, Henrissat B,  
649 Rensing SA, Grigoriev IV, Corradi N, Roux C, Martin F (2013) Genome of an arbuscular  
650 mycorrhizal fungus provides insight into the oldest plant symbiosis. Proc Natl Acad Sci U S A  
651 110:20117-20122. doi: 10.1073/pnas.1313452110

652 Tollot M, Wong Sak Hoi J, van Tuinen D, Arnould C, Chatagnier O, Dumas B, Gianinazzi-Pearson  
653 V, Seddas PM (2009) An STE12 gene identified in the mycorrhizal fungus *Glomus intraradices*  
654 restores infectivity of a hemibiotrophic plant pathogen. New Phytol 181:693-707. doi:  
655 10.1111/j.1469-8137.2008.02696.x

656 Villarreal-Ruiz L, Anderson IC, Alexander IJ (2004) Interaction between an isolate from the  
657 *Hymenoscyphus ericae* aggregate and roots of *Pinus* and *Vaccinium*. New Phytol 164:183-192. doi:  
658 10.1111/j.1469-8137.2004.01167.x

659 Young JPW (2015) Genome diversity in arbuscular mycorrhizal fungi. Curr Opin Plant Biol  
660 23:113-119. doi: 10.1016/j.pbi.2015.06.005

661  
662  
663

664 **FIGURE LEGENDS**

665 **Figure 1** *RiPEIP1* is up-regulated in the intraradical mycelium. Expression of *RiPEIP1* (relative to  
666 *RiTef*) assessed by qRT-PCR in intraradical mycelium (IRM) and extraradical mycelium (ERM)  
667 from mycorrhizal roots of *M. truncatula* grown in the sandwich system (n= 5). Single data for each  
668 condition are shown as dots and the median as black bars. Asterisks indicate a statistically  
669 significant difference ( $p < 0.01$ , ANOVA)

670 **Figure 2** Confocal imaging of RiPEIP1::GFP localization in yeast cells. The observed fluorescence  
671 pattern (a) is compatible with GFP localization in the endoplasmic reticulum and nuclear (n)  
672 envelope. A brightfield image of the same cells is shown in panel b. RiPEIP1::GFP localization is  
673 confirmed by a comparison with the fluorescence pattern from constitutively expressed Sec13::RFP  
674 (c), which labels the endoplasmic reticulum/nuclear envelope (n) and Golgi stacks, and Cop1::GFP  
675 (d), which targets the early Golgi stacks (arrowheads). Bars: 5  $\mu\text{m}$

676 **Figure 3** *RiPEIP1* gene expression along the AM colonization process. Relative expression of  
677 *MtPT4* (a) and *RiPEIP1* (b) assessed by qRT-PCR in a time course experiment of root colonization  
678 at 7, 14, 28 and 60 days post-inoculation (dpi). Single data for each condition are shown as dots and  
679 the median as black bars. Different letters indicate statistically significant difference ( $p < 0.05$ ,  
680 ANOVA). (c) Gel electrophoresis of RT-PCR products obtained from two independent samples of  
681 RNA from laser-microdissected arbuscule-containing cells (ARB) and one sample of not colonized  
682 cortical cells from mycorrhizal roots (MNM) using primers specific for *MtPT4*, *RiTef* or *RiPEIP1*.  
683 No RNA sample (-)

684 **Figure 4** *RiPEIP1* gene expression is affected in the *mtpt4-2* mutant line. The AM colonization of  
685 wt and *mtpt4-2* genotypes was evaluated through the assessment of fungal *RiTef* mRNA abundance  
686 (a); *MtBCP* expression was used as a marker of AM intraradical phase (b). The relative expression  
687 of *RiPEIP1* in wt and *mtpt4-2* roots is shown in panel c. The positive correlation on a linear  
688 regression model between the expression values of *RiPEIP1* and *MtBCP* and the high R-squared

689 value demonstrated that the two genes have similar expression profiles in wt (grey rhombi) or  
690 *mtp4-2* (black rhombi) genotypes (**d**). Asterisks indicate a statistically significant difference ( $p <$   
691 0.01, ANOVA)

692 **Figure 5** Expression of RiPEIP1 in *Oidiodendron maius* does not affect the growth of free-living  
693 mycelia. Gel electrophoresis of RT-PCR products obtained from wt and three *RiPEIP1*-expressing  
694 (BA2, BA4, BC6) free-living strains using *RiPEIP1* specific primers (**a**). Dry weight of free-living  
695 mycelia of wt and transgenic strains grown in liquid cultures (**b**)

696 **Figure 6** *RiPEIP1*-expressing strains led to a higher *Vaccinium myrtillus* root colonization level  
697 compared to the WT strain. (**a**) *In vitro* mycorrhization system between *V. myrtillus* seedlings and  
698 *O. maius*. Non inoculated *V. myrtillus* seedlings were unable to correctly develop (right panel) (**b**)  
699 The percentage of root colonization of *V. myrtillus* seedlings colonized with the *O. maius* wt or the  
700 three *RiPEIP1*-expressing strains was quantified after staining with acid fuchsin. Different letters  
701 indicate statistically significant difference ( $p < 0.05$ , ANOVA)

702 **Figure 7** Representative details of the *V. myrtillus* root system colonized by wt (**a**) or BC6  
703 *RiPEIP1*-expressing (**b**) strains after two months of inoculation. Note the stimulation of root  
704 branching in roots colonized by the *RiPEIP1*-expressing strain. (**C**) Average values and standard  
705 deviation of the number of lateral roots of the different orders in plant colonized by the wt or the  
706 transgenic strains (BA2, BA4, BC6). Bar = 1 cm

707

## 708 **Supplementary material**

709 **Figure S1** Nucleotide and deduced amino acid sequences of *RiPEIP1*. **a**) *RiPEIP1* genomic DNA  
710 sequence showing the presence of five introns. **b**) *RiPEIP1* protein sequence showing the 4  
711 transmembrane domains (underlined), the typical ER-retention/retrieval motifs (bold) and the  
712 predicted phosphorylation sites (red). See text for details

713 **Figure S2** Colonization level of *M. truncatula* roots at 28 and 60 days post inoculation (dpi)  
714 assessed accordingly to Trouvelot et al (1986). F%: frequency of mycorrhization in the root system  
715 (a), a%: arbuscules abundance in mycorrhizal pars of root fragments (b). Different letters indicate  
716 statistically significant difference ( $p < 0.05$  ANOVA)

717 **Figure S3** Mycorrhizal phenotype of *M. truncatula* wt (a, b) and *mtpt4-2* (c, d) roots colonized by  
718 *R. irregularis*. Roots were harvested 60 dpi, stained with acid fuchsin and observed with a confocal  
719 microscope. Arbuscules in *mtpt4-2* are degenerated as described in Javot et al. (2011). Bars = 25  
720  $\mu\text{m}$

721 **Figure S4** Molecular analyses of *O. maius* transgenic strains expressing *RiPEIP1*. (a) Gel  
722 electrophoresis of PCR products obtained from genomic DNA of wt and transgenic strains using  
723 *RiPEIP1* specific primers (b) Southern blot of genomic DNA from wt and transgenic strains  
724 restricted with *BglIII* enzyme and hybridized with the *RiPEIP1* probe. Lanes corresponding to BC6,  
725 BA2, BA4 samples exhibited a single genomic insertion

726 **Figure S5** Phenotype of *O. maius* free living mycelia from wt and *RiPEIP1*-expressing strain BA2  
727 as revealed by calcoflour white staining. Laser-scanning microscope observation of one-month-old  
728 *O. maius* wt and transgenic strains stained with calcofluor white. Transmitted light images are  
729 shown on the right (b, d) and the corresponding fluorescence images on the left (a, c). Bars: 10  $\mu\text{m}$

730 **Figure S6** Mycorrhizal phenotype of *O. maius* wt and *RiPEIP1*-expressing strain BC6.  
731 Mycorrhized *V. myrtillus* roots were stained with acid fuchsin and observed 2 months after fungal  
732 inoculation. *O. maius* transgenic strains showed an increased number of coils (asterisk) in epidermal  
733 cells compared to the wt.

734

735 **Table S1.** List of primers used in this study. Sites for GATEWAY recombination or restriction  
 736 enzymes are underlined.

Primer ID	Primer sequences [5'-3']
RiEF $\alpha$ f	GCTATTTTGATCATTGCCGCC
RiEF $\alpha$ r	TCATTA <del>AAA</del> ACGTTCTTCCGACC
MtTEFf	AAGCTAGGAGGTATTGACAAG
MtTEFr	ACTGTGCAGTAGTACTTGGTG
MtPT4 f	TCGCGCGCCATGTTTGTGT
MtPT4r	CGCAAGAAGAATGTTAGCCC
RiPEIP1-attB-forward	<u>GGGGACAAGTTTGTACAAAAAAGCAGGCT</u> ATGTCAGCTAAATTTATCAAGC
RiPEIP1-attB-reverse	<u>GGGGACCACTTTGTACAAGAAAGCTGGGT</u> CTTTAAACATTTTCATTAACA <del>CTC</del>
RiPEIP1fF:	ATGTCAGCTAAATTTATCAAGC
RiPEIP1fR:	CTTTAAACATTTTCATTAACA <del>CTC</del> CATCTCG
RiPEIP1-N	<u>GTCAGCGGCCGC</u> CTTTAAACATTTTCATTAAC
RiPEIP1-K	<u>GATCGGTACC</u> ATGTCAGCTAAATTTATC
RiPEIP1-X	<u>GCATCCCGGG</u> CTTTAAACATTTTCATTAAC
RiPEIP1-race-forward	AGTAGAAGCACTAAAGGTGCCAAGAAAAGT
RiPEIP1-race-reverse	TAACACTCATCTCGGGACTGACTTCATTCT
RiPEIP1-qpcrF	AAGAAAGTAAACGTGTGGCT
RiPEIP1-qpcrR	TAACACTCATCTCGGGACTG
OmTubulin-forward	GTTTCCATGAAGGAGGTTGAGG
OmTubulin-reverse	CAGAGAGCAGTCTGGACGTTGT

737

738

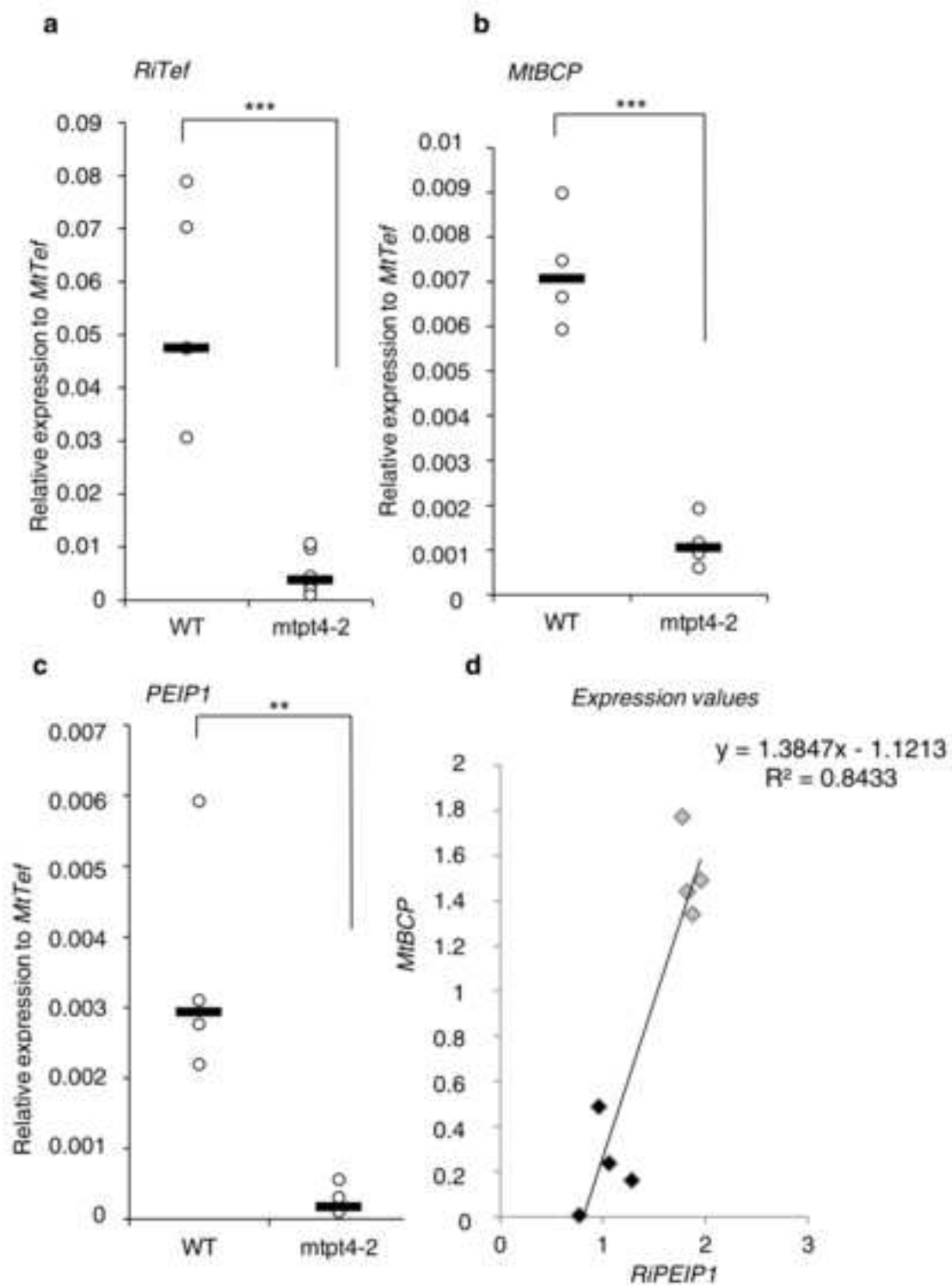
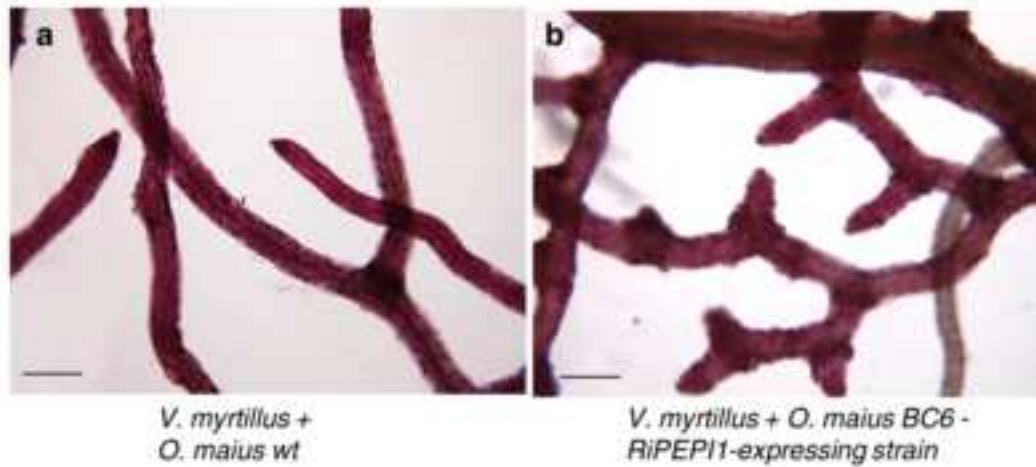


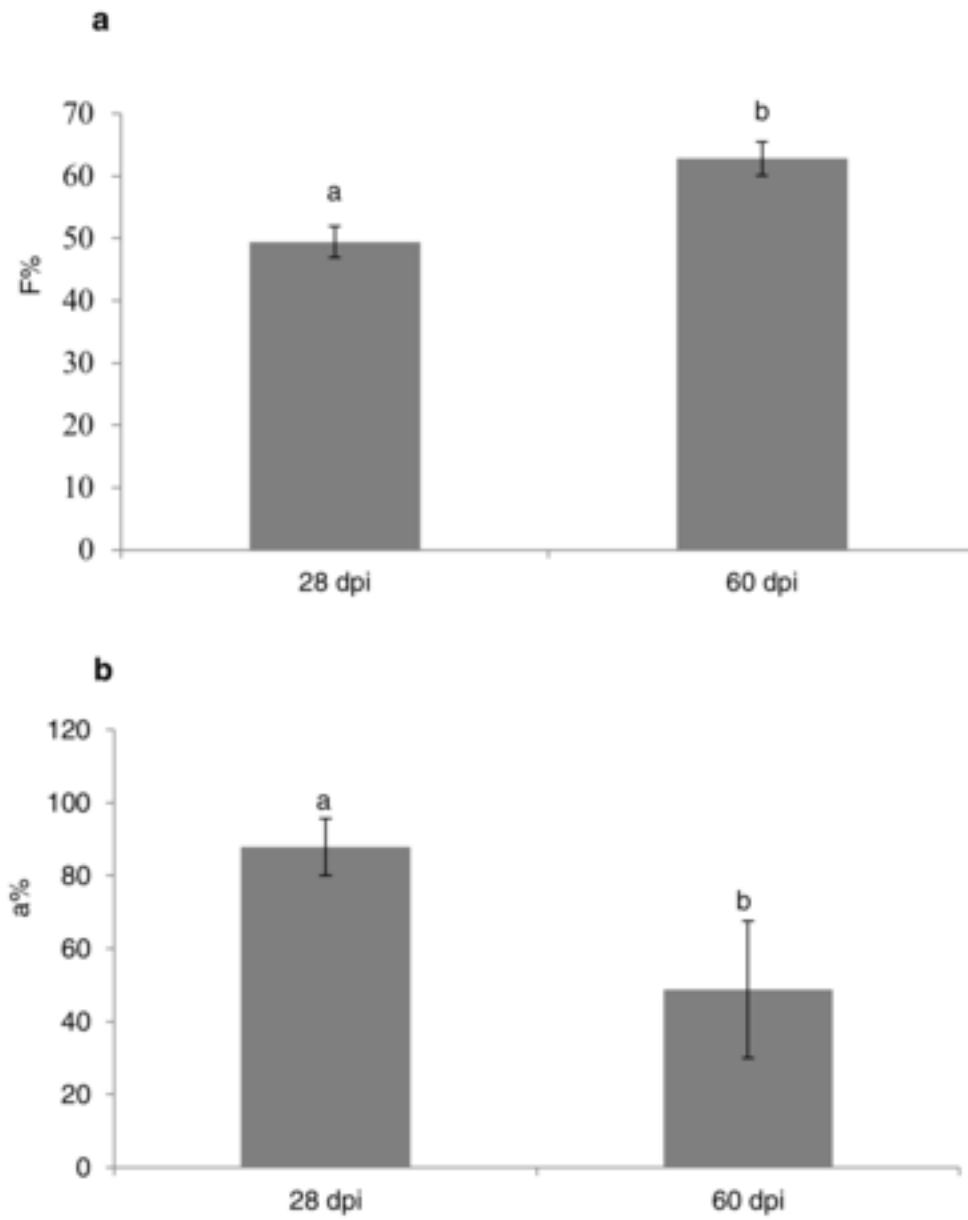
Figure 4



**c**

	Root orders	samples			
		BA2	BA4	BC6	WT
Lateral roots average values	1°	14 ± 7	14.6 ± 7.2	16 ± 10.3	9.6 ± 2
	2°	33.3 ± 25	39 ± 14.9	51.6 ± 38.4	17.3 ± 4
	3°	23 ± 24	31 ± 18.1	52 ± 28.7	10.3 ± 1.1
	4°	8.6 ± 9.8	15 ± 14	27 ± 18.5	2.3 ± 4
	5°	0.7 ± 1.1	6.3 ± 7	13.3 ± 8.7	0
	6°	0.3 ± 0.5	1.7 ± 1.5	2.3 ± 1.5	0

Figure 7

**Figure S2**

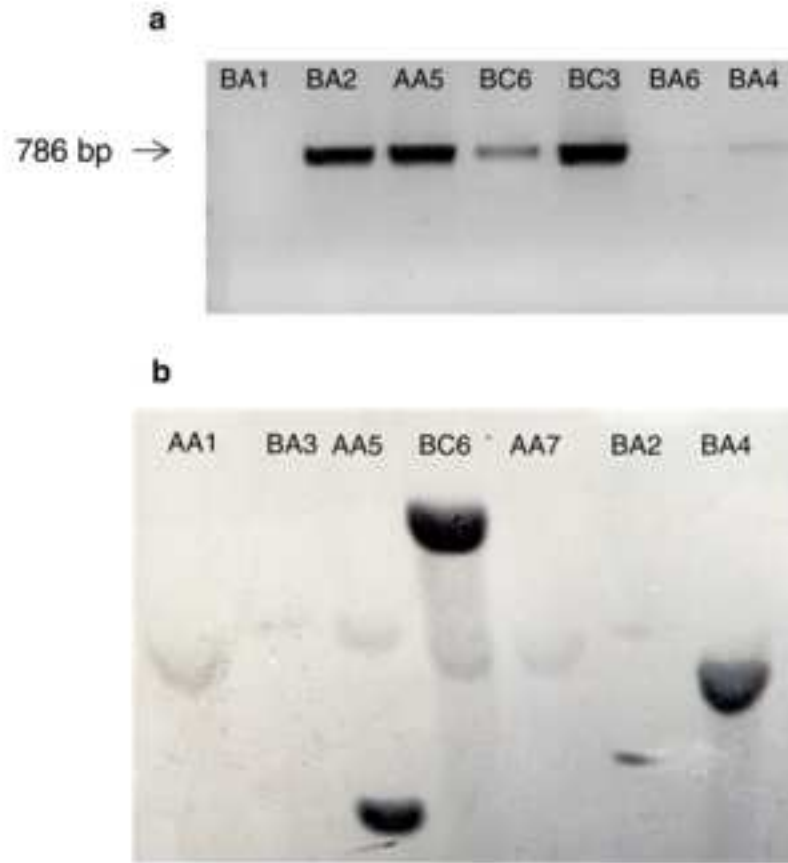


**Figure S4**